

Forecast: Data, Methods and Processing. A common description

D6.2



EU-SysFlex

| | |
|--|--|
| PROGRAMME | H2020 COMPETITIVE LOW CARBON ENERGY 2017-2-SMART-GRIDS |
| GRANT AGREEMENT NUMBER | 773505 |
| PROJECT ACRONYM | EU-SYSFLEX |
| DOCUMENT | D6.2 |
| TYPE (DISTRIBUTION LEVEL) | <input checked="" type="checkbox"/> Public <input type="checkbox"/> Confidential <input type="checkbox"/> Restricted |
| DUE DELIVERY DATE | 30/04/2020 |
| DATE OF DELIVERY | 30/04/2020 |
| STATUS AND VERSION | 1 |
| NUMBER OF PAGES | 124 |
| Work Package / TASK RELATED | WP6/T6.3 |
| Work Package / TASK RESPONSIBLE | Carmen Calpe, innogy / Sebatsian Wende-von Berg, Fraunhofer IEE |
| AUTHOR (S) | Arne Wessel, Katharina Brauns, Sebastian Wende-von Berg, Malte Siefert – Fraunhofer IEE/ Uni-Kassel "e2n" Wiebke Albers, Carmen Calpe – innogy Carla Marino, Luigi D’Orazio, Simone Tegas– e-distribuzione Daniele Clerici – RSE Corentin Evens, Poria Divshali, Sergio Motta, Pekka Koponen– VTT Suvi Takala, Antti Hyttinen –Helen Pirjo Heine, Atte Pihkala – Helen Electricity Network Maik Staudt – MITNETZ STROM |

DOCUMENT HISTORY

| VERS | ISSUE DATE | CONTENT AND CHANGES |
|------|------------|----------------------|
| 0.1 | 31.10.2019 | First draft version |
| 0.2 | 27.02.2020 | Second draft version |
| 0.3 | 12.03.2020 | Third draft version |
| 0.4 | 26.03.2020 | Fourth draft version |
| 1.0 | 30.04.2020 | Final version |

DOCUMENT APPROVERS

PARTNER

innogy
EDF
EIRGRID

APPROVER

Carmen Calpe/ WP leader
Marie-Ann Evans / Project Technical Manager
John Lowry / Project Coordinator, with PMB review

TABLE OF CONTENTS

| | | |
|----------|--|-----------|
| 1 | EXECUTIVE SUMMARY | 10 |
| 2 | INTRODUCTION..... | 13 |
| 2.1 | WP 6 OBJECTIVES AND RELATIONSHIPS BETWEEN TASKS | 13 |
| 2.2 | SCOPE AND OBJECTIVE OF THIS DELIVERABLE | 16 |
| 2.3 | STRUCTURE OF THIS DELIVERABLE | 20 |
| 3 | FORECASTING OF GENERATION AND LOAD FOR THE GERMAN DEMONSTRATOR | 21 |
| 3.1 | INTRODUCTION | 21 |
| 3.1.1 | NEED FOR A FORECAST..... | 21 |
| 3.1.2 | INNOVATION OF THE FORECAST COMPARED TO EXISTING ONES..... | 22 |
| 3.2 | DESCRIPTION OF THE FORECASTING PROCESS..... | 22 |
| 3.2.1 | CONCEPT OF THE FORECASTING SYSTEM..... | 22 |
| 3.2.2 | INITIAL DATA: MEASUREMENTS, WEATHER FORECASTS AND META DATA | 24 |
| 3.2.3 | ALGORITHMS AND MODELLING | 25 |
| 3.2.4 | REALIZATION OF THE FORECAST SYSTEM..... | 30 |
| 3.3 | FORECASTING RESULTS | 31 |
| 3.3.1 | FORECASTING QUALITY BASED ON HISTORICAL DATA..... | 32 |
| 3.3.2 | PERFORMANCE OF THE DEMONSTRATION SYSTEM | 38 |
| 3.3.3 | APPLICATIONS | 39 |
| 3.4 | PRELIMINARY CONCLUSION | 40 |
| 4 | FORECASTING OF POWER AND LOAD FOR THE ITALIAN DEMONSTRATOR..... | 41 |
| 4.1 | INTRODUCTION | 41 |
| 4.1.1 | NEED FOR A FORECAST..... | 41 |
| 4.1.2 | INNOVATION OF THE FORECAST COMPARED TO EXISTING ONES..... | 42 |
| 4.2 | DESCRIPTION OF THE FORECASTING PROCESS..... | 43 |
| 4.2.1 | CONCEPT OF THE FORECASTING SYSTEM..... | 43 |
| 4.2.2 | INITIAL DATA: MEASUREMENTS, WEATHER FORECASTS AND META DATA | 43 |
| 4.2.3 | ALGORITHMS AND MODELLING | 44 |
| 4.2.4 | REALIZATION OF THE FORECAST SYSTEM..... | 45 |
| 4.3 | FORECASTING RESULTS | 47 |
| 4.3.1 | FORECASTING QUALITY BASED ON HISTORICAL DATA..... | 50 |
| 4.3.2 | PERFORMANCE OF THE DEMONSTRATION SYSTEM | 53 |
| 4.3.3 | APPLICATIONS | 53 |
| 4.4 | PRELIMINARY CONCLUSION | 53 |
| 5 | FORECASTING TOOLS FOR THE FINNISH DEMONSTRATOR..... | 55 |
| 5.1 | INTRODUCTION | 55 |
| 5.1.1 | NEED FOR A FORECAST..... | 55 |
| 5.1.2 | INNOVATION OF THE FORECAST COMPARED TO EXISTING ONES..... | 56 |
| 5.2 | FORECASTING THE REACTIVE POWER NEEDS TO COMPLY WITH THE PQ-WINDOW REQUIREMENTS | 58 |
| 5.2.1 | INTRODUCTION | 58 |
| 5.2.2 | DESCRIPTION OF THE FORECASTING PROCESS..... | 62 |
| 5.2.3 | FORECASTING RESULTS | 71 |
| 5.2.4 | PERFORMANCE OF THE FORECAST SYSTEM | 77 |
| 5.2.5 | APPLICATIONS | 77 |
| 5.3 | AMR-CONTROLLED ELECTRIC HEATING HOUSES FORECASTING | 78 |
| 5.3.1 | INTRODUCTION | 78 |
| 5.3.2 | DESCRIPTION OF THE FORECASTING PROCESS..... | 79 |
| 5.3.3 | FORECASTING RESULTS | 81 |
| 5.3.4 | PERFORMANCE OF THE FORECAST SYSTEM | 86 |
| 5.3.5 | APPLICATIONS | 87 |
| 5.4 | EV CHARGING STATION FORECASTING | 88 |
| 5.4.1 | INTRODUCTION | 88 |
| 5.4.2 | DESCRIPTION OF THE FORECASTING PROCESS..... | 88 |
| 5.4.3 | FORECASTING RESULTS | 96 |
| 5.4.4 | PERFORMANCE OF THE FORECAST SYSTEM | 100 |
| 5.4.5 | APPLICATIONS | 100 |
| 5.5 | FORECAST FOR CUSTOMER-OWNED BATTERIES..... | 101 |
| 5.5.1 | INTRODUCTION | 101 |
| 5.5.2 | DESCRIPTION OF THE FORECASTING PROCESS..... | 101 |
| 5.5.3 | FORECASTING RESULTS | 105 |

| | | |
|----------|---|------------|
| 5.5.4 | PERFORMANCE OF THE DEMONSTRATION SYSTEM | 107 |
| 5.5.5 | APPLICATIONS | 108 |
| 5.6 | PRELIMINARY CONCLUSIONS FOR THE FINNISH DEMONSTRATOR | 108 |
| 6 | SIMILARITIES, DIFFERENCES AND TRANSFERABILITY OF FORECAST APPROACHES | 110 |
| 6.1 | OVERVIEW OF THE DIFFERENT APPROACHES AND TECHNIQUES | 110 |
| 6.2 | COMPARISON BETWEEN THE APPROACHES FROM THE THREE DEMONSTRATIONS | 115 |
| 6.2.1 | SCOPE AND INNOVATIONS | 115 |
| 6.2.2 | INPUT DATA AND MODELLING | 116 |
| 6.2.3 | APPLICATIONS AND LIMITATIONS | 116 |
| 7 | CONCLUSION | 118 |
| 8 | REFERENCES | 121 |
| 9 | COPYRIGHT | 124 |

LIST OF FIGURES

| | |
|---|----|
| FIGURE 1 – WP6 OVERVIEW AND RELATIONSHIPS WITHIN TASKS..... | 15 |
| FIGURE 2 - SCHEMA OF THE FORECAST POINT AND THE RELATED ENERGY SOURCES IN THE MEDIUM AND LOW VOLTAGE GRID | 23 |
| FIGURE 3: SCHEDULE OF THE FORECAST..... | 23 |
| FIGURE 4 - SCHEMATIC REPRESENTATION OF THE PV FORECAST MODEL | 25 |
| FIGURE 5 - FORECAST CHAIN OF THE WIND POWER FORECAST | 26 |
| FIGURE 6 - TRAINING STEP OF THE LSTM ARTIFICIAL NETWORK..... | 27 |
| FIGURE 7 - LSTM IN OPERATIONAL MODE..... | 28 |
| FIGURE 8 - LSTM MODEL ARCHITECTURE | 29 |
| FIGURE 9: DATA FLOW BETWEEN DSO AND THE TWO FORECAST SYSTEMS (EXTERNAL DATA FROM THE WEATHER SERVICES IS NOT INCLUDED)..... | 31 |
| FIGURE 10 - COMPARISON OF MEASUREMENT AND FORECAST TIME SERIES WITH THREE DIFFERENT FORECAST HORIZON (1 HOURS, 4 HOURS AND 48 HOURS)..... | 34 |
| FIGURE 11 - METRICS BAR PLOT WITH NORMALIZED RMSE, MAE AND CORRELATION FOR SIX CHOSEN FORECAST HORIZON FOR TRANSFORMER 1. THE FORECAST HORIZON INCREASES FROM LEFT TO RIGHT FOR EACH METRICS. | 35 |
| FIGURE 12 - SCATTER PLOTS FOR SIX DIFFERENT FORECAST HORIZON (1H, 4H, 8H, 16H, 32H, 48H) FOR TRANSFORMER 1. THE TRUE MEASUREMENT VALUES ARE PLOTTED AGAINST THE FORECAST VALUES. THE LEFT UPPER FIGURE SHOWS THE RESULT FOR THE COMPARISON WITH LOWEST LEAD TIME OF 1 HOUR. THE LEAD TIME INCREASES FROM THE UPPER FIGURES TO THE LOWER FIGURES FROM LEFT TO RIGHT. THE HIGHEST LEAD TIME OF 48 HOUR AND ITS COMPARISON IS THEN SHOWN IN THE LOWER RIGHT FIGURE. | 36 |
| FIGURE 13 - BOX PLOT FOR THE NORMALIZED MAE OVER ALL TRANSFORMER FORECASTS AND FOR 7 DIFFERENT FORECAST HORIZON ... | 37 |
| FIGURE 14 - BOX PLOT FOR THE NORMALIZED RMSE OVER ALL TRANSFORMER FORECASTS AND FOR 7 DIFFERENT FORECAST HORIZON.. | 37 |
| FIGURE 15 - BOX PLOT FOR THE NORMALIZED CORRELATION OVER ALL TRANSFORMER FORECASTS AND FOR 7 DIFFERENT FORECAST HORIZON | 38 |
| FIGURE 16 - EVALUATION OF THE PROCESSING TIME FOR 1,000 AND 3,000 MODELS. THE MEAN DURATION FOR FORECASTING 48H AHEAD FOR ONE TIME STEP FOR 1,000 AND 3,000 MODELS IN SECONDS IS PLOTTED OVER THE NUMBER OF USED CPU'S. | 39 |
| FIGURE 17 - SCHEDULE OF THE POWER FORECAST | 43 |
| FIGURE 18 - DIAGRAM OF PV GENERATION FORECAST. | 44 |
| FIGURE 19 - MAE AND NMAE RELATED TO SUMMER PERIOD..... | 48 |
| FIGURE 20 - MAE AND NMAE ₂ RELATED TO SUMMER PERIOD | 48 |
| FIGURE 21 - MAE AND NMAE RELATED TO WINTER PERIOD..... | 49 |
| FIGURE 22 - MAE AND NMAE ₂ RELATED TO WINTER PERIOD | 49 |
| FIGURE 23 - CLUSTERED CUSTOMER CURVES IN A WORKING DAY IN SUMMER..... | 51 |
| FIGURE 24 - CLUSTERED CUSTOMER CURVES IN A SATURDAY (DAY BEFORE HOLIDAY) IN SUMMER. | 51 |
| FIGURE 25 - CLUSTERED CUSTOMER CURVES IN A SUNDAY (HOLIDAY) IN SUMMER. | 52 |
| FIGURE 26 - MV PV GENERATOR CURVES DURING A WEEK IN JULY..... | 52 |
| FIGURE 27 - A) MAXIMUM, B) MINIMUM, C) AVERAGE ANNUAL REACTIVE POWER AND TAN Φ FOR THE YEARS 2003 TO 2017. THE MEASUREMENTS REPRESENT THE SUM OF HV/MV TRANSFORMER MEASUREMENT ON THE MV SIDE..... | 59 |
| FIGURE 28 - PQ WINDOW IN THE FINNISH ELECTRICITY SYSTEM, CASE HELSINKI..... | 61 |
| FIGURE 29 - DATAPOINT IS LOCATED BETWEEN THE TSO AND THE DSO | 62 |
| FIGURE 30 - PQ PROFILE OF THE DSO NETWORK WITH ($Q_{network}$) INFLUENCE OF COMPENSATION DEVICES AND UNDERGROUND CABLES; (Q_{uncomp}) INFLUENCE OF ONLY UNDERGROUND CABLES; (Q_{loads}) THE REACTIVE POWER FRACTION THAT IS UNKNOWN TO THE DSO BEFOREHAND, THE TARGET VARIABLE OF THE FORECAST..... | 65 |
| FIGURE 31 - DIFFERENT FORECAST TARGETS YIELD DIFFERENT STAGES OF THE REACTIVE POWER FORECAST. | 65 |
| FIGURE 32 - GRADIENT BOOSTING METHOD IMPLEMENTATION ALGORITHM..... | 67 |
| FIGURE 33 - LSTM METHOD IMPLEMENTATION ALGORITHM..... | 68 |
| FIGURE 34 - STATISTICAL CLUSTERING FORECAST METHOD | 69 |
| FIGURE 35 - GRADIENT BOOSTING INPUT AND OUTPUT FORMATS | 70 |

| | |
|--|-----|
| FIGURE 36 - LSTM INPUT AND OUTPUT FORMATS | 70 |
| FIGURE 37 - STATISTICAL CLUSTERING INPUT AND OUTPUT FORMATS | 71 |
| FIGURE 38 - DAY-AHEAD FORECAST CURVES FOR ALL THREE APPROACHES | 73 |
| FIGURE 39 - WEEK-AHEAD FORECAST FOR THE THREE FORECASTING METHODS | 74 |
| FIGURE 40 - MONTH-AHEAD FORECAST FOR $Q_{loads}(t)$ WITH THE THREE FORECASTING METHODS | 76 |
| FIGURE 41 - REPRESENTATION OF THE PARTLY PHYSICALLY BASED MODEL FOR ELECTRICALLY HEATED HOUSES WITH AMR-CONTROL CAPABILITIES | 80 |
| FIGURE 42 - DIAGRAM FOR THE HYBRID FORECASTING MODEL | 81 |
| FIGURE 43 - PHYSICALLY BASED LOAD FORECAST: OVERVIEW, OVER A 20-DAY AND OVER A 3-DAY LONG PERIOD. | 82 |
| FIGURE 44 - POTENTIAL FOR AN HOUR-LONG LOAD INCREASE OR DECREASE: OVERVIEW AND OVER A 3-WEEK PERIOD | 84 |
| FIGURE 45 - FORECAST RESULTS FOR THE AGGREGATED POWER OF THE 727 HOUSES | 85 |
| FIGURE 46 - FORECASTING ERROR OVER THE VERIFICATION PERIOD | 86 |
| FIGURE 47 - THE SIMPLE CHARGING PROFILE AND AVERAGE POWER CHARGING OF AN EV | 89 |
| FIGURE 48 - THE CHARGING PROFILES PROVIDING UP-REGULATION RESERVES | 90 |
| FIGURE 49 - THE CHARGING PROFILES PROVIDING DOWN-REGULATION RESERVES | 90 |
| FIGURE 50 - PROCESS USED TO CALCULATE THE AGGREGATED PDF FOR A GROUP OF EVS | 93 |
| FIGURE 51 - THE PROBABILITY DENSITY OF EVS ARRIVAL TIME, T_{Ar} , TO CHARGING STATIONS DURING 2018 | 96 |
| FIGURE 52 - THE PROBABILITY DENSITY OF EVS CHARGING DURATION, $T_D - T_A$, AND THE BEST WEIBULL DISTRIBUTION FIT TO THIS PROBABILITY DENSITY | 97 |
| FIGURE 53 - THE PROBABILITY DENSITY OF EVS CHARGING ENERGY, E , (KWH) AND THE BEST LOG-LOGISTIC DISTRIBUTION FIT TO THIS PROBABILITY DENSITY | 97 |
| FIGURE 54 - THE CUMULATIVE DENSITY FUNCTION (CDF) OF A) FCR-N, B) FCR-D, AND C) FCR-DN FLEXIBILITY EACH TIME OF A DAY PROVIDED BY EVS | 98 |
| FIGURE 55 - THE EXPECTED FLEXIBILITY PROFILES OF EVS CHARGED IN HELSINKI AREA | 98 |
| FIGURE 56 - THE OPTIMUM FLEXIBILITY PROFILES OF EVS CHARGED IN HELSINKI. | 99 |
| FIGURE 57 - PRODUCTION AND CONSUMPTION CURVES FOR "CONSUMER 1" DURING AUGUST 16 TH , 2019. | 102 |
| FIGURE 58 - PV PRODUCTION MEASURED AND A MODELLED FORECASTED CAP | 103 |
| FIGURE 59 -RELATIONSHIP BETWEEN THE ENERGY USED DURING THE DAY AND THE OUTDOOR TEMPERATURE FOR A SINGLE HOUSEHOLD | 104 |
| FIGURE 60 - ENERGY CONSUMPTION FOR A SINGLE HOUSEHOLD DURING THE DAY FOR THE DAYS SIMILAR TO AUGUST 16 TH , 2019. .. | 104 |
| FIGURE 61 - FORECASTED, ENERGYWISE LOWER BOUND AND ACTUAL CONSUMPTION FOR AUGUST 16 TH , 2019. | 105 |
| FIGURE 62 - FORECASTED UPPER BOUND ON THE PRODUCTION AND ACTUAL PRODUCTION FOR AUGUST 16 TH , 2019 | 105 |
| FIGURE 63 - STATE OF CHARGE, FORECASTED "WORST" CASE AND ACTUAL FOR AUGUST 16 TH 2019 | 106 |
| FIGURE 64 - DAILY MAXIMUM SOC MEASURED AND FORECASTED FOR A SINGLE HOUSEHOLD BETWEEN DEC. 9 TH , 2018 AND JAN 28 TH , 2019. | 107 |

LIST OF TABLES

| | |
|---|-----|
| TABLE 1 - LISTING OF THE HYPER PARAMETER AND THEIR VALUES USED FOR THE DNN..... | 33 |
| TABLE 2 - ACCURACY METRICS AND INPUT-OUTPUT FORMATS FOR FORECASTING METHODS FOR FULL TEST DATA FOR 2019 | 72 |
| TABLE 3 - ACCURACY VALUES AND INPUT-OUTPUTS FOR DAY-AHEAD FORECAST | 74 |
| TABLE 4 - ACCURACY FOR EACH FORECASTING METHOD USING THE WEEK-AHEAD FORECASTING HORIZON..... | 75 |
| TABLE 5 - ACCURACY FOR THE MONTH -AHEAD FORECAST WITH DIFFERENT METHODS | 76 |
| TABLE 6 - COMPARISON OF THE FORECASTING ACCURACY OF THE MODELS..... | 85 |
| TABLE 7 - AVERAGE DAILY PROFIT (IN €) CALCULATED FOR PROVIDING FLEXIBILITY PRODUCTS DURING OCT. 2018 | 99 |
| TABLE 8 - SUMMARY OF THE RESULTS OF THE FORECASTING TOOL BASED ON ONE YEAR OF HISTORICAL DATA | 106 |
| TABLE 9 - FAILED DAYS, WHEN THE FORECASTED MAXIMUM DAILY SOC IS BELOW THE MEASURED ONE..... | 107 |
| TABLE 10: OVERVIEW OF THE FORECAST APPROACHES AND TECHNIQUES IN THE THREE DEMONSTRATORS WITHIN THE EU-SYSFLEX PROJECT. | 111 |

ABBREVIATIONS AND ACRONYMS

| | |
|------------|---|
| AC | Alternating Current |
| AMR | Automatic meter reading |
| AutoML | Automated Machine Learning |
| BESS | Battery Energy Storage System |
| CDF | Cumulative Density Function |
| CIM | Common Information Model |
| CPU | Central Processing Units |
| DC | Direct Current |
| DER | Distributed Energy Resource |
| DG | Distributed Generators |
| DNN | Deep Neural Networks |
| DSO | Distribution System Operator |
| DWD | German Weather Service |
| EC-GA | Grant Agreement |
| ECMWF | European Centre for Medium-Range Weather Forecasts |
| EHV | Extra High Voltage |
| ENTSO-E | European Network of Transmission System Operators for Electricity |
| EU-SYSFLEX | Pan-European System with an efficient coordinated use of flexibilities for the integration of a large share of Renewable Energy Sources (RES) |
| EV | Electric Vehicle |
| FCR | Frequency Containment Reserves |
| FCR-D | Frequency Containment Reserves for Disturbances |
| FCR-N | Frequency Containment Reserves for Normal Operation |
| ForEx | Forecast Experiments |
| FRR | Frequency Restoration Reserve |
| GB | Gradient Boosting |
| GLDPM | Generation and Load Data Provision Methodology |
| HDNN | Hierarchical Deep Neural Network |
| HV | high voltage |
| IEE | Fraunhofer Institute for Energy Economics and Energy System Technology |
| LeakyReLU | Leaky Rectified Linear Unit |
| LSTM | Long Short-Term Memory |
| LV | Low Voltage |
| MAE | Mean Absolute Error |
| MAGO | Monitoring and control of Active distribution Grid Operation |
| mFRR | Manual Frequency Restoration Reserve |
| MLP | Multi Layer Perceptron |
| MV | Medium Voltage |
| NMAE | Normalized Mean Absolute Error |
| NRMSE | Normalised Root Mean Square Error |
| OLTC | On-Load Tap Changer |
| P | Active Power |
| PAG | Generated Active Power |
| PAS | Exchanged Active Power |

| | |
|-------|--|
| PDF | Probability Density Function |
| PGM | Physical Grid Model |
| PI | Installed power |
| PMB | Project Management Board |
| PV | Photovoltaics |
| PVUSA | Photovoltaics for Utility Scale Applications |
| Q | Reactive Power |
| ReLU | Rectified Linear Unit |
| RES | Renewable Energy Sources |
| RMSE | Root Mean Squared Error |
| RNN | Recurrent Neural Network |
| SOC | State Of Charge |
| SO GL | System Operation Guideline |
| SUC | System Use Cases |
| SVR | Support Vector Regression |
| ToD | Time Of Day |
| TSO | Transmission System Operator |
| WP | Work Package |

1 EXECUTIVE SUMMARY

The EU-SysFlex H2020 project aims at a large-scale deployment of solutions, including technical options, system control and novel market designs to integrate a large share of renewable electricity, increasingly variable, maintaining the security and reliability of the European power system. The project results will contribute to enhance system flexibility, resorting to both existing assets and new technologies in an integrated manner, based on seven European large scale demonstrators (WP 6, 7, 8 and 9). The overall objective of WP6 is the analysis and demonstration of the exploitation of decentralized flexibility resources connected to the distribution grid for system services provision to the TSOs; this objective is pursued by the means of three physical demonstrators located in Germany, Italy and Finland, using different assets located at complementary voltage levels (high, medium and low voltage) of the distribution grid. These demonstrations showcase innovative approaches in flexibility management targeted to support transmission system operators' (TSO) and distribution system operators' (DSO) needs and their related services, identified within the EU-SysFlex H2020 funded project. These approaches are followed by the means of suitable system processes which have been described in terms of System Use Cases (SUC) and presented in deliverable D6.1. The functionalities identified within the SUC modelling have been mapped into four main software tools groups, namely forecast tools (D6.2), simulation tools (D6.3), communication tools (D6.4) and optimisation tools (D6.5), the development of which is the main goal of Task 6.3. These tools are described in four corresponding deliverables: this deliverable, D6.2, is part of this set and addresses the methods and tools which provide forecast information and first results of these tools.

Forecasting became one of the most important disciplines in the energy systems. This is mainly due to the, still growing, amount of volatile, weather dependent renewable energy sources (RES) like wind and photovoltaic (PV) plants. But also forecasts of consumers are becoming more and more important, since the regular household is not behaving in regular patterns like it was about 50 years ago. The whole life has become more volatile and consumers often becoming prosumers, meaning they also produce energy in their houses. Due to these reasons plannable operation became even more important. Forecasts can help grid operators and energy markets to schedule their actions, decide on operational strategies and take the actions required. In addition, ENTSO-E (European Network of Transmission System Operators for Electricity) has agreed with the European National Regulatory Authorities on processes called Generation and Load Data Provision Methodology (GLDPM) and System Operation Guideline (SO GL). In those, the determination of predicted grid states for the next 48 hours (or even more) and the forecasting of load and generation are key pieces of information.

Within WP6 of EU-SysFlex, advanced and innovative forecast methods are applied to real-life field test Demonstrators in order to enable an enhanced information exchange between the distribution system operator (DSO) and transmission system operator (TSO) and also to enable sufficient flexibility forecasts for aggregators. In this deliverable, the individual, and partly quite different, forecast approaches in the three physical Demonstrators are described and compared with each other. The demonstrations have one common goal, all three use information from forecast to make their individual operations and actions plannable and hence more controllable. For the Finnish demonstration, this means forecasting and optimizing the use of assets in order to

sell flexibilities through an aggregator to TSO ancillary services and on the other hand to the reactive power needs of a DSO. These assets and prosumers are located in the low and medium voltage grids and include households with electric heating, customer-scale batteries, office-scale battery, large-scale battery energy storage system (BESS) and electric vehicles charging stations to forecast and optimize the use of the assets in order to sell flexibilities through an aggregator to the TSO ancillary services. On the other hand, Finnish demonstrator aims for a technical proof of concept for a reactive power market and therefore forecast is needed by the DSO to determine reactive and active power flows at the connection point of TSO and DSO (PQ-window). The Italian and German demonstrators also act at the interfaces between DSOs and TSOs. The aim is to determine active (P) and reactive (Q) power flexibilities at TSO-DSO interface via optimization methods. The flexibility is provided by volatile renewable energy sources and is therefore strongly dependent on the weather and, raising the need of energy forecasts for these renewable resources. All three Demonstrators use partly individual approaches but also for some applications have similar basic assumptions and methods.

The German Demonstrator is focusing on the TSO-DSO interface between high voltage (HV) and extra high voltage (EHV) grids. The aim is to provide PQ-flexibility to ensure a secure, stable and efficient grid operation. In this case, a bottom up approach is used which forecasts energy sources from low and medium voltage grids and aggregates them onto high voltage (HV)/medium voltage (MV) substations. With measurements at these substations, residual load can be determined and be used to improve the forecasts via artificial intelligence and self learning algorithms. Furthermore, with machine learning approaches it is possible to forecast the consumption taking place at the lower voltage levels. For the latter approach, Long Short-Term Memory (LSTM) models are utilized, which takes advantage of historical time series. Generation is predicted via the usage of physical models and also historical data in combination with information about weather conditions. Both approaches result in time series for individual grid points (production and consumption) which are then harnessed to generate complete future grid states. These grid states serve as basis for optimization routines, which determines PQ-flexibility for usage in distribution grids themselves, but also for transmission grid operations. The predicted time span is up to 72 hours in this project.

The Italian demonstration also deals with the TSO-DSO interface, but between HV and MV. (The grid levels controlled by TSO and DSO are different in Germany and Italy.)

The aim of forecast in this case is, on the one hand estimation of current energy injection from PV plants and decentral generators (DG) in order to estimate current grid states and power exchange over HV/MV substations (nowcast) and on the other hand, to forecast these generating units for the next 72 hours. This current and predicted information about generation at MV/LV and, in aggregated form, at HV/MV substations serve in combination with standard load profiles for consumers as basis for operational planning and optimization approaches. The basis for this forecast approach is built by physical models in combination with weather data. In the project, these methods leads eventually to an enhanced observability for TSO and improved grid management for DSO.

Last but not least, in the Finnish Demonstrator, three different kinds of forecasts are needed for the aggregator's side: forecast of the electricity consumption of electrically heated houses with large hot water tanks, forecast of the expected flexibility of a set of public electric vehicle charging stations and forecast of customer-scale batteries availability to the TSO ancillary markets. In addition, one forecast is created for the DSO to determine active and reactive power flow at the TSO-DSO connection point. In all cases, the forecast is strongly entangled with optimization of the final predicted schedules. In order to reach the goal of optimized use of flexibilities, different forecast approaches are used within this demonstration. Statistical analysis is, besides other techniques, used in the analysis and prediction of data for the determination of charging behaviour and PQ-windows. In the latter case, also machine learning techniques are utilized to train models (Long ShortTerm Memory, LSTM) to the data which then can predict such data. In order to analyse and model household electric heating consumption, physical based models are set up and complemented with deep neural networks (DNN) for the residuals. First results are promising and can resemble the expected behaviour.

In all three cases first applications and results (partly on real data, partly on simulated or generic data) show, that the evaluated and applied approaches can fulfil the demands and requirements within the individual Demonstrators. In a next step, the approaches will be implemented and deployed in order to use them in the field test phase in EU-SysFlex.

2 INTRODUCTION

In the electricity industry, a key challenge is to precisely balance the supply and consumption of electricity and to ensure the secure transmission and distribution of energy from producers to consumers via the electricity grid. In order to meet both requirements and to take and implement appropriate measures in time, it is necessary to balance the generation and consumption in advance. Consumption behaviour has been known for a very long time, as it shows a recurring pattern over time. In addition, wind power forecasts have been used for two decades, and more recently also PV power forecasts, in order to determine the use of power plants in advance via market mechanisms on the one hand, and to identify and eliminate congestion in the electrical grid at an early stage on the other.

The forecasts were initially used by transmission system operators and in the electricity market sector. Due to the increasingly high share of renewable energies, the existing concepts have reached their limits and new solutions must be developed to improve the accuracy of the forecasts. Up to now, forecasts have been made without explicitly taking into account the network structures below the transmission grid. This approximation still works well, but shows its limits with most renewable energy generation taking place in the distribution grids. The European Regulation 2017/1485, establishing a guideline on electricity transmission system operation, therefore requires distribution system operators to prepare forecasts and exchange them with other network operators and in particular with the transmission system operators. Not only wind power forecasts and PV power forecasts play a role here, but also forecasts of the vertical power flows which flow between the grid levels and which include wind power, PV power, consumption and all other producers and consumers. These forecasts are exchanged between the grid operators and serve as input into forward-looking grid calculations.

The primary source of uncertainty in these forecasts is the weather dependency. Therefore, weather forecasts are an important input variable in power forecasting. Only for very short-term forecasts with a forecast horizon of a few hours, direct measurements of the current performance are another input variable. In the coming years, other influences will play an increasingly important role in the forecasts: Interventions in the generation of renewable energies such as feed-in management, redispatch by renewable energies, electric vehicles, sector coupling, flexible consumption, battery storage and many more must be represented in forecasts. In three different demonstrators, various of the above-mentioned challenges will be investigated and tested.

2.1 WP 6 OBJECTIVES AND RELATIONSHIPS BETWEEN TASKS

WP6 is one of the demonstration work packages within EU-SysFlex. It consists of three Demonstrators set up in Germany, Italy and Finland. The main objective is to analyze and test the use of distributed flexibility resources, with a focus on enabling provision of system services from resources connected to the distribution grids in accordance with the requirements of DSOs and TSOs. Two main requirements are:

1. DSO and TSO need to follow the current policies for the decarbonization of the energy systems in integrating large amount of renewable energy sources (RES) in their grid structures.
2. The DSOs must ensure the security and resilience of their networks.

For this, the DSOs need besides an adequate amount of "freedom" in the operation of their networks also a reasonable operational planning horizon in order to avoid overloads and restrictions in advance. This can be currently "superimposed" in certain operating conditions by requirements of TSOs, which have to take care about the problems in their grids like frequency stability or reverse power flows caused by the increase penetration of RES. These partly contradictory requirements can be met by an improved cooperation between TSOs and DSOs using RES's active and reactive power flexibilities. With this said, three sub-objectives can be identified for WP6:

- Improve TSO-DSO coordination;
- Provide ancillary services to TSOs from distribution system flexibilities;
- Investigate how these flexibilities could meet the needs of both TSOs and DSOs.

Besides this, the decisions made by the DSO needs to be made on a plannable basis. Since Wind and PV feed-in cannot be scheduled like conventional power plants, forecast methods are required in order to enable the grid operators to archive the above objectives. Furthermore, the consumption also needs improved forecasting due to its significant influence on grid states, especially when electric vehicles rise even more in number. The latter and possible distributed storage in households can also help reaching the above goals.

WP6 addresses these objectives through five interlinked tasks. Task 6.1 refers to the required coordination of the work package. Task 6.2 focuses on the definition of System Use Cases (SUC) based on the Business Use Cases (BUC) coming from WP 3. Within Task 6.3, systems and tools are being developed in order to set up the SUC. In Task 6.4, field tests are carried out in the three demonstrators. In addition, the results of these field tests will be analyzed and common conclusions will be drawn in Task 6.5. A schematic overview of all the relationships described above is depicted in Figure 1.

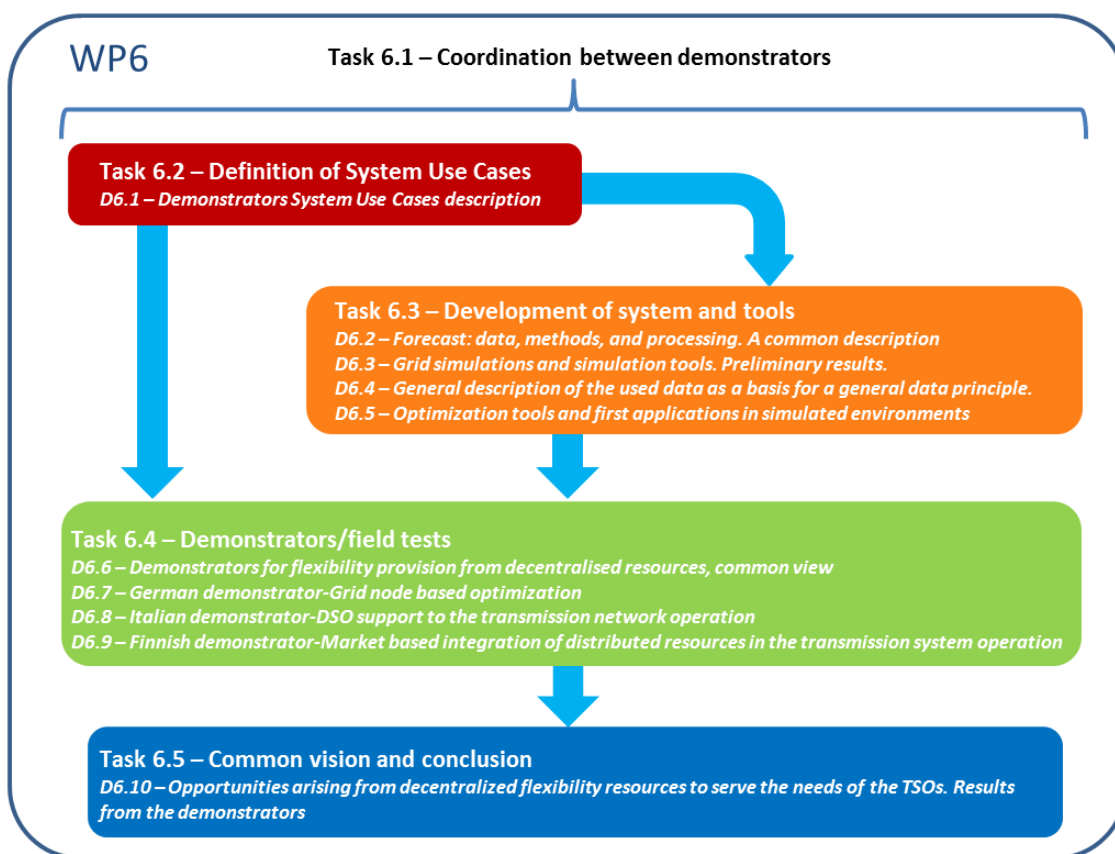


FIGURE 1 – WP6 OVERVIEW AND RELATIONSHIPS WITHIN TASKS

The activities and achievements of each Task, and of the whole Work Package itself, will be presented through a comprehensive set of Deliverables. In the following, they are shortly described, divided by Task:

- Task 6.2 “Definition of System Use Cases”:
 - Deliverable 6.1 “*Demonstrators Use Cases description*” presents the “translation” of Business Use Cases from WP3 into System Use Cases
- Task 6.3 “Development of systems and tools”:
 - Deliverable 6.2 “*Forecast: Data, Methods and Processing. A common description*” presents the description of requirements of the DSO/TSO interface, in order to harmonize the data formats and models for all the trials;
 - Deliverable 6.3 “*Grid simulations and simulation tools*” presents the first results about network models and simulations from the demonstrators;
 - Deliverable 6.4 “*General description of the used data as a basis for a general data principle*” presents the description of communication interfaces between the actors involved in the demonstrators;
 - Deliverable 6.5 “*Optimization tools and first applications in simulated environments*” presents the description of the optimization tools and the range of flexibilities used in the demonstrators;
- Task 6.4 “Demonstrators/field tests”:

- Deliverable 6.6 *“Demonstrators for flexibility provision from decentralized resources, common view”* presents the deployment plan, including technical specifications, procurement procedures for technical equipment, timeline for installations, and monitoring procedures;
- Deliverable 6.7 *“German demonstrator - Grid node based optimization”* presents the information about the German demonstrator results, including the description of the working framework;
- Deliverable 6.8 *“Italian demonstrator - DSO support to the transmission network operations”* presents the information about the Italian demonstrator results, including the description of the working framework;
- Deliverable 6.9 *“Finnish demonstrator – Market based integration of distributed resources in the transmission system operations”* presents the information about the Finnish demonstrator results, including the description of the working framework;
- Task 6.5 *“Common vision and conclusion”*:
 - Deliverable 6.10 *“Opportunities arising from the decentralized flexibility resources to serve the needs of the TSOs. Results from the demonstrators”* presents common conclusions and recommendations from the demonstrators’ activities, in order to contribute to the WP objectives and overall Project results.

The current deliverable D6.2 *“Forecast: Data, Methods and Processing. A common description”* is part of Task 6.3 *“Development of systems and tools”*. The scope of this task is to develop the algorithms and the software tools, which embed the innovative functionalities and the corresponding requirements defined in the System Use Cases, presented in Deliverable 6.1. Task 6.3 deals with four groups of tools, divided by the type of application (forecast, simulation, communication and optimization). They are presented and described in four corresponding Deliverables (D6.2 to D6.5). This group of tools will be integrated in the demonstrator set-ups in order to carry out the field tests, which are the scope of Task 6.4 and will be described in a dedicated set of deliverables (D6.7, D6.8 and D6.9 respectively). This Deliverable (D6.2) deals with the description of the developed and applied forecast techniques. These forecast approaches utilize a variety of mathematical and physical model descriptions, ranging from statistical analysis over usage of artificial intelligence approaches, to purely mathematical approaches. In this deliverable, the applied methods will be described and first (simulated) results are presented.

2.2 SCOPE AND OBJECTIVE OF THIS DELIVERABLE

The objective of this deliverable is to get a comprehensive overview of the different forecasts developed within the German, Italian and Finnish demonstrator. Therefore, the different forecast systems and their concepts are described including the corresponding input data, the algorithm and modelling as well as the realization of these forecast systems. In order to be able to classify the forecasts correctly, the need and the innovation of forecasts are introduced. To complement this, the forecasts and their qualities are analysed and evaluated.

German demonstration

In the German Demonstrator, the provision of active and reactive power at DSO high-voltage grid-level to the TSO at extra-high-voltage transmission grid in the form of P-Q flexibility ranges and maps is being determined via optimization. These flexibility ranges and maps are based on the current state of the electrical network. This planning is to be continued into the near future for a schedule based process, e.g. the next hours, for which forecasts for the generators and loads in the high voltage grid as well as the underlying medium-voltage grid are required. Therefore, forecast based on the voltage level below the high voltage level, i.e. medium voltage level, are included in order to forecast the vertical power flow going into the high voltage level. This advanced forecasting routine is being set up within the German demonstrator.

The forecast is especially important for the next few hours in terms of optimization. Therefore, the forecast quality and accuracy must be very high for this time range in particular. In the German demonstrator, only measurements at the interface between the medium-voltage grid and the high voltage grid are available. These measurements are an aggregation of all generators. However, the prediction is made for the individual grid stations in the medium-voltage grid, broken down by the various generators and loads. In order to provide a high quality forecast for the next hours, direct measurements at the generators and loads are required. As these are not available, it is to be investigated whether a similarly good forecast can be made using other approaches, in which the existing measurements are integrated.

Italian demonstration

This demonstration set-up is applied in a portion of the Italian medium voltage distribution network; its main scope is to exploit the controllable assets connected to distribution network for supporting ancillary service provision to the TSO. Its goal is to demonstrate that the already connected DERs plus some dedicated assets (BESS, STATCOM) may be managed and optimised locally by the DSO in order to provide suitable P-Q flexibility range for TSO at primary substation. This goal is pursued through the provision of aggregated reactive power capability and a cumulative parametric curve (energy/cost) for active power. The concept of the aggregation of flexible resources at distribution level is a substantial innovation for the Italian national scenario. The aim of simulations is to estimate how much flexibility could be achieved for different scenarios and to assess, which range of flexibility could be actually exploited without violating the distribution network constraints, i.e. guaranteeing safe and efficient operations of the distribution network.

This demonstration will be accomplished by using a forecast instrument developed directly by e-distribuzione and integrated with Central and Local SCADAs. This instrument is useful to support the monitoring and control of distribution network to plan the activities (work, optimal schemes etc) and, consequently, act on the grid for operating it. Considering that it also exploits weather forecast data for state estimation scopes, it is useful to satisfy also the EU-SysFlex objectives in managing flexibilities owned by the DSO and involved in the project in addition to RES.

Finnish demonstration

The Finnish demonstrator deals with aggregator activities related to flexible resources in medium and low voltage networks. Its main scope is to manage the flexible resources, in order to allow them to be exploited in the TSO ancillary service market and for reactive power services to the DSO. Its goal is to increase the revenues and value achievable from the operations of flexible assets and it is pursued through innovative aggregation approaches and a novel reactive power market concept. The forecasting in the Finnish demonstration is divided in four different forecasts, one forecast for the DSO (Helen Electricity Network) and three forecasts for the aggregator (Helen, energy company in Finland). The main purpose of the forecasts for an aggregator is to forecast the available flexibility from the assets to the TSO ancillary services. The forecasts presented in this deliverable are created by VTT, Technical Research Centre of Finland, and are based on information and historical data at Helen or at Helen DSO as well on open data sources, such as solar radiation and outdoor temperatures.

The forecast for a DSO:

- PQ-window compliance forecasting tool: The research question that the tool is targeted to answer is how much reactive power services the DSO should procure from the market in order to minimize the costs charged by the TSO when the exchanges between the distribution and transmission networks are out of bounds. The created forecast is used in the technical proof of concept of a reactive power market.

The forecasts for an aggregator:

- Forecast for households with electric storage heating that can be controlled through their Automatic Meter Reading (AMR) systems: This tool forecasts the heating needs throughout the day, but can also predict how the heating system will react to changes and commands resulting from the operation of the AMR-connected switches.
- Flexibility forecast of electric vehicle (EV) charging stations: The forecast is intended to give an estimate of how much capacity can be made available for specific markets. In this case, the target markets are the frequency containment reserves (FCR) markets.
- Forecast of customer-scale batteries availability to flexibility markets: This tool forecasts the State of Charge (SOC) of batteries installed in individual households

The scopes and goals described above, even if specifically focused to the needs of each demonstration, are aligned with the overall objective of the WP6, i.e. “analyse the opportunities arising from decentralised flexibility resources connected to the distribution grid to serve the needs of the overall power system”. Forecast tools and approaches described so far represent a part of the whole demonstrations set-ups, so they may not completely fulfil the WP6 objectives solely on their own, since the demonstrations activities in their entirety are targeted to that. Besides this, it is clear from the above descriptions that the utilization and application of forecast itself and further applications of it support the Work Package objectives described in section 2.1, here reported again for clarity:

- Improvement of TSO-DSO coordination
- Provision of ancillary services to TSOs from flexibilities in the distribution system.

- Demonstrating how flexibilities in the distribution grid can be used to meet the requirements of both DSO and TSO.

2.3 STRUCTURE OF THIS DELIVERABLE

This deliverable is meant to be comprehensible and self-contained in content but, since it is part of the set of deliverables in Task 6.3, it must be always considered as one part of a larger series.

The document structure is as follows:

- Chapter 3, 4 and 5 describe the individual approaches, realizations and first results of forecast within the three different demonstrators from the three participating countries;
- Chapter 6 outlines a comparison and overview of the afore presented forecast methods;
- Chapter 7, as a conclusive chapter, provides a summary and an outlook with ongoing research and open questions.

3 FORECASTING OF GENERATION AND LOAD FOR THE GERMAN DEMONSTRATOR

3.1 INTRODUCTION

In the German demonstrator an optimization of the electrical grid regarding active and reactive power as well as congestions is carried out by the DSO in the high voltage distribution grid. One component of this optimization is the generation and residual load forecast aggregated to individual power transformers at high and medium voltage level, which are performed for both intra-day and day-ahead forecasts. Therefore, a forecast tool is set up, which should meet the new requirements of a vertical power flow forecast with a high spatial and temporal resolution. Vertical power flow is defined as the power flow between grids with different voltage level.

So far in Germany, forecasts for wind and PV generation have usually been made for complete DSO and TSO regions or, on the contrary, for individual power plants. Having an increasing focus on the local power grid, with the goal of optimizing grid operations, the assumption of a copperplate for connecting wind and PV plants is no longer valid. It is now a matter of individual cable strands connecting renewable energies to the transformer stations to optimize the power flow with regard of congestions and reactive power deficits. In order to be able to estimate these optimizations for the next hours and days, local forecasts for the renewables are needed at the MV/HV substations.

On the DSO level, the focus lies in the feed-in from medium to high voltage level and depends on the detail level of the transformer station, the transformers or the busbar. Additionally, at those points, a greater mix of production and consumption will occur, which can be summarized as a vertical power flow.

Forecasting the feed-in of renewable energies is not enough anymore. The production of the other resources and the consumption of loads need to be forecasted too. This forecasting is done for every renewable energy type separately and give a consistent sum at the end.

Some of the generators are connected to the medium-voltage grid, the low-voltage grid or feed directly into the high-voltage grid. The simplest case is the high-voltage grid, where renewable energies are directly connected to the transformer stations. Feeding into the medium-voltage grid is more complicated, since the configuration of the grid may change at irregular intervals due to changes in the switching state of the grid, which must be taken into account by the forecast algorithm.

The actual forecast must be made at the medium and low voltage levels, where the generators are located and then summed up, depending on the switching state of the grid, to provide the forecast at the high voltage level.

3.1.1 NEED FOR A FORECAST

In order to establish schedule based active and reactive power management for congestion management and voltage control for transmission and distribution grid, it is imperative to predict future load flows in distribution grid. In Germany DSOs operate HV, MV and LV grids. Therefore, a high-quality forecast for the next few hours of infeed and load at grid connections in HV and aggregated at HV/MV substations are necessary to predict future

grid states. The German demonstration processes these forecasts together with other grid data to optimise power flow in future grid states.

3.1.2 INNOVATION OF THE FORECAST COMPARED TO EXISTING ONES

There are existing forecasting systems on the market that forecast the feed-in of vertical loads and renewable energies. These often do not take into account the existing grid condition of the medium and low-voltage grids situated below the high-voltage level. In this project, these structures are mapped in a high level of detail in the forecasting system.

Due to the lack of measurements in the medium and low voltage grid, a short-term forecast is often not possible. A new forecasting approach is therefore to be applied in the project, which allows a short-term forecast to be made that is adjusted every quarter of an hour to the prevailing conditions.

3.2 DESCRIPTION OF THE FORECASTING PROCESS

This chapter provides an overview of the forecasting system. First the concept of the system is introduced. This includes a detailed description of what exactly is predicted and how it is done.

Then the underlying input data is described, followed by the description of the used algorithms and at the end the technical realization takes place. The realization is divided into two steps. The first step defined in this deliverable considers the implementation of the baseline model which will be extended in the expansion stage in a second step. The results from the expansion stage and the according implementation steps will then be discussed in deliverable D6.7 'German demonstrator - Grid node based optimization'.

3.2.1 CONCEPT OF THE FORECASTING SYSTEM

The optimisation of the grid state is carried out in the high-voltage grid, but the generators themselves are located in the medium and low voltage grid and feed into the high voltage grid from there. For this reason, the vertical power flow on the busbars of the substations are forecasted at the transition from medium to high voltage.

The vertical power flow is decomposed in order to include the influence of the individual renewable energies. The decomposition is divided into wind, PV and the residual load, which includes traditional power plants, loads and due to the uniform energy supply: biogas power plants. The active power is forecasted for these components separately, while the reactive power is forecasted for the complete vertical load. A schema of the forecast point and decomposition with the related energy sources in the medium and low voltage grid is shown in Figure 2.

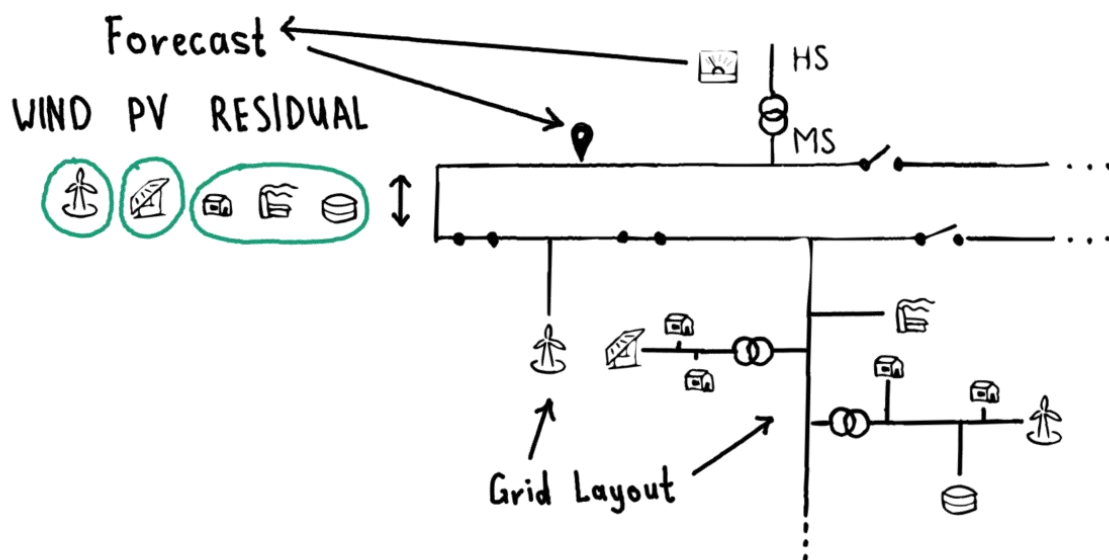


FIGURE 2 - SCHEMA OF THE FORECAST POINT AND THE RELATED ENERGY SOURCES IN THE MEDIUM AND LOW VOLTAGE GRID

In Figure 3 the different time constraints are described. The maximal lead time is 48 hours in advance in the baseline model and will be extended to 72 hours in the expansion stage. According to the temporal resolution of the electrical grid the time step will be 15 minutes. At initial time the calculation of the forecast begins, which includes values which are valid at each forecast horizon within the interval from zero to the maximum lead time. After the calculation of the forecast is completed, the forecast is delivered with a certain delay at 'wall clock time'. The forecast is updated every 15 minutes to create an intraday forecast (update cycle). This prediction incorporates current measurements into the process in order to determine near points in time more accurately. In the baseline system this is only done for the vertical loads, in the expansion stage the wind and PV forecasts also use this data.

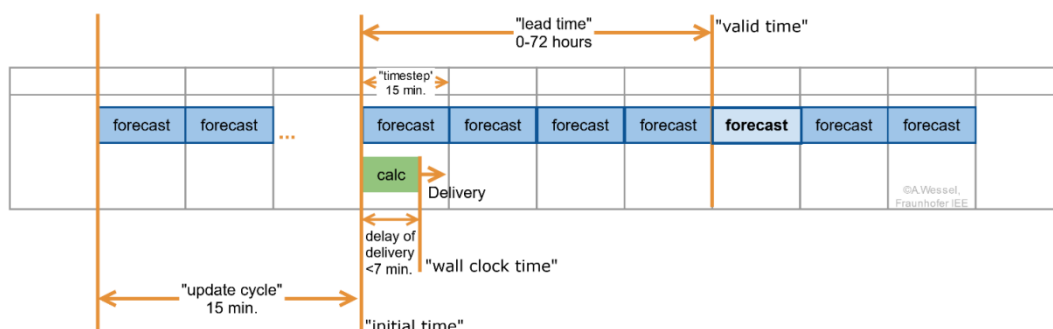


FIGURE 3: SCHEDULE OF THE FORECAST

The forecasting system is based on several numerical weather models: The Cosmo-D2 and the ICON-EU model of the German Weather Service (DWD) and the IFS model of the European Centre for Medium-Range Weather

Forecasts (ECMWF). From the Cosmo-D2 and the ICON-EU model the deterministic variant is used as well as the ensemble version of the models (Cosmo-D2 EPS, ICON-EU EPS), which allows the probabilistic forecast.

In addition to the weather forecasts, the measurements of the current grid status are included, as already mentioned above. However, these are only available at the transformers from medium to high voltage and not directly at the busbar where the points, to be forecasted, are located.

3.2.2 INITIAL DATA: MEASUREMENTS, WEATHER FORECASTS AND META DATA

The forecasting system is based on forecasts of the weather models Cosmo-D2 (EPS), ICON-EU (EPS) from German Weather Service and IFS from European Centre for Medium-Range Weather Forecasts.

The Cosmo-D2 model was chosen, especially for the intraday forecast, because of its update cycle of three hours, the high spatial resolution of 2.2 km and the close time delivery, i.e. the delay of delivery, which is only 1.5 hours. The disadvantage of the model lies in the low maximum lead time of 27 hours for each model run. Only the 3 o'clock run has an extended lead time of 45 hours. This is just about the limit of the required 48 hours prediction time required for the baseline version (so that the next day can be completely covered).

In order to soften this limit, the ICON-EU model is to be added to the forecast process in the expansion stage. This model offers a maximum lead time of 120h hours at a spatial resolution of 6.5km across Europe.

Since each wind or PV generator is to be predicted individually, the high spatial resolution of the Cosmo-D2 model should contribute to better reproduce spatial effects in the forecast.

The IFS forecast model is added to the list, as it is among the best European weather models in terms of forecast quality. The spatial resolution of 9km together with the temporal resolution, a time step of three hours, is rather low. However, this is compensated by the good forecast skills.

For the wind power prediction, the wind speeds and the wind directions for several heights up to about 120m above ground are used as parameters from the weather models. These heights are chosen so that they cover most hub heights of the installed wind turbines. In addition, the temperature at the wind levels and the air pressure are considered in an experimental status in order to include the effects of air density on the power characteristics of the wind turbines. The PV forecast uses direct and diffuse radiation from the weather models as parameters. In the second version of the forecast system, measurements of power at the MV/HV points will be included from wind farms/ PV plants, which are directly connected to the power stations. All measurements at the MV/HV points are 5 minutes snapshots and after 15 minutes a mean value is calculated which then is used as input.

The residual load forecast for the active power P is based on the forecast of the wind and PV power together with the vertical power flow measurements at the MV/HV stations and general weather forecasts (pressure, temperature, wind). For the typical load profiles, information such as the hour of the day and the position of the sun are also included. For the reactive power a forecast is created based on the same input, only that the wind and PV power forecasts are not included.

The meta data contain among other things information about the EEG energy source at either the substation or the underlying local grid stations with according coordinates, the summarized installed capacity at the station and the plant type and key at the local grid stations. All these information are connected to the so called prediction

point which is either a transformer or a busbar for which the forecast is then calculated. Additional information includes which one of two transformers at one station is used and also if the grid station is operated in ring operation or not. This meta data is delivered regularly every few days as a table extract from a database of Mitnetz.

3.2.3 ALGORITHMS AND MODELLING

When setting up a forecasting system, it is possible to choose either statistical or physical approaches for the individual models to predict generation and consumption. Here, as a limitation, the historical measurements used for the training of the models only contain the sum signal of all the individual generators/loads connected to the transformer. Therefore, the forecast is split into a part forecasting wind and PV and a part forecasting the residual loads, which contain the loads and other power sources and apply two different types of models, the physical and the statistical approaches which are described below.

PHYSICAL APPROACH FOR THE WIND AND PV POWER FORECASTS

For the wind and PV forecast a physical approach was chosen. With this physical approach, a first guess forecast for the historical time span can be created. This is then subtracted from the data measured at the transformer station and the resulting power time series is used for training the residual model, which is then based on machine learning procedures.

The physical model for the wind and PV forecast is based on the approach of the Physical Grid Model (PGM), introduced in context of the research project Fritz et al. (2017). It is used here in a slightly modified variant:

The wind power and PV forecast is first calculated on the grid points of the weather model and output as a normalized value.

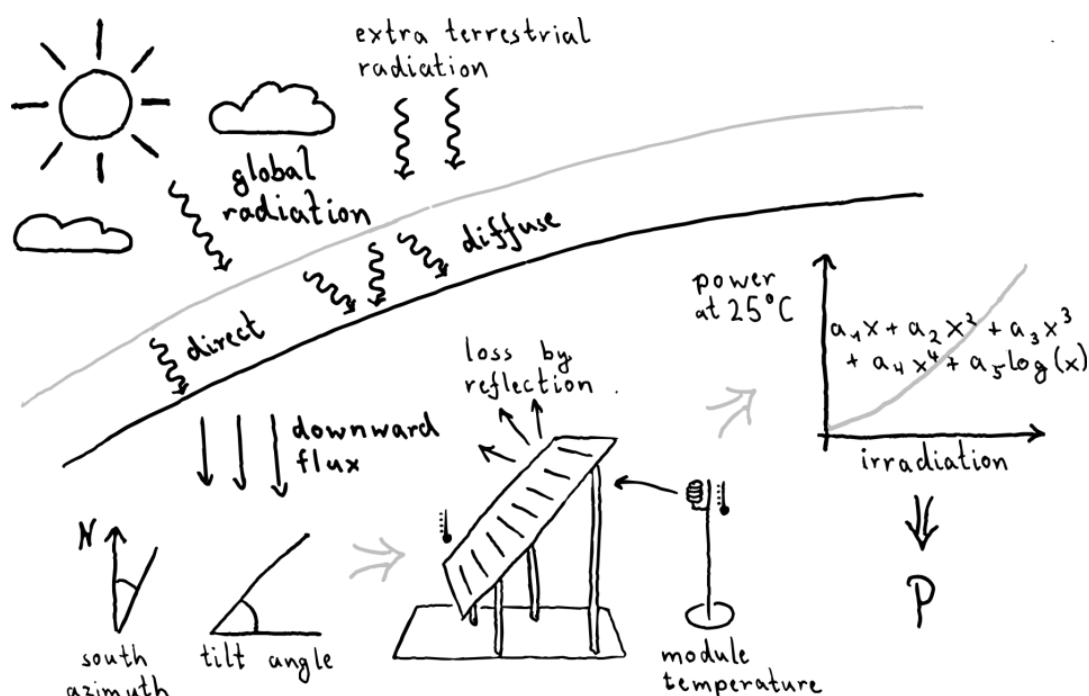


FIGURE 4 - SCHEMATIC REPRESENTATION OF THE PV FORECAST MODEL

Then the grid is interpolated to the actual power plants and scaled with the nominal power of the generators. The conversion of wind speed into power or irradiation into power is therefore carried out with universal models, i.e. for wind the universal power curve from the Tradewind project McLean (2008) is taken as a first approach and the PV model uses the SPS from the Fraunhofer IEE described in Saint-Drenan et al. (2015) and schematically shown in Figure 4.

The normalized power values on the grid points have to be interpolated on the single plants. This is done with radial basis functions, which allows later an additional selective spatial weighting, depending for example on the local orography or special weather situations. In the basic version of the forecast, the interpolation is set to a symmetrical radial basis function covering 2x2 gridpoints.

Of the wind turbines and PV panels, only the rated power is known in addition to the location. Therefore, the PGM has been extended to handle combinations of different parameterizations. For wind these would be scenarios for different hub heights and for solar different orientations of the modules. These scenarios are then combined according to local wind and PV plant statistics, as seen in Figure 5 for the model chain wind as an example.

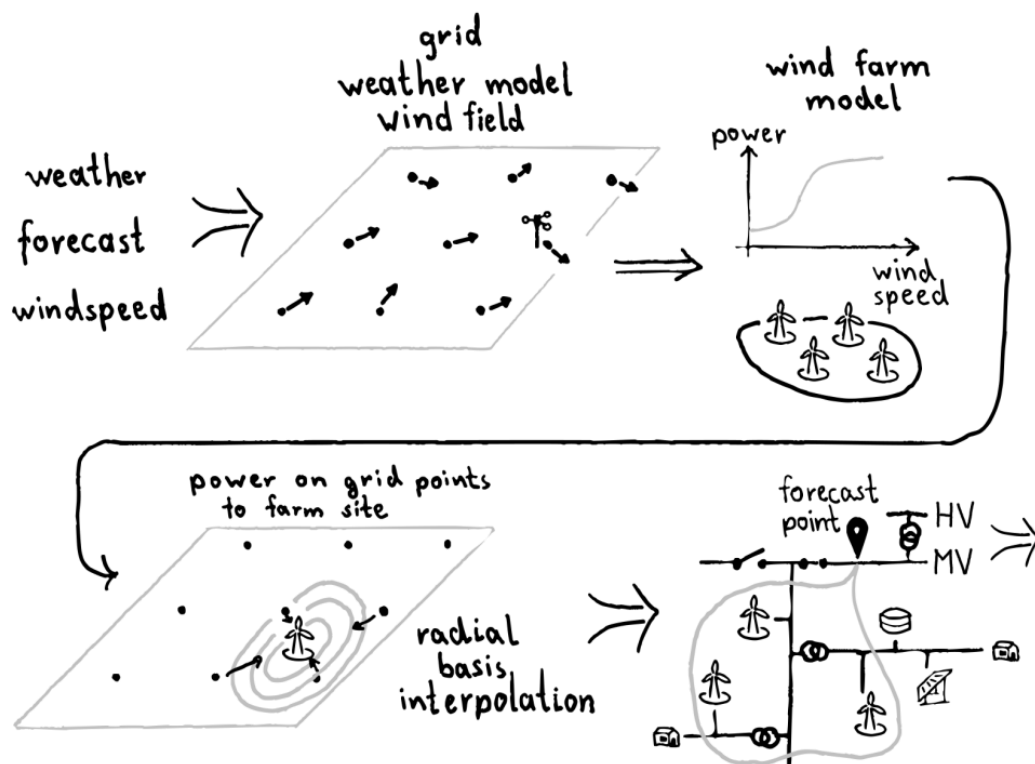


FIGURE 5 - FORECAST CHAIN OF THE WIND POWER FORECAST

Beneath the deterministic part, a probability forecast for wind and PV will be included in the expansion stage. This is based on the Cosmo-D2 EPS Ensemble weather model. Here often the spread of the different members (weather predictions) in the weather ensembles is not sufficient for the power forecast. Therefore, it will be calibrated with historical data at transformer stations, where either only wind or PV feed-in takes place. The results are then transferred to the other grid nodes in the nearby region.

In order to include the measurements in the short term forecasts, a new method based on ensemble forecasts is developed. Therefore, measurements at transformer station with only wind or PV feed-in should be used to weight the ensemble member according to the best fitting member for the last hours. These weights are then used to create deterministic short time forecasts based on the weighted ensembles for the surrounding wind and PV plants. Thus, measurements of the last hours are used to create a local improved forecast for the region. After interpolation on the coordinates of the plants, the summation of all producer at each transformer is calculated with a matrix, based on meta data, provided by the DSO, which includes the relationship between power producers and busbars. In the special event of ring circuits, when a producer is assigned to two transformers, the matrix contains a weighting for both transformers based on the impedance of the power lines. Based on this wind and PV forecast a first guess forecast for the historical data is calculated for each transformer station. By subtracting the shortest forecast of these wind and PV forecasts from the historical measurements at the transformer, the residual load is calculated and used to train the model.

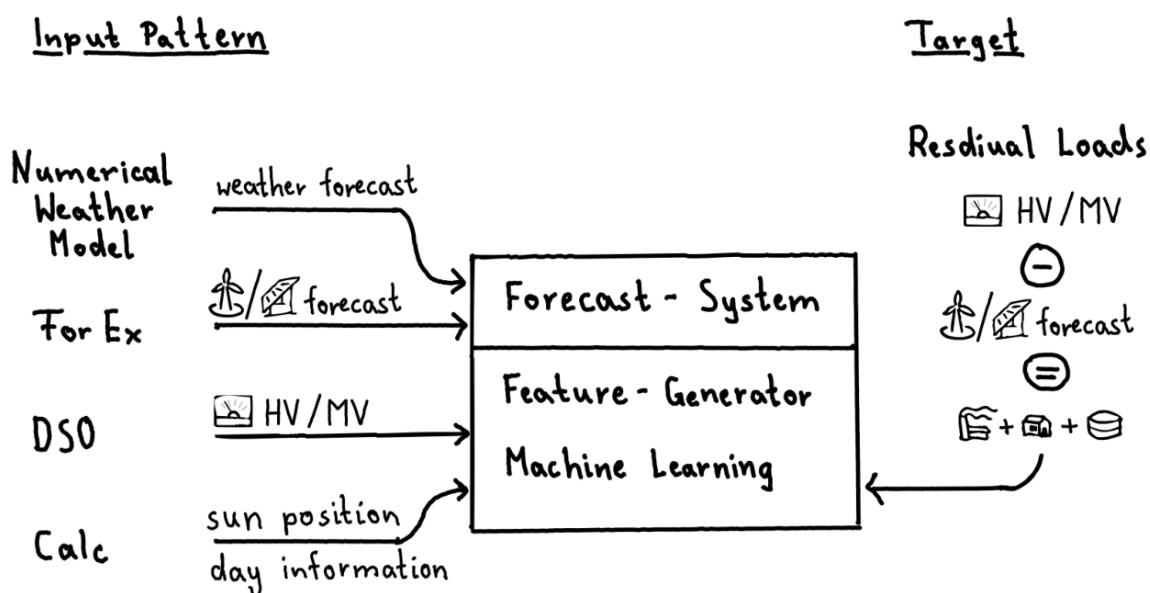


FIGURE 6 - TRAINING STEP OF THE LSTM ARTIFICIAL NETWORK

STATISTICAL APPROACH FOR THE RESIDUAL LOAD FORECASTS

For the residual load forecast, shown in Figure 6 and Figure 7, the Long Short-Term Memory (LSTM) [Hochreiter and Schmidhuber (1997)] as machine learning algorithm model is chosen, which is a special type of (recurrent) neural networks for the basic system. Recurrent neural networks [Rumelhart et al. (1986)] remember their past and are normally used for time series modelling.

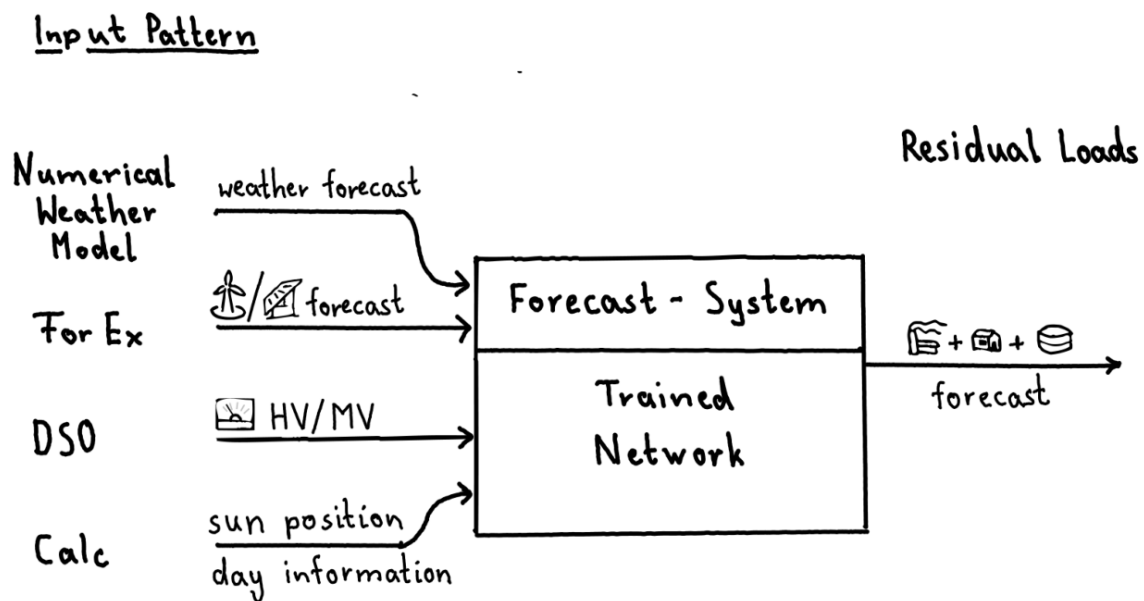


FIGURE 7 - LSTM IN OPERATIONAL MODE

Depending on the availability of input data three different cases are distinguished for the residual load forecast. The first one is the combination of two inputs, the weather forecasts on the one hand and on the other hand the last 24 hour measurements of the vertical power flow. Both other two strategies with just the weather forecasts or just the measurements as input can be used as a fall back or redundancy strategy, if either the weather forecasts or the measurements are not available. But for the baseline only the first approach is used, since only the models for this approach are already trained. If here some of the measurements are not available during the last 24 hours, first of all an interpolation method is chosen to keep the process running. For a deep neural network (DNN) the input data is usually separated into several batches which is done with a generator function. The used DNN model architecture can be seen in Figure 8. At the beginning, there are two input layers which describes the vertical power flow and the residual load respectively (input_1) on the one hand the weather forecasts (input_2). After the LSTM layers which use recurrent dropout and are concatenated with both inputs, two fully connected layers are used with a pending dropout layer. The usage of recurrent dropout and the additional dropout layer are used in order to prevent overfitting. And at last a fully connected output layer is used.

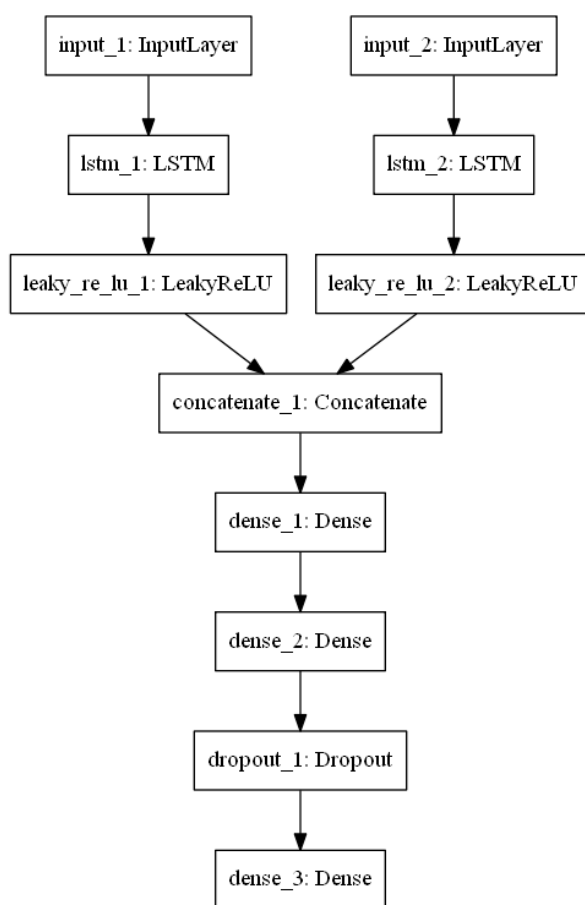


FIGURE 8 - LSTM MODEL ARCHITECTURE

As activation function the Leaky Rectified Linear Unit 'LeakyReLU' for the LSTM layer is applied which suited best the range of the input data and for the densely connected layers 'ReLU' (Rectified Linear Unit) is used.

For the optimization the 'Adam' optimizer with the loss metric of the mean absolute error (MAE) is used. For these hyper parameters some values are chosen partly from the paper 'LSTM: A Search Space Odyssey' [Greff et al. (2017)] and partly from experiences gained in different experiments connected to other projects. The results are additionally compared and verified with a hyper parameter optimization with an Automated Machine Learning (AutoML) approach investigated by Salz in the master theses 'Hyperparameter Tuning mit AutoML für Zeitreihenprognosen im Energiesektor' [Salz (2020)]. There it could be shown that the used hyper parameter are leading to similar results than the results from the AutoML approach.

There are still other ongoing investigations in several master thesis which deal with an AutoML architecture search to find the best model architecture which is an add-on to the hyper parameter optimization with AutoML and also with transfer learning. The transfer learning approach [Pan and Yang (2010)] is set-up, which should deal with the extreme changes in the characteristics of the transformer behaviour due to e.g. dynamic grid topologies, changes in the installed assets and maintenance at the transformers itself. This approach considers the influences of the horizontal power flow between several related transformers. The results from these master thesis should complete the model in combination with a regular update process in order to facilitate the modification of the grid topologies.

In the update process the previous trained model is retrained assuming that new measurements are available at least on a daily basis. This update process is generated every day to capture the most recent changes.

All these approaches are still investigated and it is not yet sure, if they will be added in the expansion stage to the baseline method for the demonstrator.

3.2.4 REALIZATION OF THE FORECAST SYSTEM

According to the functional splitting of the forecasts the realization will also be done in two separate software systems: one System for the wind and PV forecast, another for the residual loads.

First have a look at the data flows: In the operational model, the systems get meta data about the producers and the state of the grid for the mapping of the producer to transformer in regular base every few days as table dump from a database. This has to be processed to create current assignment matrices, as well as saved with change time to get a history for a later improvement of the models. The processing is done in a relational database with an additional toolbox for archiving the historical changes. The size of the meta data is limited and can be processed in under 30 seconds, which goes well with the schedule, because it can be processed in parallel to the main forecast processing.

A second data flow delivers the actual state of the grid concerning vertical loads at the medium/high voltage transformers as file in CIM format, which are needed for the intraday forecast. These CIM structured files have to be parsed to the systems. Originally the processing time was over 10 minutes, but could be reduced to half a minute to a minute (depending on file size) by using external libraries. This is still a relevant time factor and has to be considered.

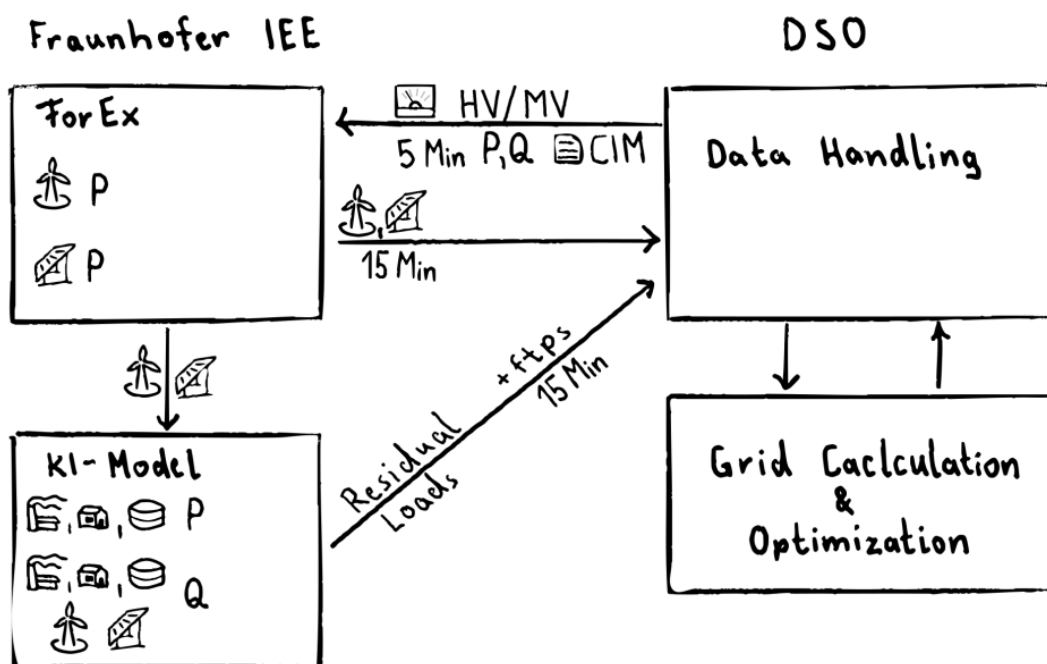


FIGURE 9: DATA FLOW BETWEEN DSO AND THE TWO FORECAST SYSTEMS (EXTERNAL DATA FROM THE WEATHER SERVICES IS NOT INCLUDED)

The actual wind/PV forecast is then calculated under MATLAB with the forecast framework ForEx (Forecast Experiments) of the Fraunhofer IEE. For the German demonstrator the forecast has to be done for 549 wind farms and 7364 solar plants. Regarding the demonstrator's process requirements the calculation time should not exceed two minutes. Therefore, processing is distributed among individual modules that are permanently available in the memory to avoid start-up times of the forecast. The orchestration is done by a central scheduler. In this way the calculation time could be reduced drastically to fulfil the requirements of being faster than two minutes.

Once the wind/PV forecast has been completed, it is transferred to Mitnetz(DSO) and to the load forecast system in parallel which is shown in Figure 9. This is done to the DSO internally via ftps due to security reasons.

The prediction is then used to determine the residual from the measured power at the transformer, so that the residual load model can use it as an input. The load forecast is set up under Python. After completing this forecast, it will also be transferred to Mitnetz, where the optimization process is then started.

3.3 FORECASTING RESULTS

Since the realization of the forecast into the demonstrator is still in progress and will be discussed in the deliverable D6.7, results are only presented for the vertical power flow forecast as a pre step of the residual load forecast. This means that we do not differentiate between generation and load yet, but use the measurements at the MV/HV stations to train the LSTM based models. The data preparation, usage and the evaluation of these models are following the same steps as for the residual load forecast models except that for this the wind and PV

generation is subtracted beforehand. In this context the now evaluated vertical power flow forecasts give a good overview of how the range of the forecast quality can be expected for the residual load forecast.

So far 585 vertical power flow models were generated and are used for developing the forecasting system. These models are also used for investigations in work package 5.3 in subtask C.3. The objective in T5.3 C.3 are optimized processes due to the topic of massive data flows for the forecasting system. Thus, the processing time for the online evaluation of one forecast point and 48 hours lead time with an increasing number of models from one to 10,000 are investigated in three different settings (Hadoop cluster, CPU server and GPU Server). Since there are 1,415 models to be calculated for P and for Q in T6.2, the focus is to evaluate around 3,000 models simultaneously in an appropriate time of under at least 10 minutes with loading and saving of the input and output data and the models. The specification of less than 10 minutes comes from the fact that a maximum of 15 minutes are available for the delivery of the forecasts to the demonstrator.

In addition to the investigations for work package 5.3 which are highly correlated with the constraints of the forecast system developed here in T6.2, the models were evaluated with historical data. The results for one transformer are shown as an example. Therefore the forecast quality of the vertical power flow forecast of one transformer station with historical data is evaluated in 3.3.1 and in a second step the performance of the demonstration system is evaluated with the total number of available vertical power flow models 3.3.2. Finally, in 3.3.3 it is explained how the forecasts of wind, PV and the residual load are used and are embedded in the demonstrator.

3.3.1 FORECASTING QUALITY BASED ON HISTORICAL DATA

For the evaluation of the vertical power flow forecast models historical data from 2016 to 2018 is available. Data from the year 2019 are currently being processed and will be used for retraining the models. The historical data is split into training data with 85%, validation data with 6.5% and test data with 8.5%. The splitting takes place for exact dates like the 1st of January 2018, the 1st of March 2018 and till the end of the available data with the focus on getting the most possible training data set. Each transformer has its own reference number which is mapped to a coordinate in order to get the according weather forecast parameter.

The historical weather data has a time resolution of three hours and needs therefore to be interpolated to 15 minute values. This is done with linear interpolation.

As in 3.2.2 described the input data consists of the weather forecast parameters like temperature, wind speed, solar radiation, but also day information and the vertical power flow measurements. These inputs scale differently, so that a normalization to similar scales for training a neural network is necessary in general. For this normalization the data is subtracted by its mean and then divided by its standard deviation, both calculated from the training dataset, i.e.

$$x_{scaled} = \frac{x - \bar{x}}{\sigma}, \quad (1)$$

where x is the original value, \bar{x} the mean and σ is the standard deviation. To fully pre-process the input data for the calculation of the deep neural network models the data is allocated into batches. The chosen model hyper parameters are listed in the following Table 1.

TABLE 1 - LISTING OF THE HYPER PARAMETER AND THEIR VALUES USED FOR THE DNN

| Model Hyper Parameter | Number |
|------------------------------|--------|
| Number neurons LSTM layer | 100 |
| Number neurons dense layer 1 | 500 |
| Number neurons dense layer 2 | 500 |
| Recurrent dropout | 0.5 |
| Dropout | 0.5 |
| Batch size | 192 |
| Number epochs | 40 |
| Steps per epoch | 50 |

For the training procedure the validation dataset is evaluated through 40 epochs and the best weights which are achieved by using the 'EarlyStopping' and 'ModelCheckpoint' callback functions of the Python Keras library are saved. The test data is then processed similar to the training data and is used for the evaluation part. For the evaluation and the calculation of the metrics the forecast values needs to be inverted back to absolute values and then to be re-normalized to values between 0 and 1. The normalization of the absolute forecast values to values between 0 and 1 for the calculation of the metrics is done with the scaling defined in equation (2),

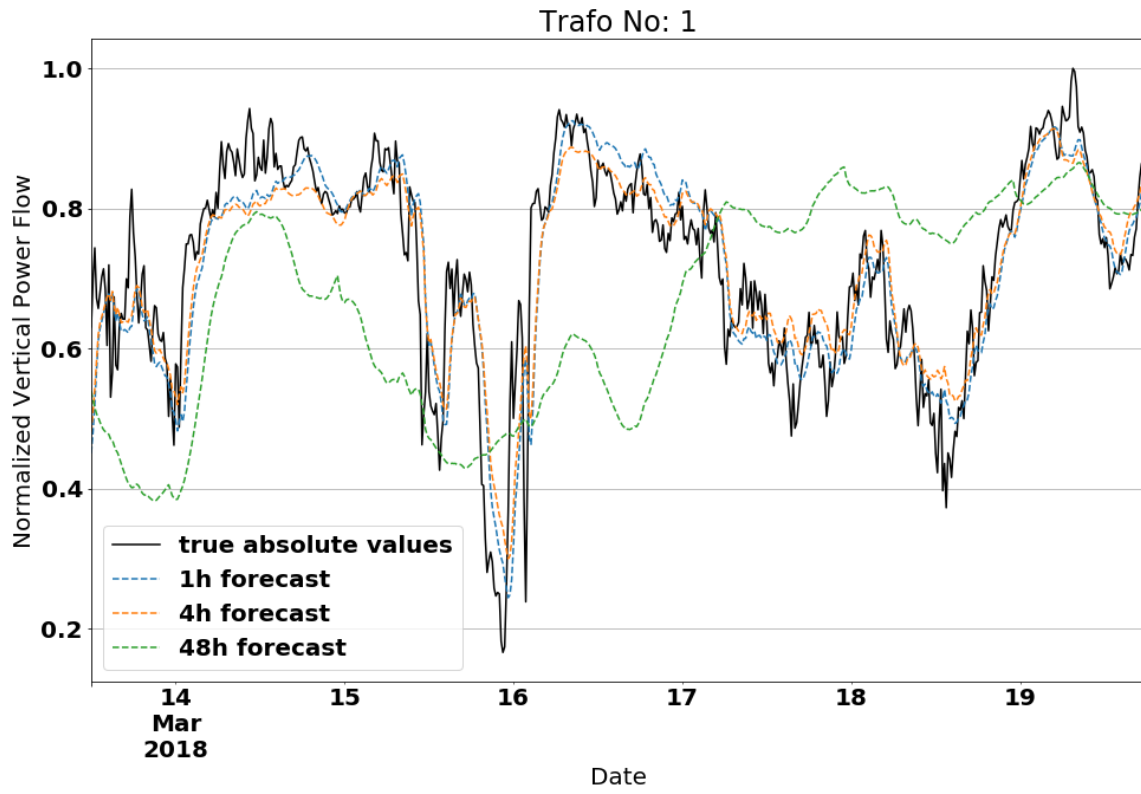


FIGURE 10 - COMPARISON OF MEASUREMENT AND FORECAST TIME SERIES WITH THREE DIFFERENT FORECAST HORIZON (1 HOURS, 4 HOURS AND 48 HOURS)

$$x_{scaled} = \frac{x - Q_{0.03}(x)}{Q_{99.7}(x) - Q_{0.03}(x)} \quad (2)$$

where x is the original value and x_{scaled} is the normalized value. For prevention of using outliers for the maximum and minimum values of x , the quantile values of the 99.7% quantile ($Q_{99.7}$) and the 0.03% quantile ($Q_{0.03}$) respectively are used instead as maximum and minimum.

In Figure 10 the time series of the measurements' absolute true values are plotted against the predicted absolute values with three different forecast horizons. The time frame is about 6 days, which are cut out exemplarily from the entire test data set. The comparison shows that the shorter two forecast horizon with 1 and 4 hours respectively have a high correlation of about 85% and 84% respectively to the true measurement values. For the 48 hours forecast horizon the correlation of about 18% is very low which also can be seen in Figure 11 and in Figure 12. In Figure 11 three different metrics are estimated and shown as a bar plot. It can be seen that for all forecast horizon the root mean squared error (RMSE) and mean absolute error (MAE) seem to have a relatively good result. As expected, the RMSE and MAE results increase with increasing lead time and

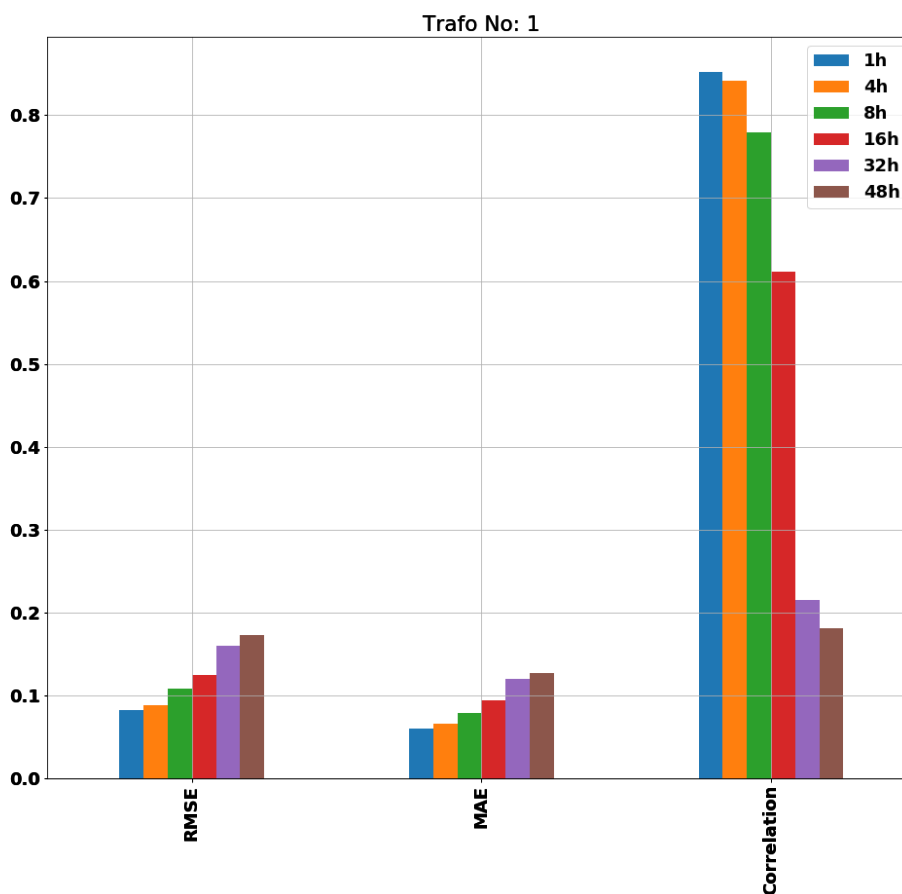


FIGURE 11 - METRICS BAR PLOT WITH NORMALIZED RMSE, MAE AND CORRELATION FOR SIX CHOSEN FORECAST HORIZON FOR TRANSFORMER 1. THE FORECAST HORIZON INCREASES FROM LEFT TO RIGHT FOR EACH METRICS.

the correlation values decrease. For the RMSE all values are below 18% and for the MAE below 13% for the vertical power flow forecast of transformer number 1. But the correlation of the last two forecast horizon of 32 and 48 hours ahead do not yield such good results which could already be seen in Figure 10 for the forecast horizon of 48 hours. Another method to analyze the results is the usage of scatter plots like in Figure 12. Each forecast horizon also used in the bar plot in Figure 11 of 1h, 4h, 8h, 16h, 32h and 48h is plotted against the true vertical power flow measurement values of the test dataset. Additionally, a line for comparison shows the case if the model had learned the exact relationship between the explanatory variables and the vertical power flow measurements. The size of the spread of all data points corresponds to the quality measure, the larger the spread, the worse the quality. As expected, it can be seen that the larger the forecast horizon the worse the quality gets. For both axes, showing the measurement true values and the forecast values of the specific forecast horizon respectively, a histogram is also appended where the corresponding distribution gives an overview of how many points are overlapped.

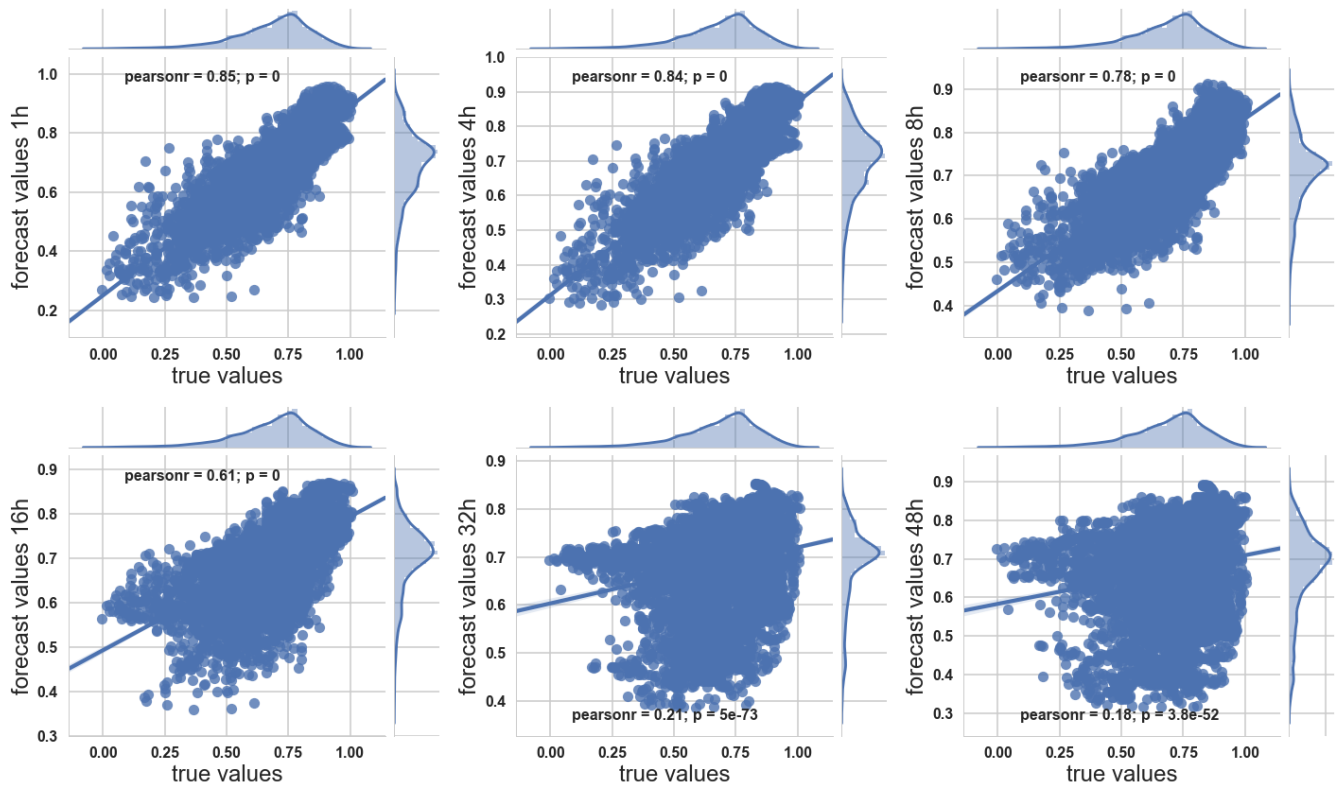


FIGURE 12 - SCATTER PLOTS FOR SIX DIFFERENT FORECAST HORIZON (1H, 4H, 8H, 16H, 32H, 48H) FOR TRANSFORMER 1. THE TRUE MEASUREMENT VALUES ARE PLOTTED AGAINST THE FORECAST VALUES. THE LEFT UPPER FIGURE SHOWS THE RESULT FOR THE COMPARISON WITH LOWEST LEAD TIME OF 1 HOUR. THE LEAD TIME INCREASES FROM THE UPPER FIGURES TO THE LOWER FIGURES FROM LEFT TO RIGHT. THE HIGHEST LEAD TIME OF 48 HOUR AND ITS COMPARISON IS THEN SHOWN IN THE LOWER RIGHT FIGURE.

OVERVIEW OVER ALL FORECAST RESULTS

For the evaluation of all forecast results from all available transformer models, the above used metrics, i.e. MAE, RMSE and correlation from these transformers are used and displayed in box plot diagrams. The box plot is chosen in order to get a better understanding of the error distribution instead of just using the overall mean value. In Figure 13 the box plot of MAE is shown. The 24 hour horizon is added to test the thesis that in the data a daily seasonal effect occurs. Thus, the model does not yet seem to be optimized well enough, as the input of the information of the day is not yet properly processed. This effect can also be seen in the Figure 14 and Figure 15. This needs further investigation and a fine tuning of the models. The results of this fine tuning will be shown in the deliverable D6.7. What also can be seen in these figures is that for the forecast horizon of one and four hours the quality over all forecast is still good, especially for the one hour horizon where the distribution is very close together. Here 75% of all forecasts with an one hour horizon have a MAE below 7.5%, a RMSE below 12% and simultaneously only 25% of all these forecasts have a correlation lower than 84%. The higher the forecast horizon, the worse gets the forecast quality. The MAE and RMSE get higher and the correlation gets lower, except for the already discussed forecast horizon of 24 and 48 hours. For these two forecast horizon it also stands out that the median is not exactly in the middle. Thus, 50% of all forecast results have a MAE lower than 8%, a RMSE lower than 14% and a correlation higher than 79% for the 24 hour horizon which is similar to the discussed results of the one hour forecast horizon for the 75% quantile.

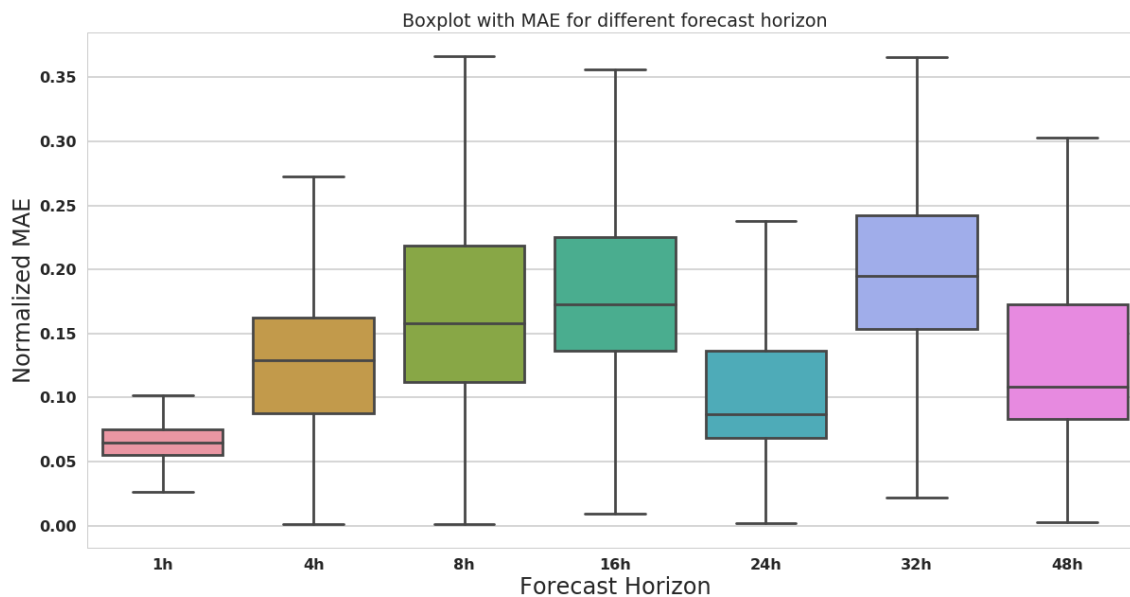


FIGURE 13 - BOX PLOT FOR THE NORMALIZED MAE OVER ALL TRANSFORMER FORECASTS AND FOR 7 DIFFERENT FORECAST HORIZON

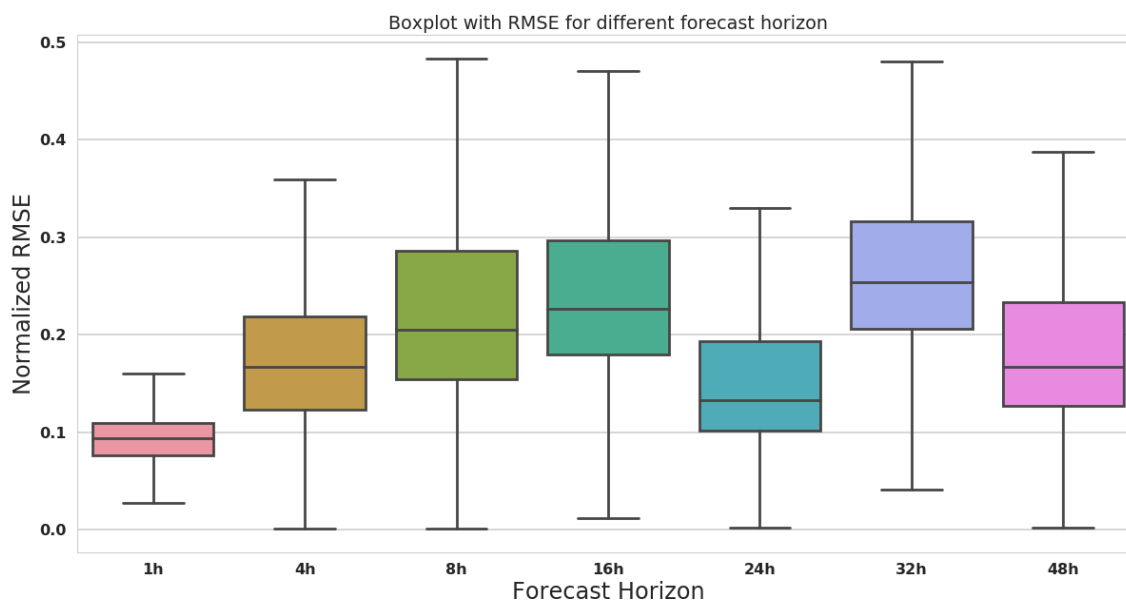


FIGURE 14 - BOX PLOT FOR THE NORMALIZED RMSE OVER ALL TRANSFORMER FORECASTS AND FOR 7 DIFFERENT FORECAST HORIZON

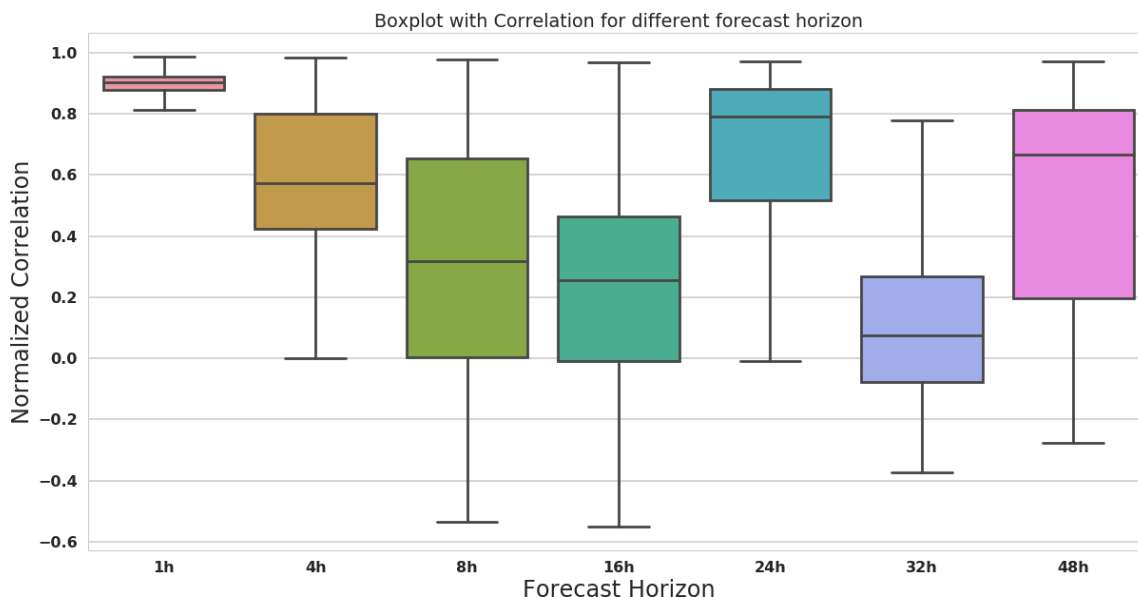


FIGURE 15 - BOX PLOT FOR THE NORMALIZED CORRELATION OVER ALL TRANSFORMER FORECASTS AND FOR 7 DIFFERENT FORECAST HORIZON

3.3.2 PERFORMANCE OF THE DEMONSTRATION SYSTEM

Until a few years ago, forecasts were only required for individual portfolios or entire control zones. This has changed in recent years, as not only transmission system operators but alsoas well as distribution system operators need forecasts for all substations in order to get a better overview of their network. The number of substations of the transmission grid is in the order of hundrets. In this project, forecasts are calculated for the substations of the distribution system operators of the high voltage level. For the distribution grid about ten times more forecasts have to be calculated, i.e. a total number in the order of thousand. The requirements for a high-performance calculation of the forecasts are correspondingly high. The measurement data required for the forecast are processed in just under a minute. The wind and PV power forecasts are also calculated in under two minutes. In a next step, the forecasts of the residual load are produced. In total, the entire process takes less than 15 minutes until the forecasts are delivered to the user. The exact time is not yet measured, due to the fact that the development of all components and their combination to a full system described above including reading the input measurements, building the wind and PV forecasts, building the residual load forecast and saving the results in a specified csv format has not yet reach its final step. The bottleneck of the forecasts mainly consists in the sequential processing of the data preparation and the renewable energy forecasts followed by the forecast of the residual load. Another bottleneck is the loading and evaluation of the Keras residual load models which should be done more efficient, e.g. with caching in the future. Below are the results for the evaluation of 1,000 and 3,000 models of the experiments of work package 5.3 C.3 (Figure 16).

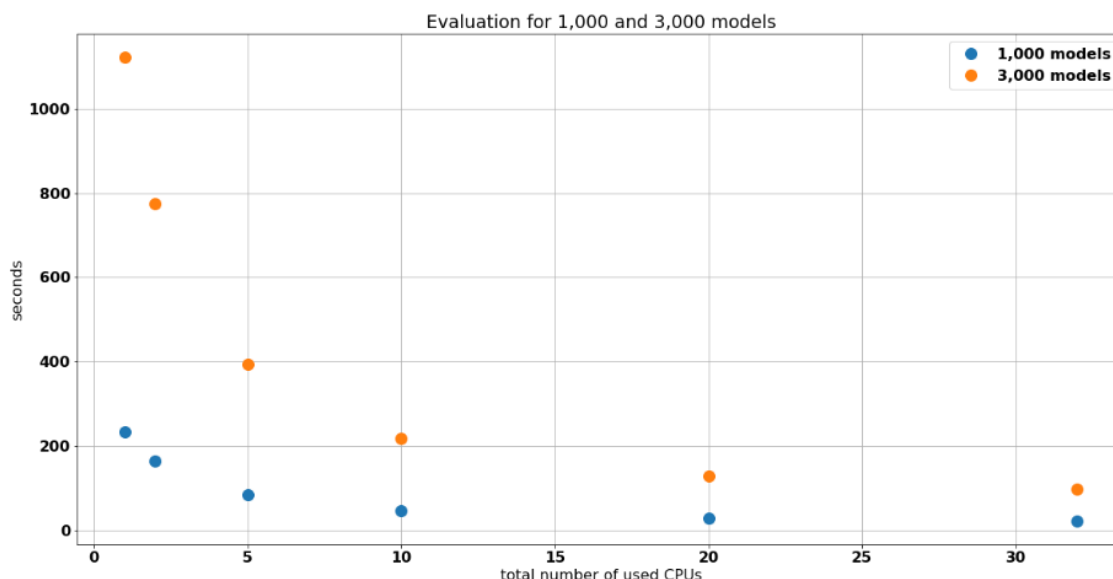


FIGURE 16 - EVALUATION OF THE PROCESSING TIME FOR 1,000 AND 3,000 MODELS. THE MEAN DURATION FOR FORECASTING 48H AHEAD FOR ONE TIME STEP FOR 1,000 AND 3,000 MODELS IN SECONDS IS PLOTTED OVER THE NUMBER OF USED CPU'S.

These experiments are evaluated for the following number of models: 1, 10, 100, 585, 1.000, 3.000 and 10.000. In Figure 16 only the results from the experiments which have a number of models corresponding to the real number of about 1415 available transformers are shown. Since not only the forecast of the active power but also the forecast of the reactive power is needed, twice the number of models needs to be considered. Thus, the results for 1,000 and for 3,000 respectively are shown. Each experiment was made on a server with a maximum number of 32 Central Processing Units (CPUs). In order to see how the processing time for the mentioned number of models changes by using a different number of CPUs, experiments were made for 1, 2, 5, 10, 20 and 32 CPUs. Additionally, each experiment was evaluated 10 times in order to better verify the results and then the mean value was calculated. For the delivery of the residual load forecast the deployment will take place on a server of about 5 CPUs. With the focus on these 5 CPUs a processing time for 1,000 models will be around 1.4 minutes and for 3,000 models around 6.6 minutes which can be seen in Figure 16.

3.3.3 APPLICATIONS

Since one of the main foci of the German Demonstrator lies on determination of PQ-flexibility bands, forecast is utilized in order to create predicted grid states for the next 72 hours. From the forecast, aggregated P and Q values for all HV/MV substations in the high voltage grid of MITNETZ Strom are available. The timely resolution of this data will be at least 1 hour and can go down to 15 minutes. The grid states for the upcoming 4 – 6 hours will be computed on the finer resolution and from 6 – 72 hours on, a resolution of 1 hour may be enough. But this is to evaluate during the field test. The forecast values for P and Q can be assigned to the related substations and with this knowledge a complete determined system of power flow equations can be solved via a simple power flow calculation. The results are predicted grid states which correlate with the forecast data. On these grid models

for each time step in the future, optimization methods are applied and PQ-flexibility bands are determined. Based on these bands, TSO and DSO can adjust their operational strategies and decisions.

3.4 PRELIMINARY CONCLUSION

In this chapter a baseline forecast for the German demonstrator is described. The forecast system consists of two approaches, the physical modelling for the wind and PV forecasts and the machine learning approach by using a LSTM in a deep neural network architecture for the residual load forecast. Both approaches are used in order to achieve the objectives at hand by taking into account the existing grid conditions in the medium voltage grid in the best possible way. One of the greater challenges is the usage of the vertical power flow measurement values as input for the short-term forecasts whose outputs are only subsets of the original vertical power flow. For example, the vertical power flow measurement needs to be adapted as input for the short-term residual load forecast. The wind and PV forecasts are subtracted from the vertical power flow and can only then be used as input. Analysis of the system and the final deployment steps are still in progress so that a final evaluation is yet to be done in Deliverable 6.7. Thus, the performance time of the whole forecast process could not yet be determined in detail. First results for the vertical power flow forecast for one transformer are shown in more detail and an overview of the results for all transformer is given. Forecasts with a shorter forecast horizon of up to 4 hours perform well, especially for the forecast horizon up to one hour. This could be shown especially by the narrow distributions in the box plots for all transformer results for the one-hour horizon. Here 75% of the MAE values for all transformer forecasts are lower than 7.5%, lower than 12% for the RMSE and simultaneously only 25% of all Correlation values are below 84%. But the results also show that there is still some investigation needed. The forecast quality of the 24 and 48 hour forecast horizons increase against e.g. the 16 and 32 hour forecast horizons which indicates that there is still a daily seasonality in the data, which is not yet sufficiently well represented by the models. The result of these evaluations and the addition of wind and PV forecasts are finally shown in Deliverable D6.7. For the residual load forecast backup strategies for redundancy tasks are developed, where a forecast at each time step of 15 minutes can be guaranteed. But due to the long forecast horizon and the high update cycle of about 15 minutes, the very need of such fall-back strategies is yet to be defined.

4 FORECASTING OF POWER AND LOAD FOR THE ITALIAN DEMONSTRATOR

4.1 INTRODUCTION

The forecast tool implemented in the Italian Demonstration is called MAGO (Monitoring and control of Active distribution Grid Operation) and is a web-based application oriented to the real-time monitoring and estimation of distributed generation in the distribution network managed by e-distribuzione.

The forecast tool is arranged in the SCADA owned by e-distribuzione and is based on an algorithm developed by University of Siena. The related technical requirements and developments about the web application based tool and SCADA integration are also included in Baldi et al. (2012) and Mistesi et al. (2011).

By monitoring the characteristics parameters of DERs, it is able to provide the forecast of generated Active Power.

4.1.1 NEED FOR A FORECAST

In the past, the Italian electrical system was defined by assuming that a mono-directional power flow comes from the transmission network. In this scenario, all the customers in the distribution network are represented by passive loads which can be represented by a load diagram in terms of shape and value. Indeed, during the years was determined, by means gathering of data of consumption and dedicated measuring campaign, the typical diagram for different kinds of customers, organized in clusters: voltage level, residential, commercial and so on. Taking into account the huge penetration of distributed generation (DG) from 2005, the need to change the paradigm became clear, assuming new criteria for planning and operation of distribution system, developing new tools to reach this new frontier.

Distributed generation, in particular the Generation from Renewable sources, is characterized by a stochastic behaviour, depending on the variability of primary source. In this context, the new instrument to support the DSO in the operational activities should have had a robust generation's forecast algorithm as primary engine. A forecasting tool makes it possible to estimate the generation level in the real-time and, two or three days ahead, it allows to the network operator to guarantee the right level of security of the grid, in terms of efficiency of monitoring and control. The knowledge of level of generated power provided by the forecast tool allows: to continue to estimate and make the load flow of system in a good way; to manage the organization of scheme, having a good cognition about the amount of power flowing to the HV/MV substation as well as to the feeders and all section of network, due to the contribution of generations and consumptions of customer at MV and LV level.

In this scenario, all the customers in the distribution network are represented by passive loads which cannot be controlled according to the regulatory framework; on the contrary, in a centralized scenario, it is possible to control the generators which are connected to the transmission network, among other things for balancing operations.

Thanks to Finance Acts approved by the Italian Parliament between 2007 and 2012 [Gazzetta Ufficiale della Repubblica Italiana], state funding and incentives were granted exclusively for the production of electricity produced from renewable energy sources. For this reason, there was an increasing of small size generation plants, called Distributed Generation (DG), in the medium and low voltage network. This kind of resources are not

programmable because the owner of this kind of plant can decide autonomously to produce or not energy and also because the energy generate can be affected by the weather. This determines a new decentralized scenario with a multi-directional power flow, in which passive loads absorb and a new category of active loads inject energy in the electrical network.

This multi-directional power flow causes bottlenecks and back feeding phenomena which can be faced by performing advanced regulation techniques and forecasting day by day the renewable resources (in particular PV plants) production through weather forecast.

4.1.2 INNOVATION OF THE FORECAST COMPARED TO EXISTING ONES

In comparison to the developments pursued within the Grid4EU project and which will be applied within the EU-SysFlex project, a new *aggregation for observability* functionality has been developed.

Its main purpose is to provide, for each HV/MV transformer of the Primary substation, the active power and reactive power values of PV generators, loads and other sources, by updating them every 20 seconds.

The Local SCADA aggregates the available data by exploiting many inputs data:

- Measurements from the field sent by the Energy Regulation Interfaces installed at the plants' premises (with a time resolution of 10s, 600s and 10min);
- Measurements from meters of MV generators (with a time resolution of 15min);
- Weather data collected for the calculation of the forecast (Nowcast) of the generation from solar sources;
- Weather forecast data for the calculation of the generation forecast from solar sources.

Aggregated data about loads and losses are obtained as difference between the active power measured on the secondary windings of the transformers and the estimation of the overall generation (photovoltaic + other sources).

All these estimated data are related to the real structure of the MV network fed by each MV busbar of a primary substation.

Data are sent to the TSO every 20 seconds.

More in detail, this functionality includes the Nowcast algorithm, which performs an estimation of production from solar sources with a 20 seconds cycle. Also the accuracy of the estimation of Nowcast is evaluated by means of a KPI calculation, based on the measurements acquired by meters installed on the MV PV plants.

4.2 DESCRIPTION OF THE FORECASTING PROCESS

As stated in the Introduction, the objective of MAGO consists of determining forecast of Active Power generated by renewable resources, by means of weather forecast.

4.2.1 CONCEPT OF THE FORECASTING SYSTEM

The forecast tool developed by e-distribuzione allows the estimation of:

- generation level for MV and LV producers, aggregated for substation (point of connection for MV producers, MV/LV transformer for V producers), considering the historical data measurement and weather information

The distributed generators are divided into two main families:

- RES which are not dependent on weather variables;
- RES working in best conditions (e.g. PV plants working in case of “clear sky”).

All measurement used to forecast the generation level are collected each 24 hours. The forecast provided by the tool is 72 hours ahead.

Figure 17 shows the three-time intervals used within the forecast tool. The update cycle is the time interval beyond which the algorithm is updated; the lead time can be almost equal to 72h and indicates the depth of forecast; the timestep is the time interval between each sample of the forecast curve.

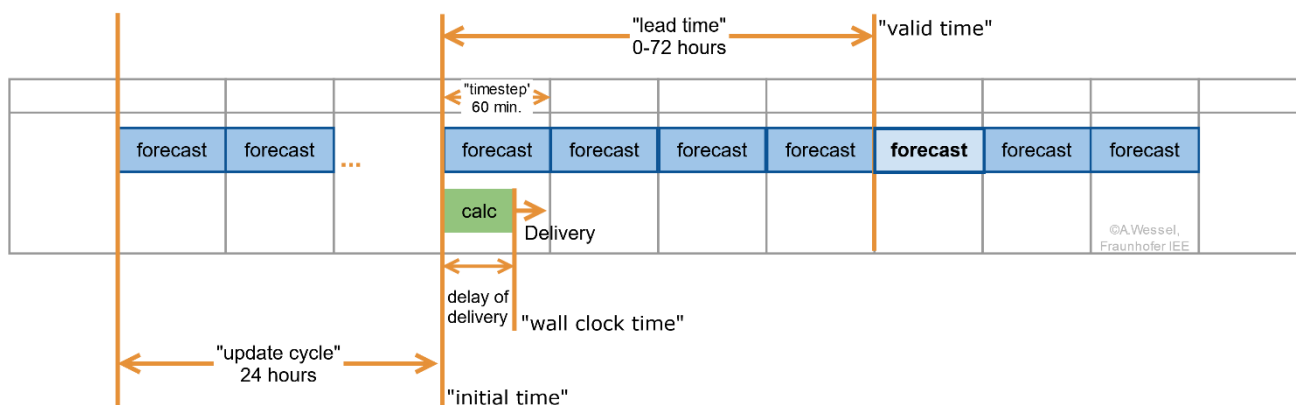


FIGURE 17 - SCHEDULE OF THE POWER FORECAST

4.2.2 INITIAL DATA: MEASUREMENTS, WEATHER FORECASTS AND META DATA

As defined in the first System Use Cases *IT NT SE – Perform Network State Estimation for the Italian Demo* described in *D6.1 – Demonstrators system use cases description*, the generation forecast information of loads and generations are sent to the local SCADA in order to trigger the state estimation and the optimization algorithms.

The forecast tool produces the forecasted information considering the measurements of installed power (PI) and the generated active power (PAG) of each plant, taking into account the primary source, even if, for pure

producers, it is possible to consider the exchanged active power (PAS); furthermore, the weather variables (including irradiation, environmental temperature and wind speed) are considered.

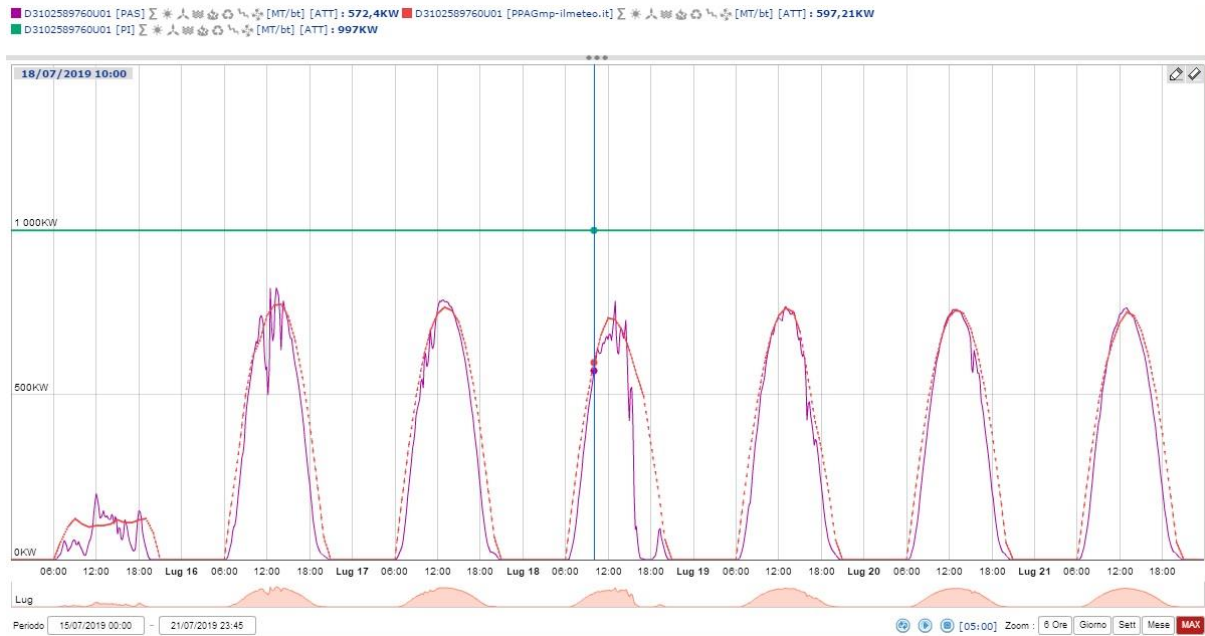


FIGURE 18 - DIAGRAM OF PV GENERATION FORECAST.

Figure 18 shows a report from the used forecast tool, in which the forecast and the real production during a week in July 2019 are compared. By performing this ex post analysis, it is possible to observe similarities and differences between PAG and PAS profiles.

Forecast results can be then evaluated according to the methods explained in Forecasting Results.

4.2.3 ALGORITHMS AND MODELLING

As described in D6.4, the adopted method for the forecast of solar energy is based on the PVUSA [Dows and Gough (1995)] model for PV plant, in which the generated power is expressed as a function of irradiation and environmental temperature [Bianchini et al. (2013)], as shown in the equation (3) below:

$$P = aI + bI^2 + cIT \quad (3)$$

Where P is the Generated power, I is the irradiance, T is the environmental temperature and a, b and c are the model parameters.

In case of wind energy, as shown in the equation (4), the model of the generated active power is a function of the wind speed (V) and a, b, c, d, e and w are the model parameters [Giannitrapani et al. (2015)].

$$P(V) = b + (a - b) \left(1 + e^{\frac{V-c}{w}} \right)^d \quad (4)$$

The algorithm is launched every 24 hours with a time horizon of 72 hours, with a time step of 60 minutes due to the availability of weather forecast by providers.

The algorithm can be affected by an error due to the unavailability of weather variables or plants characteristics and to a delay of the incoming measurements in Initial Data section.

In case of thermal power plant, like biomass, or gas power plant, forecast tool does not foresee any algorithm. In this case for every not renewable power plant is considered the generation level measured at the same day in the last year.

At the end, for the hydroelectric power plant is adopted a same criterion of forecast used for conventional distributed generators.

4.2.4 REALIZATION OF THE FORECAST SYSTEM

The forecast system of the Italian demonstrator can provide the level of generation related to the generators connected to the distribution network. The current development activities are aimed at enabling the exchange of information between the TSO and e-distribuzione (DSO) in real time. The data that will be exchanged are:

- Active and reactive power throughout the HV/MV transformer;
- Estimation of the active power injected into the MV network by generators directly connected to the MV distribution grid;
- Estimation of the active power injected into the MV network by LV generators directly connected to the LV network;
- Total amount of the active and reactive power absorbed by MV customers directly connected to the MV network.

Relevant data related to the power generated and installed on the distribution network connected to every HV/MV transformer are available in a cluster, organized according their types (producers/prosumers - i.e. producers and consumers at the same time) and different primary sources (PV, wind, hydro, thermal and others). These data are updated in real time according to the actual grid configuration and to the measurements acquired directly by the meters. Thanks to all these shared data, the TSO could be able to correctly evaluate the level of security of the power system and the needed reserve.

THE NOWCAST ESTIMATION ALGORITHM

The algorithm works on MV generators that are not equipped with the Energy Regulation Interface and on all LV generators behind to the MV/LV transformers. It retrieves the estimated real-time values of P and Q.

It receives the following data as input:

- Power master data of all generators of the MV network;
- Real-time weather data (temperature and solar irradiation);
- Near-real-time data from the generation meters of power sources different from PV (P and Q);
- Periodic data from PV plants meters (P and Q).

Generation from photovoltaic power plants acquires weather data regarding solar radiation with "near real time" frequency; generation from other sources considers of "real time" recordings (every 15 minutes) of P and Q from the related meters.

In particular, for all the MV producers where Energy Regulation Interfaces or meters are not installed and for all the LV generators in general, it is assumed that the power factor production is equal to one (zero exchange of reactive power with the grid).

NOWCAST OF GENERATION

The Nowcast functionality is included in the Local SCADA.

For the solar sources, the application receives weather data from a weather provider or from weather stations with "near real time" frequency.

There could be multiple data sources related to a subset of MV producers and MV/LV transformers.

The application uses this data to run the generation forecasting algorithm for all the MV producers from solar sources and to MV/LV transformers with photovoltaic generation.

For all the MV generators which are not PV generators, MAGO receives data from meters as input with "near real time" frequency. It exploits the acquired generation data as "Nowcast" until a new acquisition is done. When this flow is not active, the "Nowcast" coincides with the forecast currently calculated with the weather data updated every 24 hours.

The Local SCADA, through MAGO, calculates the "Nowcast" data for all MV production plants and MV/LV transformers. These values are stored in the Real Time Database of the central SCADA in order to be sent to the operator workstations and to the TSO in an aggregate form (including the entire MV network behind the secondary/tertiary branch of the HV/MV Transformer).

The local SCADA, through the Remote Terminal Unit installed in the Primary Substation, acquires the active and reactive power data related to the MV generation plants equipped with Energy Regulation Interface.

The aggregated values of active (P) and reactive (Q) power are calculated every 20 seconds by considering the generation from multiple sources (PV plants on one side and others on the other) and the loads connected to every branch of secondary/tertiary of the HV/MV transformer on which the functionality of observability is available and activated. After the calculation, these aggregated values are saved into the Real Time Database of the DSO central system and then sent to the TSO central system, together with all the other measurements related to the primary substation.

The aggregated data are composed of data estimated by MAGO and data sent by Energy Regulation Interfaces at the MV generator (where installed).

In case of failure in updating the aggregated data to be transmitted to the TSO, it is expected that a null value "invalid" is sent, as required by the TSO central system. There is also the possibility for the TSO to activate/deactivate the delivery of aggregations for observability.

4.3 FORECASTING RESULTS

Forecast performances are evaluated considering a set of parameters, which are calculated after the algorithm generates the forecast results.

A set of samples N is considered, the first parameter is the mean absolute error (MAE), which is the PV forecast quality and consists of the mean absolute error (evaluated with the expression (5)) of PV plants expressed in kW between the exchanged power PAS and the forecast of generated power based on weather forecast ($PPAG_{mp}$).

$$MAE = \frac{1}{N} \sum_{i=1}^N |PAS(i) - PPAG_{mp}(i)| \quad (5)$$

This index does not take into account the ageing phenomena of power plant, depending on any primary source, or the unavailability of generating modules, for instance for planned or not maintenance interventions.

Considering a solar power plant, during the central part of the day (from 8 to 15 o'clock) when there is the maximum level of generation, the more the forecast has optimal performances the more its MAE is near to zero.

The part of generation diagram where MAE is representative is on the border, where the generation level is very low. In that case, measurements and forecast are similar.

The normalized mean absolute error of PV plants could be evaluated using the expression (6) by dividing the MAE for the nominal power of the plant, obtaining the NMAE.

$$NMAE = \frac{MAE}{P_{nom}} \quad (6)$$

This error could be also evaluated, using the expression (7), by dividing for the measurements of the generated active power PAS .

$$NMAE_2 = \frac{1}{N} \sum_{i=1}^N \frac{|PAS(i) - PPAG_{mp}(i)|}{PAS(i)} \quad (7)$$

The graphs included below show the trend of the KPIs evaluated for one of the four remote controlled PV plant of the demonstrator in two different weeks of the year.

Figure 19 and Figure 20 show respectively each index referred to the summer period 2019; Figure 21 and Figure 22 are related to the winter period 2020.

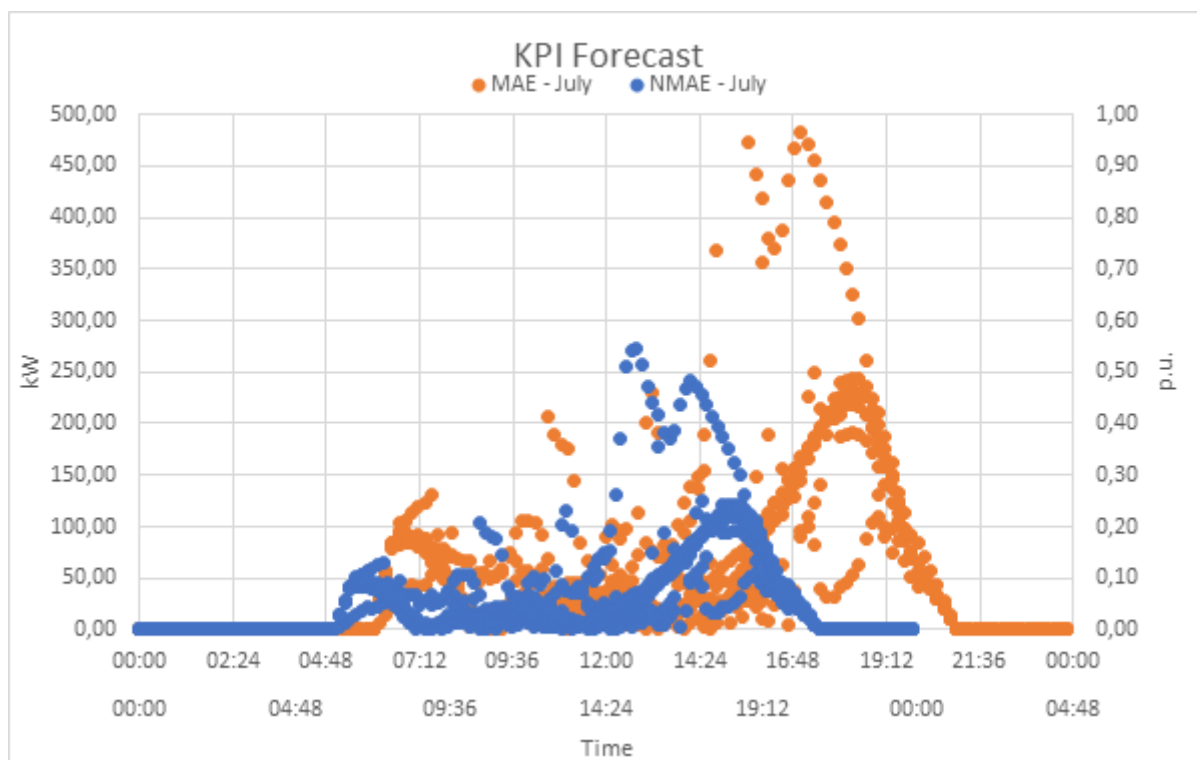


FIGURE 19 - MAE AND NMAE RELATED TO SUMMER PERIOD

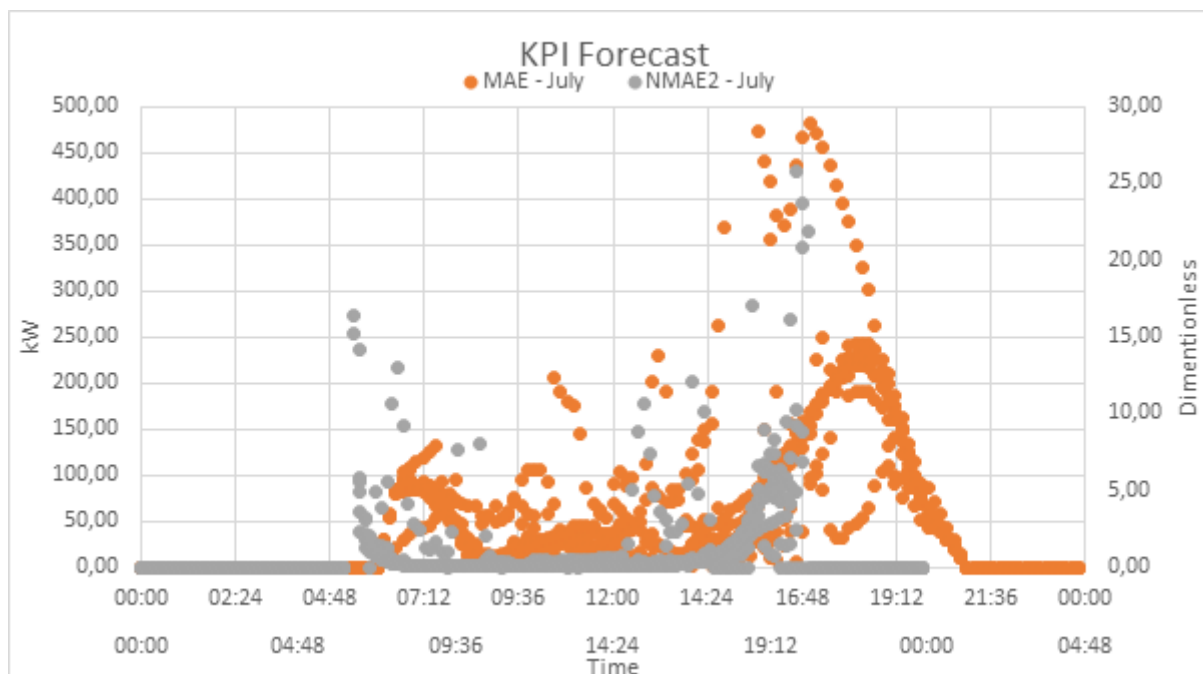


FIGURE 20 - MAE AND NMAE₂ RELATED TO SUMMER PERIOD

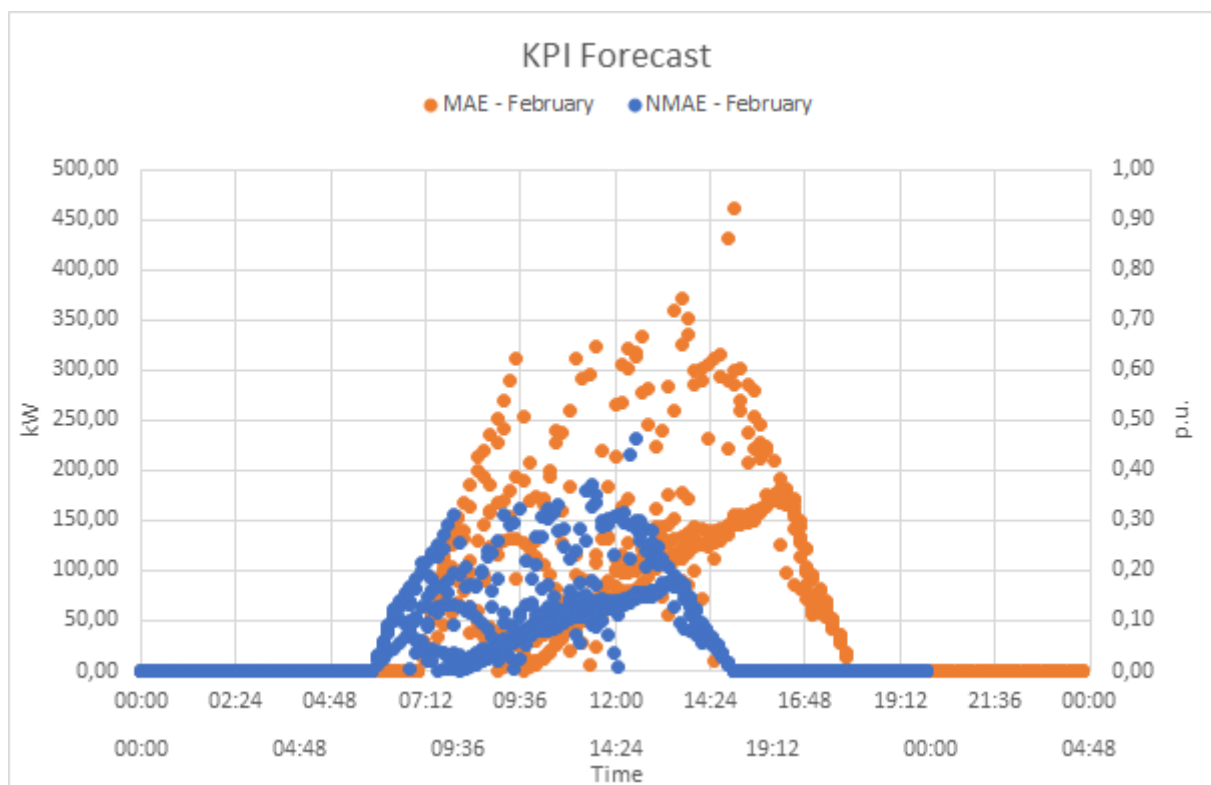


FIGURE 21 - MAE AND NMAE RELATED TO WINTER PERIOD

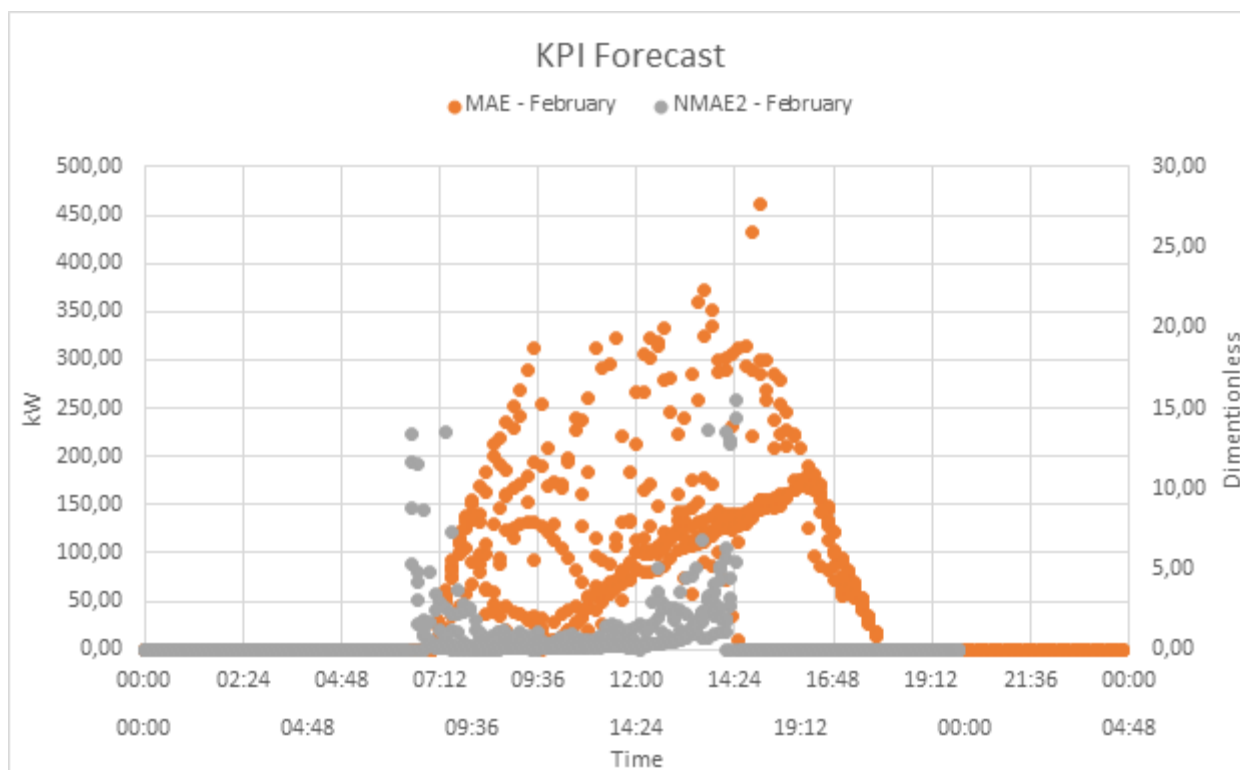


FIGURE 22 - MAE AND NMAE₂ RELATED TO WINTER PERIOD

It is possible to see how the forecast algorithms can estimate, with satisfactory results, the level of generation for every single power plant (PV, in this specific example) during the period of day characterized by the maximum of power injection. The deviation between each estimation sample and the corresponding measurement is due mainly to the time width of the sample itself. More in detail, the measurement system calculates the average value of the active power exchanged by the power plant each 10 minutes. In this timeframe the estimation algorithm, based on the weather forecast for the same time period, assumes the level of power injection as constant and, consequently, the level of generation is assumed as fixed for the same period of 10 minutes. On the contrary, the measurements are based on elementary samples computed in accordance with the EN 61000-4-30 (international standard for the metering devices). The meter computes an average value for each minute first and finally another average value of active power referred to the last 10 minutes. The generation level, for each single sample of 10 minutes can vary strongly and rapidly and every meter takes into consideration this.

Another phenomenon that it is important to consider is the aging phenomena of power plants. The implemented forecasting tool takes to provide an estimation of generation power for each power plant, considering the weather condition and characteristics of generating modules, assuming for them ever the same level of efficiency (steady performance). So, during the typical period of maximum level of producibility, it could be possible to do an over estimation of generation.

For this reason, MAE index is not very representative, if considered alone. The performances of the tool estimator have to be evaluated considering NMAE and $NMAE_2$ also. Indeed, with NMAE it is possible to normalize the deviation between generated power (measured and estimated) respect to rated power of power plant. This allow to know the real weight of MAE.

4.3.1 FORECASTING QUALITY BASED ON HISTORICAL DATA

Within the Italian Demonstration, forecast based on historical data is usually performed for the passive loads. The curves coming from meters are elaborated from e-distribuzione SCADAs and then categorized by considering the installed power and the customer class: these are respectively Residential, Agricultural, Industrial, Commercial and LV generation classes.

Figure 23, Figure 24 and Figure 25 show the clustered curves, in each summer scenario, of the customers behind a MV/LV transformer, based on historical recorded curves and current measurements.

The curves are clustered based on the season (winter, spring, summer and autumn) and the day of the week (working day, Saturday and Sunday). Saturday and Sunday are equivalent to a day before holiday and holiday.

LV customers do not follow this categorization since they are single customers which have an installed power higher than 55kW; it is not clustered in a particular class but recorded with its individual meter curve. Furthermore, it is possible to observe that the consumption is lower during Saturday and Sunday.

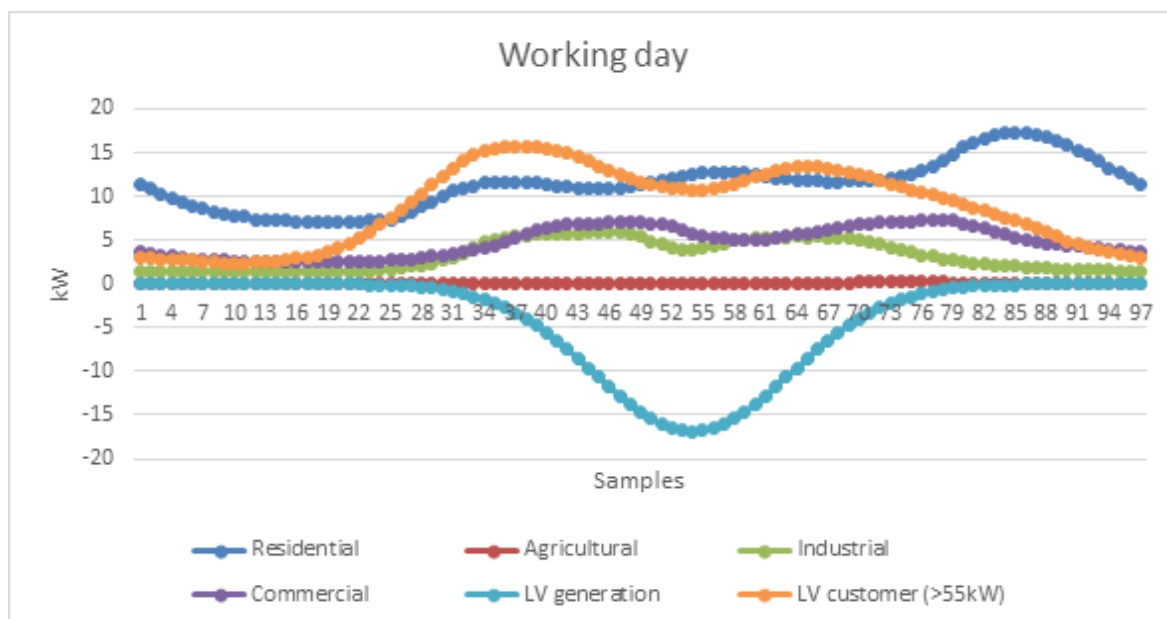


FIGURE 23 - CLUSTERED CUSTOMER CURVES IN A WORKING DAY IN SUMMER.

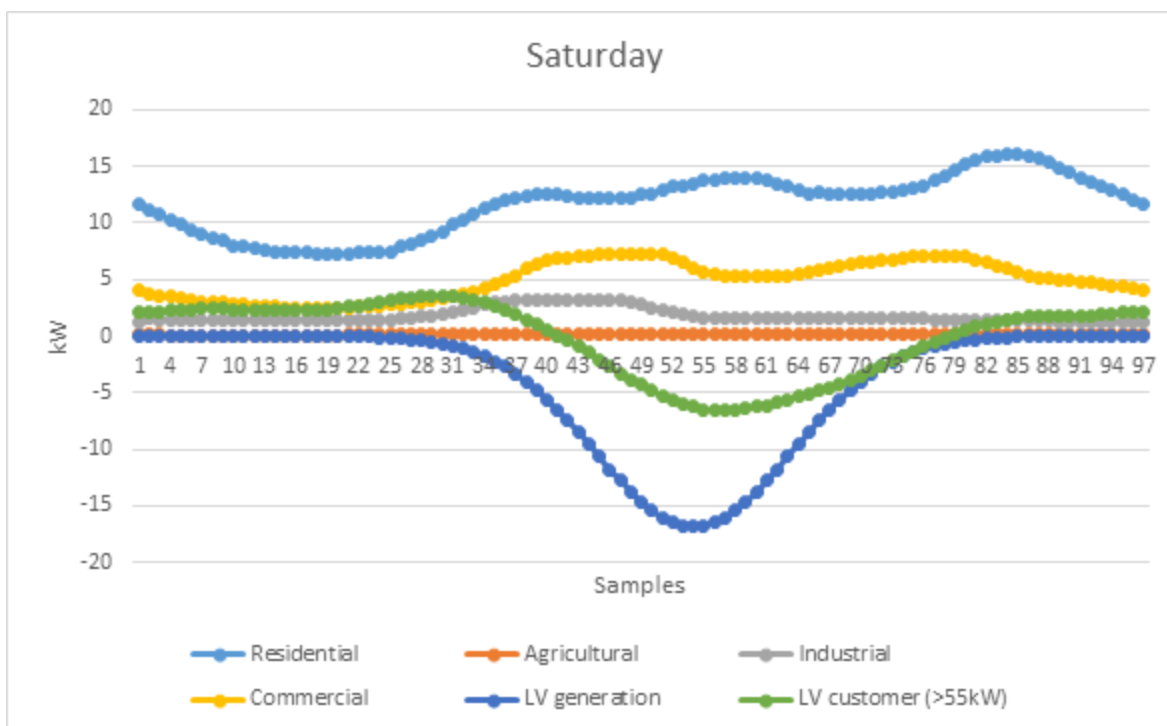


FIGURE 24 - CLUSTERED CUSTOMER CURVES IN A SATURDAY (DAY BEFORE HOLIDAY) IN SUMMER.

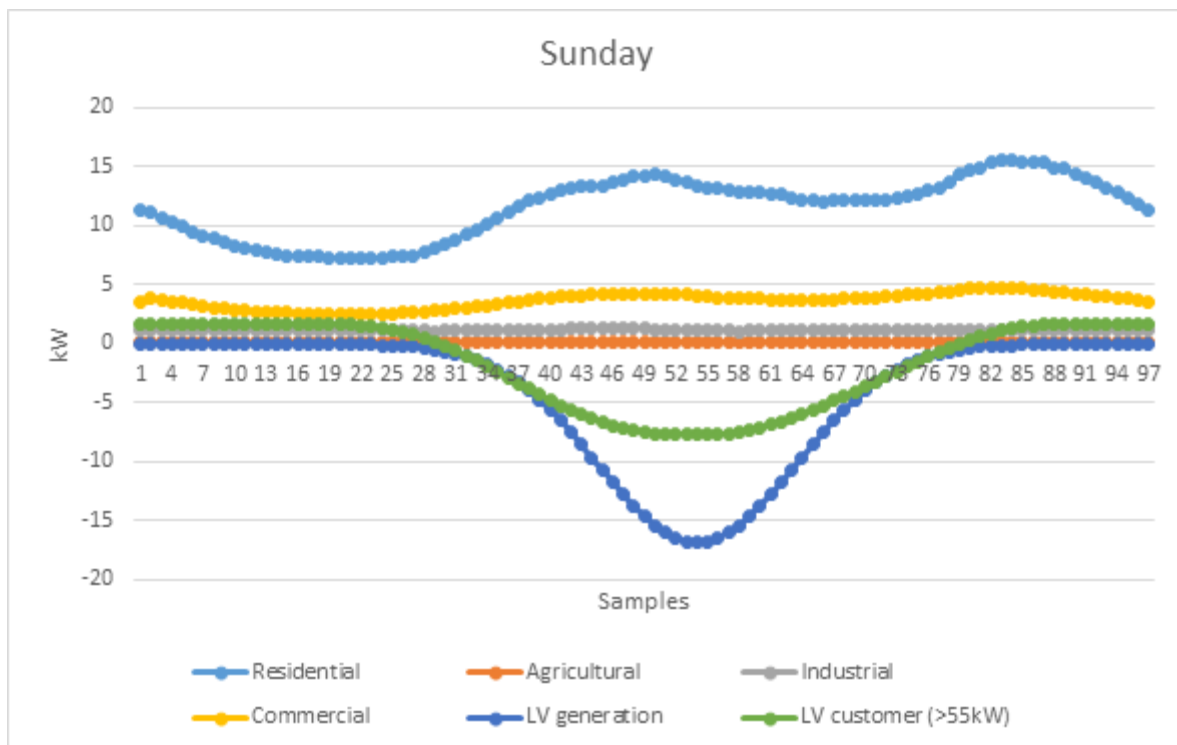


FIGURE 25 - CLUSTERED CUSTOMER CURVES IN A SUNDAY (HOLIDAY) IN SUMMER.

MV customers connected to the MV busbars of the secondary substations have also their specific meter curve. They can be passive loads, active loads or both, like the LV customer shown in the previous figures.

Figure 26 shows the three scenarios for a week on July related to a single MV customer; going in detail, this customer consists of a PV plant connected to the distribution grid. It is possible to appreciate that the production does not vary so much during the three days.

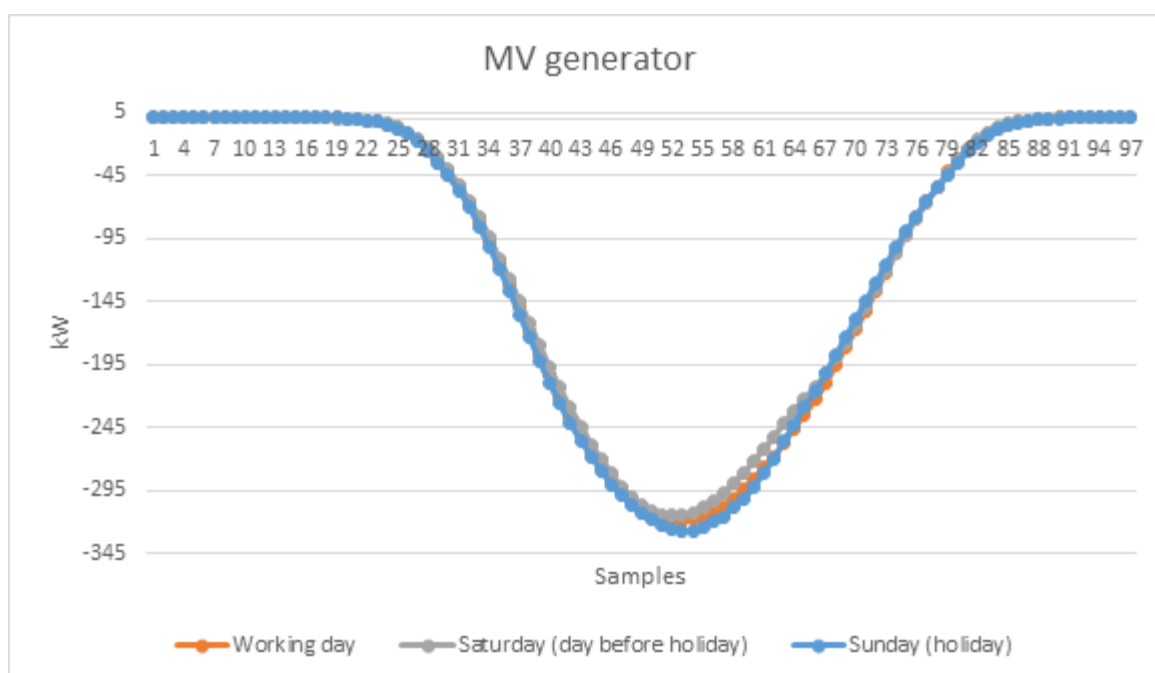


FIGURE 26 - MV PV GENERATOR CURVES DURING A WEEK IN JULY.

Once the historical curve related to a certain period is recorded, it is clustered considering also any change which can occur, according to the real time measurements acquired thanks to intelligent electronic devices.

Forecast based on the historical data is then performed also for active loads. These data are used as an input for state estimation and optimization if forecast results from MAGO are not available.

Forecast quality can be then improved inside distribution network state estimation algorithms, by adjusting the forecast curves once the curve from smart metering is stored. In this way the forecast curve is modelled according to the day of the week and the season but takes also into account of the real field data. This mostly solves any lack of data from forecast tool.

4.3.2 PERFORMANCE OF THE DEMONSTRATION SYSTEM

The performance of the Italian Demonstrator about forecast tool can be evaluated according to proposed KPIs within *WP10 – Pan-European Scalability and Replicability Analysis and Flexibility roadmap* in *D10.1 – Report on the selection of KPIs for the demonstrations* [Soler et al. (2019)].

These KPIs take into account respectively of MAE and NMAE described in Forecasting Results and will be considered also in order to evaluate the benefits of the developed solutions which will be applied in EU Sysflex project after the experience in Grid4EU project, implemented in the same distribution plant.

4.3.3 APPLICATIONS

In the Italian demo, the forecast of generation is the input for the functionalities of State Estimation and Voltage Regulation integrated in the Network Calculation Algorithm System.

More in detail, for the State Estimator, in addition to network data and measurements, forecast data are used to evaluate V at slack and values of P and Q at MV nodes. These outputs, together with the same forecasts and network data, are used by the Voltage Regulator in order to evaluate the reference Voltage of the OLTC and the values of Active and Reactive power for the controllable resources.

4.4 PRELIMINARY CONCLUSION

In this chapter a baseline forecast for the Italian demonstrator is described. The forecast system consists of the estimation and real-time monitoring of distributed generation to which the nowcast functionality is added.

The forecast tool currently exploits weather forecast data and works within E-distribuzione systems for state estimation scopes, finalized to voltage regulation of OLTCs; for this reason this functionality is necessary to satisfy also EU-SysFlex objectives, in which flexibilities owned and managed by the DSO (including the OLTC itself) are involved in addition to RES. In this context, nowcast functionality will be aimed at improving the accuracy of forecast providing an “almost” real time information about renewable production. Those information will be obtained by processing weather data coming from a weather station that is going to be installed close to the demonstration site. However, it should be noted that the actual availability of distributed power plants can also

constitute a limitation to the correct functioning of the forecast tool because, according to the Italian regulatory framework, owners of DG are not required to provide updates about it.

For the residual load forecast, an historical characterization of loads is performed by clustering the customers within a specific categorization based on the season and the day of the week. This kind of elaboration is then performed also for Distributed Generation, even if the output data are used for state estimation and optimization in case forecast tool output should not be available.

5 FORECASTING TOOLS FOR THE FINNISH DEMONSTRATOR

5.1 INTRODUCTION

The Finnish demonstrator deals with aggregator activities related to flexible resources in medium and low voltage network. Its main scope is to manage the low and medium voltage flexible resources, in order to allow them to be exploited in the TSO ancillary service market and for reactive power services to the DSO. Its goal is to increase the revenues achievable from the operations of flexible assets and it is pursued through innovative aggregation approaches and a novel reactive power market concept.

In the Finnish demonstrator, four different forecasting tools have been developed. One is serving the DSO's needs to forecast its demand for reactive power compensation in its network and three aim to assist the aggregator in improving its actions on the reserves markets:

- The PQ-window compliance forecasting tool is a preliminary step in the operation of the DSO-managed reactive power market such as outlined in the System Use Cases described in deliverable D6.1. The question that needs to be solved is to know how much reactive power services the DSO should procure from the market in order to minimize the costs charged by the TSO when the exchanges between the distribution and transmission networks are out of bounds of the permitted active (P) to reactive (Q) power ratio, from here on referred to as the PQ-window.
- The forecasting tool for households with electric storage heating that can be controlled through their Automatic Meter Reading (AMR) systems forecasts the heating needs for houses with a hot water storage unit used for space heating and domestic hot water. The storage is large enough so that charging once per day for a couple of hours is enough to load up enough heat for the whole day. The forecasting tool forecasts the heating needs throughout the day but can also predict how the heating system will react to changes and commands resulting from the operation of the AMR-connected switches.
- The Electric Vehicle (EV) forecasting tool is used as a basis by an optimization tool in order to bid the capacity available from a set of public EV charging stations. The forecast is intended to give an estimate of how much capacity can be made available for specific markets. In this case, the target markets are the frequency containment reserves (FCR) markets.
- The forecasting of customer-owned batteries is made in the context of individual households owning PV panels and a battery, with its primary use being to store and use locally as much of the PV production as possible. The objective of the forecast is to identify how much of the batteries capacity has to be reserved for that purpose and cannot be used to be bid on other markets.

5.1.1 NEED FOR A FORECAST

Within the Finnish demonstrator, four different forecast approaches are developed and applied. One forecast for the need of the DSO and three forecasts for the needs of an aggregator. This chapter further discusses the current situation and describes why the developed forecasts are needed.

FORECAST FOR THE DSO

As a part of its usual operation, Helen DSO estimates and analyses the situation of the PQ-window and how the reactive power profile will develop in the future for years ahead. In addition to the long term forecasts, Helen DSO uses a short term forecasting tool (covering the present operating hour), which is predicting the need of reactive power at the TSO/DSO interface. The short-term forecast is used to control the reactive power compensation devices connected to 110 kV and owned by Helen DSO and to fulfil the requirements of the PQ-window set by the TSO. Nowadays, the DSO has also some controllable reactive power assets (110 kV reactor, 110 kV capacitors, connections of 110 kV underground cables when not endangering the reliability of the local power system, customer agreements).

The previous forecasts at Helen DSO were done for different time frames and therefore existing forecasts could not be utilized for the reactive power market demonstration. The forecast developed in EU-SysFlex by VTT is used during the reactive power market demonstration to determine reactive power compensation needs for a week ahead. The developed forecast is needed by the DSO in order to determine if there is a need for additional reactive power compensation when the present controllable assets (reactor, capacitors owned by the DSO) are insufficient. When these present reactive power resources are inadequate, the DSO could procure supplementary reactive power assets from the reactive power market according to the need resulting from the forecast of the developed tool. The reactive power market is demonstrated as a technical proof of concept during EU-SysFlex.

FORECASTS FOR THE AGGREGATOR

During the past decade Helen has been developing capabilities to integrate third party owned assets into the reserves and balancing power markets. So far, these assets in the reserves and balancing power markets have typically been industrial-sized loads or large generation capacities. In EU-SysFlex, Helen is aiming at utilising the experience gained with the larger assets to harness small distributed assets to the markets. The main difference with small assets compared with assets that are already aggregated and traded today is the even higher uncertainty of the available capacity. Therefore, different kinds of forecasting tools are needed. They are essential to the successful aggregation and usage of small, distributed assets on the ancillary services market, because they predict, how much flexibility is available from the different types of assets and provide information to form a schedule, how much and when to bid to the markets.

5.1.2 INNOVATION OF THE FORECAST COMPARED TO EXISTING ONES

FORECAST FOR THE DSO

The forecasting of the reactive power (Q) is nowadays performed continuously and automatically within the operating hour at Helen DSO. This forecast is further used and applied to control - during operating hour in question - the 110 kV reactor and capacitors. In addition, analyzation of reactive power profile in Helsinki is performed at Helen DSO to create longer term forecasts for years ahead. In the EU-SysFlex project, an innovative development is a novel day-ahead, weekly and monthly forecast covering the active power P and the reactive power Q of the PQ window. The forecast for a week and a month ahead is essential for the demonstration of reactive power market during EU-SysFlex. While demonstrating the proof of concept of the reactive power

market, the DSO needs to have a forecast of the amount of required reactive power compensation to 1) stay within the PQ window in the near future (days, weeks) 2) determine if and when reactive power compensation is asked from the reactive power market. In the forecasting method developed during EU-SysFlex, also the active power P is forecasted to be able to forecast the need of the reactive power Q .

FORECASTS FOR THE AGGREGATOR

Controlling the automatic meter reading (AMR) meters of customers has included forecasting also before the EU-SysFlex project. Historically, the AMR meters, their readings and controlling system have been used to optimize and shift the heating hours to those hours with the lowest spot price. During the night time (22:00 - 07:00), the distribution tariff is also lower than during the day time (applies to customers with time-of-day distribution tariffs). The forecasting that has been used before, estimates the heating need of the households according to the outside temperature. The outside temperature determines the number of hours that is necessary to charge the storage water tank. These hours are used during the night time when the spot price is the lowest. Recently the system was simplified a bit so that the priority order of hours during the night was fixed according to the average information about spot prices. This means that previously, the selected heating hours (e.g. 3 hours) could vary every night according to the spot-price. Nowadays, if there is a 3 hour need for heating, the 3 hours are fixed based on what typically are the hours with the lowest price (e.g. 02:00 - 05:00).

The innovation of the forecast for the houses with electric heating developed within EU-SysFlex is the forecast of the available up and down regulation potential. The developed model still estimates the heating need of the households based on the outside temperature. In addition, it gives an estimate, how much up or down regulation could be offered to the TSO ancillary service markets, e.g. to the manual frequency restoration reserve (mFRR-market) and during which hours.

The flexibility forecast for the public EV charging stations and for the customer scale batteries are applications of existing concepts to real empirical data, not typically done with data sets as sparse as available during EU-SysFlex. Both forecasts are essential if the customer-scale batteries and EV charging stations are to be aggregated and operated in the TSO ancillary services.

5.2 FORECASTING THE REACTIVE POWER NEEDS TO COMPLY WITH THE PQ-WINDOW REQUIREMENTS

5.2.1 INTRODUCTION

In Finland, the reactive power characteristics of the electricity power system have dramatically changed during the last decade from inductive reactive power towards capacitive reactive power. This has been observed also in Helsinki, Finland and the development is still continuing. Figure 27a presents the yearly maximum values of reactive power and the yearly maximum $\tan\phi$ values (Q/P , ratio of reactive and active power) for the years 2003 to 2017, and their linear regression curves. The values represent the sum of the measurements of all main transformers in Helen DSO's distribution area. It can be observed that the yearly maximum reactive power consumption has decreased in an approximately linear fashion, with a rate of decline of 8 Mvar/year. Conversely, the yearly maximum active power has not significantly changed. The maximum $\tan\phi$ value has decreased from ca. 0.30 (year 2003) to ca. 0.10 (year 2017). The linear estimation for the rate of decline of the yearly maximum $\tan\phi$ value is 0.013 /year. Similar trends can be identified for the yearly minimum and average reactive power values (Figure 27b and Figure 27c). The decrease rates for the annual average reactive power and $\tan\phi$ from 2003 to 2017 are 5 Mvar/year and 0.010 /year, respectively. [Pihkala et al. (2019)]

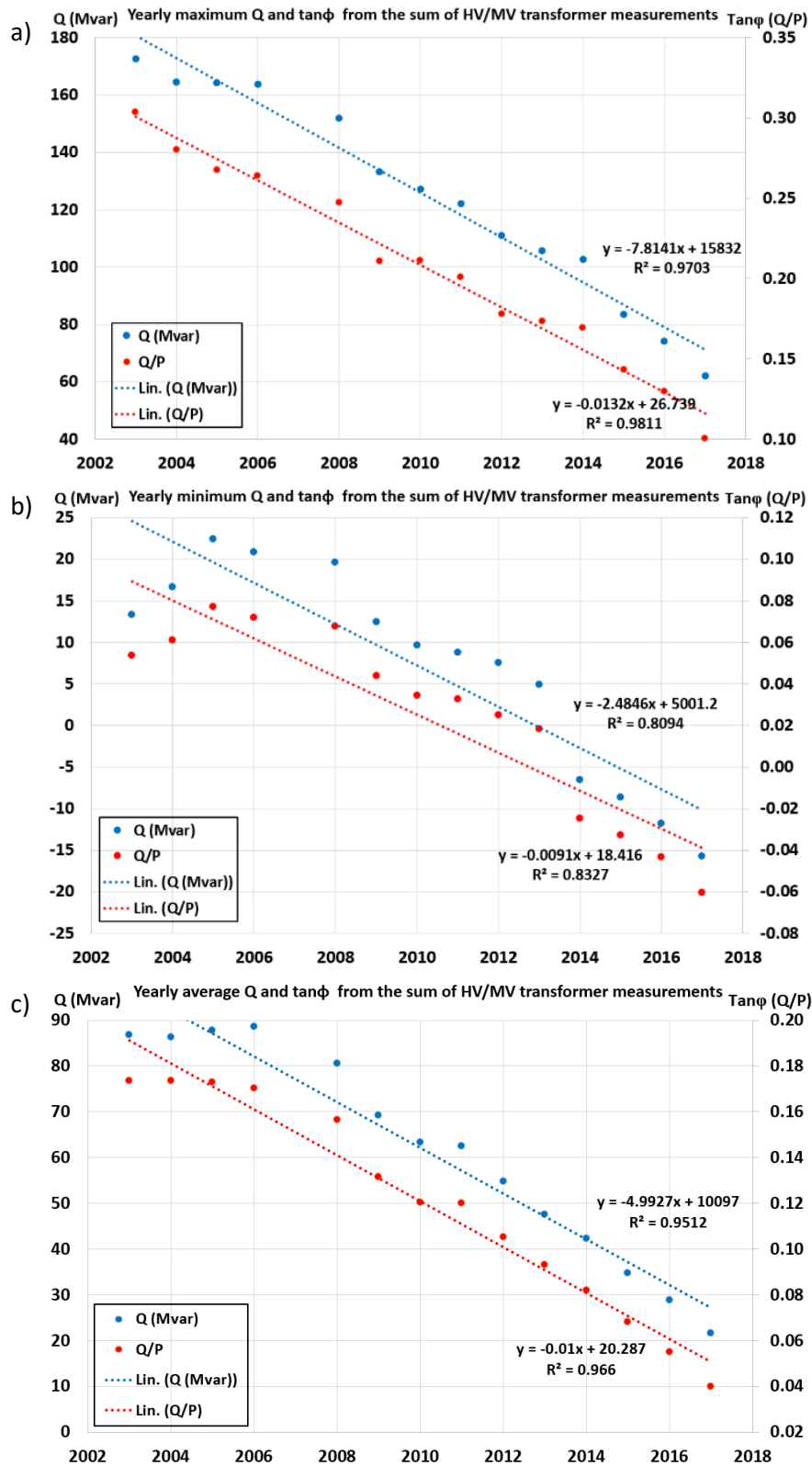


FIGURE 27 - A) MAXIMUM, B) MINIMUM, C) AVERAGE ANNUAL REACTIVE POWER AND TANφ FOR THE YEARS 2003 TO 2017. THE MEASUREMENTS REPRESENT THE SUM OF HV/MV TRANSFORMER MEASUREMENT ON THE MV SIDE.

The main reasons for this drastic development are [Pihkala et al. (2019), Takala et al. (2019)]:

- 1) The urban network in Helsinki, Finland, consists of 0.4 kV, 10 kV, and 20 kV distribution network, and the 110 kV subtransmission network. The total network length is 6400 km, and the share of 110 kV lines is 215 km. The medium voltage and low voltage networks and approximately one third of the 110 kV network consist of underground cables. When considering the reactive power in the Helsinki distribution area, the underground cable network acts like a capacitor. In the future, the city and thus also the distribution network will slightly expand meaning also an increase of capacitive reactive power that arises from the underground cable network. More remarkably, the substitution of 110 kV overhead lines with underground cables in the growing, denser city environment means especially considerable step towards additions of capacitive reactive power.
- 2) During the past decade, there has been a major change in the reactive power profiles of customers' devices. In the past, the majority of end-user equipment has been either resistive or inductive (consuming reactive power). An example of a resistive load is an incandescent lamp. Inductive loads include induction motors, fluorescent lamps with magnetic ballasts, and high pressure sodium lamps, which are commonly used in street lighting. Refrigerators, washing machines, microwave ovens, and air conditioners are examples of traditional inductive end-user equipment. However, electric loads with capacitive power factors (generating reactive power) have become more common during the last decade. Typically, electronic devices are equipped with filter capacitors. LCD TV's, personal computers, laptops, and mobile phone chargers are examples of capacitive loads. Furthermore, while directly connected induction motors consume significant amounts of reactive power, it has become increasingly common to equip motors with frequency converters, which allows operation at power factors closer to unity. An example of this development is an inverter-based air conditioner. One of the most significant changes of end-user equipment during the last decade is the replacement of incandescent lamps with energy-efficient compact fluorescent lamps and LED lamps. Both of these lamp types exhibit capacitive power factors. In street lighting, traditionally high-pressure sodium lamps have been the preferred solution. This lamp type consumes significant amounts of reactive power. However, there is a trend towards LED lights in street lighting as well. Therefore, it is expected that more inductive loads will be replaced by capacitive ones. [Pihkala et al. (2019)]

The drastic changes of the characteristics of reactive power challenge the DSOs and the TSO. In Finland, there is one TSO, Fingrid, and about 80 DSOs. DSOs are to control the reactive power balance in their distribution area. In the TSO/DSO boundaries, the desirable reactive power flow is determined via a so called PQ window set by the TSO with the aim of DSOs to stay within the limits of their PQ window. Figure 28 presents the scheme of the PQ window with Helsinki data. The vertical axis is the consumed active power P (MW) in the DSO's area. The horizontal axis is the determined, virtual reactive power flow (Mvar) between the DSO and the TSO. Hourly average active and reactive power values are used in the PQ window descriptions. From technical point of view, the PQ window limits assist the TSO in controlling the voltage of the transmission network. If a DSO exceeds the limits, penalty payments included in the TSO/DSO tariff come into force. These reactive power fees have

significantly increased during 2016 - 2019 requiring fast actions from DSOs to avoid the considerably high payments.

Simultaneously, DSOs experience and face drastic changes of reactive power characteristics and realize to have insufficient compensation capacities. When having experienced major changes of reactive power characteristics during the past decade there have been a variety of control strategies of the reactive power of the distribution area. In Helsinki, until 2016, the main reactive power control mechanism was a control agreement with a local energy producer, Helen. Along with the agreement, Helen was in charge of controlling the reactive power of the PQ window with their traditional power plants. In 2013, Helen informed it can no longer guarantee that at least one power plant would be in operation during the summer time. Consequently, the DSO decided to annul the agreement starting from 2016. Nowadays, the Helen DSO mainly compensates reactive power with its own 110 kV reactor (30 Mvar) and two capacitors (2 * 30 Mvar). The compensation demand is focused on the reactor, and the two capacitors are rarely used. Additionally, there have been some specific agreements with biggest customers and disconnection of 110 kV underground cables when the reliability of the network has not been endangered. Additionally, high, medium voltage and in addition biggest low voltage customers are determined to compensate excessive reactive power via the grid tariffs. While the capacitive reactive power is nowadays problematic, the company has also contacted and instructed individual customers with major reactive power production to keep their reactive power slightly inductive.

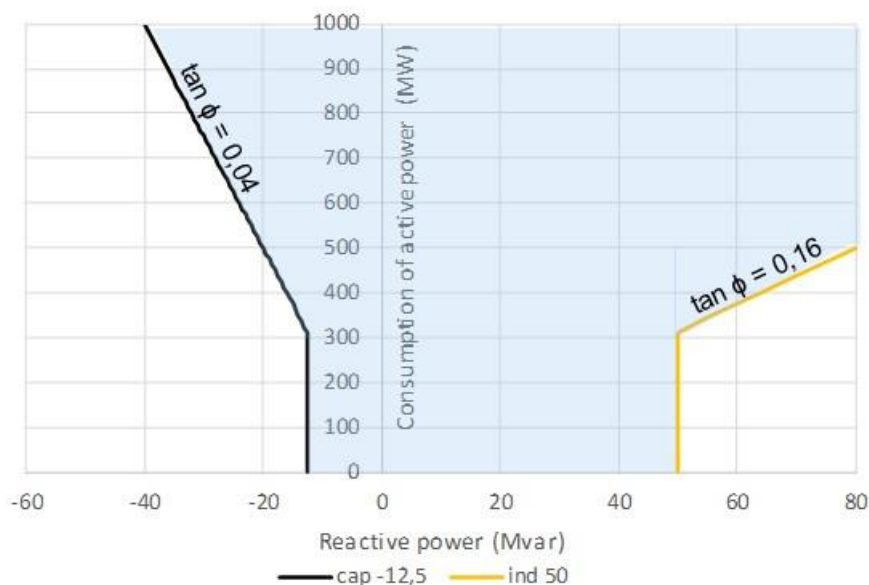


FIGURE 28 - PQ WINDOW IN THE FINNISH ELECTRICITY SYSTEM, CASE HELSINKI.

As mentioned above, in Helsinki, in order to mitigate the reactive power exchanges in the PQ window, the Helen DSO actively uses its' own 110 kV compensation devices. The most challenging time periods are those times of low consumption, that is spring, summer and early autumn weekends and nights. At those times, too little controllable inductive reactive power is currently available. Helen DSO has decided to invest into a new 50 Mvar reactor. This is one solution. However, on the other hand, in the distribution network, there are more and more

controllable reactive power assets, like power electronics of small devices. They are owned by customers and not by Helen DSO. This could be an interesting potential of controllable reactive power for Helen DSO. An alternative for this reactive power regulation lies on capturing the reactive control capabilities of the newly connected devices with power electronics by making them accessible to a reactive power market. In the market procedure, the DSO should forecast the reactive power exchanges for the future in order to be able to plan the operation of its regulating devices and to determine how much reactive power would be required from the market. Given the close connection and dependency between active and reactive power, forecasting the former is also needed in this task.

5.2.2 DESCRIPTION OF THE FORECASTING PROCESS

The forecasting system uses data of the boundary between the TSO and Helen DSO networks. The data gathered consists of historical measurements for the different points which can be summed up and interpreted as the representation of the whole DSO's grid. The connection between the TSO and DSO can be considered as a single point. This method has been selected because it is the one applied in the PQ window. This connection point is represented in the diagram shown in Figure 29. Active and reactive power flows from the TSO network to the DSO network are measured. Therefore, when the reactive power profile of the DSO network is capacitive, and thus flows towards the TSO network, it is registered in the dataset with a negative signal. Alternatively, an inductive profile for the reactive power in the DSO is given with a positive signal.

The historical data used in the forecasting are hourly measurements of active power, reactive power and temperature. Additional information that was made available included information about the capacitive contribution from the largest 110 kV underground cables in the distribution network as well as, naturally, time-related information, such as time of the day, day of the week, season of the year, etc.

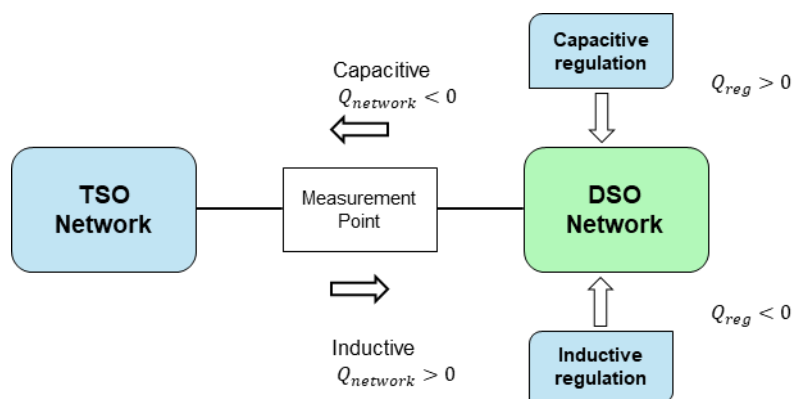


FIGURE 29 - DATAPOINT IS LOCATED BETWEEN THE TSO AND THE DSO

The first data set consists of hourly average values for the active ($P(t)$) and reactive ($Q_{network}(t)$) power flow between the TSO and the DSO networks. $Q_{network}(t)$ is the reactive power value at the measured single connection point between the TSO and DSO and $P(t)$ is the consumption of active power in the distribution area.

The second data set is the hourly average usage of the reactive power compensation resources $Q_{comp}(t)$, such as data for the reactive power compensation from one 110 kV reactor and two 110 kV capacitors, operated by the DSO. When $Q_{network}(t)$ is sufficiently negative (presenting a capacitive profile), the inductive regulation device is activated to absorb some of it. The reactive power flow from the compensation device to the DSO network in this case is negative, as it is measured arbitrarily as coming from the inductive resource to the network. Similarly, the dataset has measurements from the capacitor banks with a positive sign.

The third data set is the hourly data on the connection state of the nine most important cables, in terms of reactive power contributions, of the DSO's 110 kV underground cabling network. The overall capacitive contribution of those cables $Q_{cables}(t)$, which is considered to be independent from their loading, is also available on an hourly average. The last data set consists of temperature measurements as well as time and date related information to create, for each data point, hourly features such as time of the day (ToD), season of the year, day of the week, etc. These features have been identified as having a significant impact on the accuracy of the forecasting tools.

The forecasting targets must be defined by analyzing the portion of the total reactive power of the network that is unknown to the DSO. Therefore, from combining the measurements in the dataset, it is identified that:

$$Q_{network}(t) = Q_{loads_{network}}(t) + Q_{comp}(t) + Q_{cables_{cap}}(t) + Q_{cables_{ind}}(t) \quad (8)$$

where

- $Q_{network}(t)$ is the reactive power value at the measurement point, composed by the combination of reactive power contributions from multiple grid components (Mvar),
- $Q_{loads_{network}}(t)$ is the reactive power at the measurement point that is dependent on (i) the loads; (ii) the medium and low voltage networks; (iii) the 110kV overhead lines present in the distribution network in Helsinki. $Q_{loads_{network}}(t)$ can be seen as the reactive power that is not controllable or known by the DSO in advance (Mvar),
- $Q_{comp}(t)$ comes from the reactive power compensation resources, namely the reactor and both capacitors (Mvar),
- $Q_{cables_{cap}}(t)$ and $Q_{cables_{ind}}(t)$ are the reactive power contributions (capacitive and inductive, respectively) from the cabling system (Mvar).

Equation (8) indicates that the total reactive power measured at the connection point between the DSO and the TSO networks is a combination of the reactive power contribution of (i) the 110 kV underground cabling represented by the inductive and capacitive influences $Q_{cables_{ind}}(t)$; $Q_{cables_{cap}}(t)$; (ii) the compensation devices $Q_{comp}(t)$; and (iii) the customer loads, medium and low voltage networks and 110 kV overhead lines in the DSO network, combined into $Q_{loads_{network}}(t)$.

The capacitive contribution of the network cables to the reactive power, $Q_{cables_{cap}}(t)$, can be considered constant and known for each individual cable in the 110 kV underground network, and thus determined entirely by the connection status (connected or not) of the 110 kV cables. Its inductive counterpart, $Q_{cables_{ind}}(t)$, is

related and proportional to the cable loading. Therefore, $Q_{cables_{ind}}(t)$ can be combined to $Q_{loads_{network}}(t)$ to obtain a variable that fully represents the influence of the variation arisen from the whole distribution network including all industrial, commercial and residential contributions on the reactive power profile of the DSO. The previous equation can be simplified to:

$$Q_{network}(t) = Q_{loads}(t) + Q_{comp}(t) + Q_{cables}(t) \quad (9)$$

where

- $Q_{loads}(t) = Q_{loads_{network}}(t) + Q_{cables_{ind}}(t)$ is considered as the combination of the reactive power from the network and the inductive power from the underground 110 kV cable network (Mvar)
- $Q_{cables}(t) = Q_{cables_{cap}}(t)$ simplifies the capacitive influence of the reactive power from the underground 110 kV cable network (Mvar).

As just mentioned, $Q_{cables}(t)$ is the reactive power contribution that is known by the status of the specific 110 kV underground cables. $Q_{comp}(t)$ is dependent on the operation of the compensation resources and is controlled by the DSO. It is therefore known as well. In essence, forecasting the total $Q_{network}(t)$ comes down to forecasting $Q_{loads}(t)$. The objective of the forecasting tool is however to forecast the reactive power compensation needs. The two values of interest to forecast are therefore:

$$\begin{cases} Q_{uncomp}(t) = Q_{loads}(t) + Q_{cables}(t) \\ Q_{loads}(t) \end{cases} \quad (10)$$

where

- $Q_{uncomp}(t)$ is the reactive power measurement when the influence of the compensation devices is removed (Mvar).

Based on Equation (10), the forecast target variable is defined:

$$Q_{compensation\ needed}(t) = Q_{CN}(t) = Window\ limits \pm (Q_{loads}(t) + Q_{cables}(t)) \quad (11)$$

where

- $Q_{compensation\ needed}(t) = Q_{CN}(t)$ is the compensation required to the DSO to guarantee the reactive power remains within the agreed PQ window (Mvar),
- $Window\ limits$ are the reactive power limits of the PQ window (Mvar). It is dependent on the active power of the DSO network at all times (Mvar).

Thus, the hourly amount of regulation needed $Q_{CN}(t)$, either capacitive or inductive, is dependent on the difference between the reactive power $Q_{network}(t)$ and the limits from the PQ window (Figure 28). As such, to identify the exact limits of the PQ window at each time, which are dependent on the active power $P(t)$, the active power also can be considered as a variable to forecast. The forecasting strategy consists of forecasting $Q_{loads}(t)$, to have an idea on the status of the reactive power in the DSO network. These values are combined with the known values for $Q_{cables}(t)$, obtained from other forecasting resources in the DSO and related to the connection

of the 110 kV underground cables. This combination used in subsequent calculations from Equation (11), together with the forecasted $P(t)$ that influences the window limits.

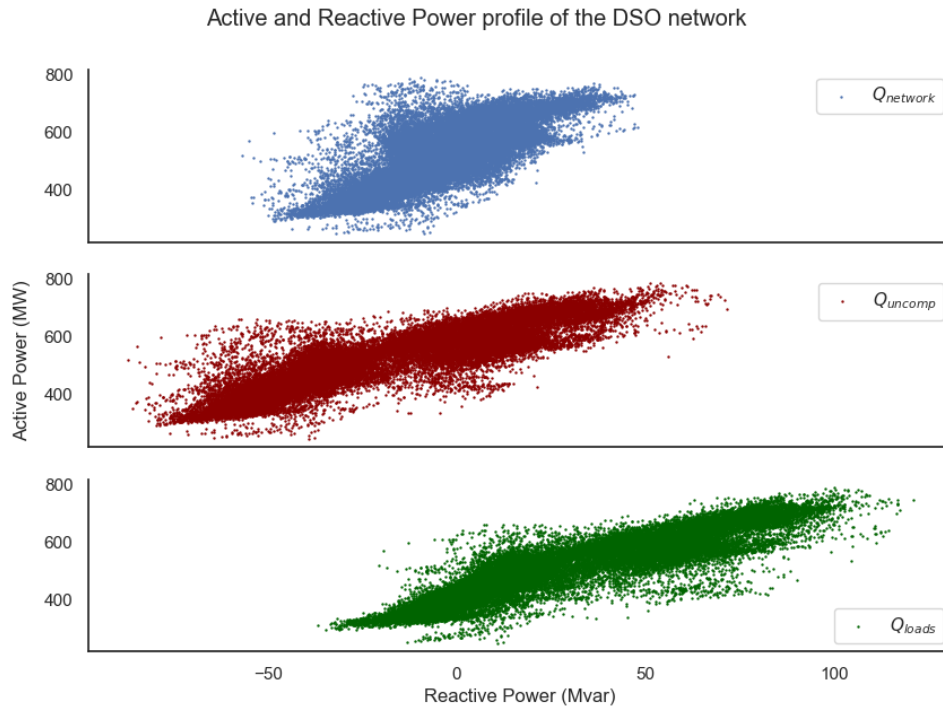


FIGURE 30 - PQ PROFILE OF THE DSO NETWORK WITH ($Q_{network}$) INFLUENCE OF COMPENSATION DEVICES AND UNDERGROUND CABLES; (Q_{uncomp}) INFLUENCE OF ONLY UNDERGROUND CABLES; (Q_{loads}) THE REACTIVE POWER FRACTION THAT IS UNKNOWN TO THE DSO BEFOREHAND, THE TARGET VARIABLE OF THE FORECAST.

The scatter plots in Figure 30 show the three data sets of reactive/active power from 2016-2019. The top one shows $Q_{network}(t)$, the original PQ window data. By removing the influence of the reactive power compensation, the reactive power values spread further and show $Q_{uncomp}(t)$. Finally, removing the capacitive contribution from the 110 kV underground cables shows shift in the reactive power profile in the plot for $Q_{loads}(t)$.

The forecasting strategy chosen is described in Figure 31. This strategy consists of forecasting initially a $Q_{target}(t) = Q_{loads}(t)$. The second stage adds the known $Q_{cables}(t)$ to yield the supplementary target, the regulation needed from the resources, $Q_{uncomp}(t) = Q_{target}(t) + Q_{cables}(t)$ (by substituting $Q_{loads}(t)$ by $Q_{target}(t)$ in Equation (10).

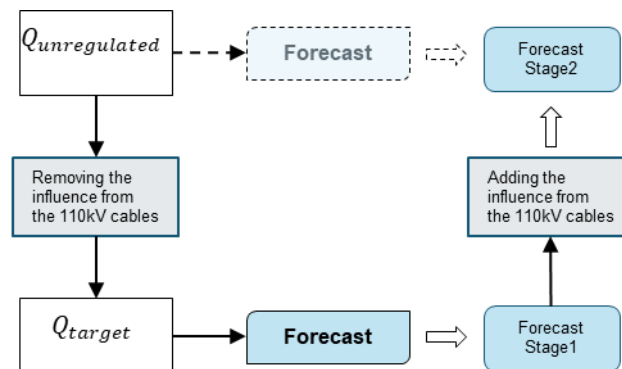


FIGURE 31 - DIFFERENT FORECAST TARGETS YIELD DIFFERENT STAGES OF THE REACTIVE POWER FORECAST.

5.2.2.1 INITIAL AND INPUT DATA

The historical data used to develop, train and test the tool is the following:

- Active power exchanges at the network interconnection points, $P(t)$
- Reactive power exchanges at the network interconnection points, $Q_{network}(t)$
- Connection status of the underground cables and their reactive power contributions, $Q_{cables}(t)$
- Status of the existing reactive power management devices (reactors and capacitors), $Q_{reg}(t)$
- Temperature, $T(t)$

for the period from 2016 to 2019. It was provided by Helen DSO to VTT.

5.2.2.2 ALGORITHM AND MODELING

The algorithms for modelling and forecasting reactive power compensation requirements were realized using Python 3.7, with methods from the *scikit-learn*[ref1] and *keras*[ref2] packages available at the time of the publication of this report.

Three different forecasting algorithms were tested, with different ranges of accuracy depending on the forecast horizon. There is also a difference in the inputs for each forecasting method. A brief description of each forecasting technique and a justification for its implementation are given in the following sections. The input and output formats for both the training and testing sections of each methods are also discussed.

GRADIENT BOOSTING REGRESSION FORECAST

The first forecasting method uses Gradient Boosting (GB), a machine learning algorithm for regression and classification. It is an ensemble technique that combines several weak prediction models to form strong predictors. Each weak predictor improves upon the last, yielding a strong combination of successive predictors that offer a high regression performance and accuracy. It is an extremely popular machine learning algorithm due to its performance per the computational power ratio, which combined with its flexibility and ease of implementation, allows for its application in multiple domains. Typically, Gradient Boosting offers unmatched accuracy at the expense of computational costs for training, especially for a large dataset. The Gradient Boosting algorithm also does not allow for great interpretability of its generated models, another disadvantage in the context of forecasting reactive power.

Figure 32 shows the proposed methodology of forecasting hourly reactive power compensation. Historical data composed of hourly measurements from 2016 to 2018 is used to create a Gradient Boosting Model. These measurements consist of hourly reactive power values associated to other measurements - features - such as active power, temperature and time-related information associated to the timestamp (day of the week, hour of the day, season of the year). The Gradient Boosting Model receives an input with N timestamps representing the N previous hours and forecasts the values of $Q_{loads}(t)$ for the forecast horizon of the next F hours.

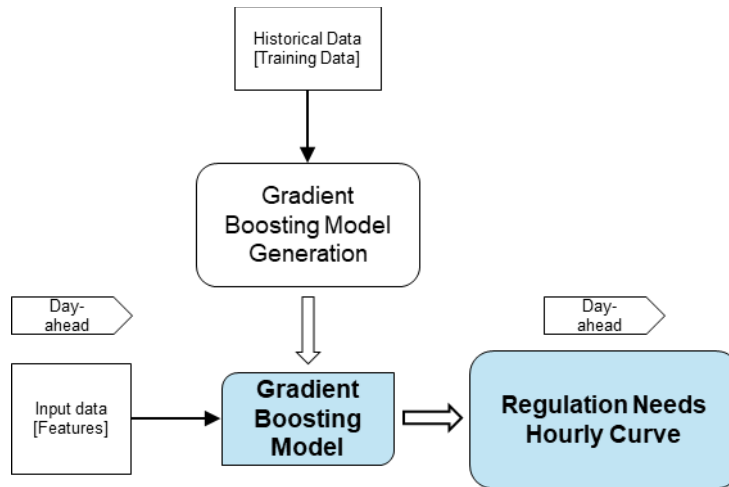


FIGURE 32 - GRADIENT BOOSTING METHOD IMPLEMENTATION ALGORITHM.

This algorithm was applied with a rolling-window to forecast all days in the period between January and May of 2019 (the test dataset). The $F=24$ timesteps (for a day-ahead forecast) were forecasted and concatenated to assess the accuracy for the whole 2019 test dataset. The accuracy is then calculated for the complete test set, which compares all time steps in 2019 to their correspondent forecast.

RECURRENT NEURAL NETWORK (RNN) FORECASTING TECHNIQUE

The second approach was to implement a Recurrent Neural Network in the form of a Long-Short-Term Memory (LSTM) network. This type of Artificial Neural Network is widely used for forecasting time series with dependency from historical values. A LSTM is capable of learning past behavior of a time series and forecast future data. As such, this technique is very appropriate for the application at hand. It also allows for inserting different features, such as active power $P(t)$, temperature $T(t)$ and day of the week, to forecast the behavior of reactive power.

Figure 33 shows the process to create an LSTM model and use this model for forecasting $Q_{loads}(t)$ for the F following timesteps. The forecast strategy was the same as adopted for the Gradient Boosting method, with a rolling window of k_{test} timesteps being input to the model to forecast the next F hours, which are then concatenated for all the duration of the test period. The LSTM method was trained for 100 epochs with a batch size of 1000 datapoints for all forecast horizons. Increasing the amount of epochs has the potential to increase the performance of the method, at the expense of computational resources and time to train the models.

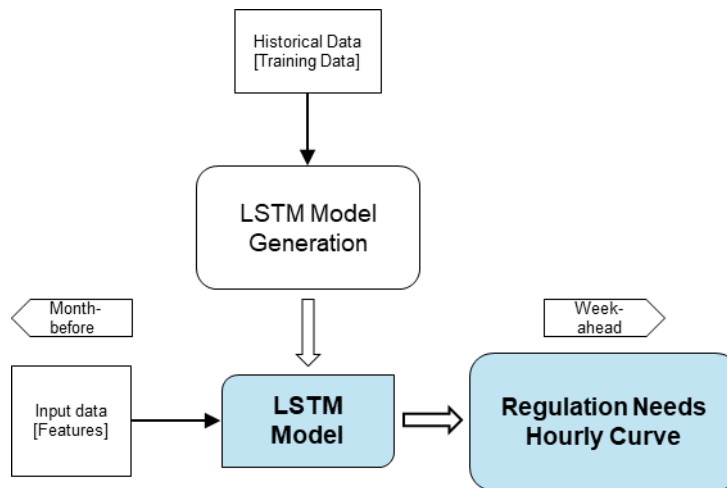


FIGURE 33 - LSTM METHOD IMPLEMENTATION ALGORITHM

STATISTICAL CLUSTERING BASED ON SCENARIO CLASSIFICATION

A probabilistic method for clustering of reactive power compensation requirements was developed based on a statistical analysis of historical data. The focus is to have a forecasting model with its main features being the explainable nature of the method and the ability to clearly show trends. The reactive power compensation needs were forecasted in terms of the probability of being within certain intervals according to time-related parameters of the forecast horizon F timestamps (time of day, day of the week, season).

Initially, the historical probability forecast depends on accurately dividing the historical data into periods of similar characteristics. From the prior data analysis of the reactive power behavior over the four-year dataset used in this task, it was decided that the higher level of separation between data scenarios would be the *season*. Therefore, historical data was clustered into Winter, Spring, Summer and Autumn periods, each consisting of three months over each year represented in the dataset. The next level of clustering was based on the day of the week. Finally, the last layer of data clustering was based on the hour of day.

Having the historical data classified in 672 different bins ($4 \text{ seasons} \times 7 \text{ days of week} \times 24 \text{ hours}$) allow us to calculate a probability distribution between the regulation needed at each one of those scenarios. A Saturday Morning on July (Summer in the pilot location) has a different $Q_{loads}(t)$ probability distribution than a Wednesday Afternoon during Winter.

Based on the scenarios, when given a date as an input, the historical probability forecast yields a probability distribution for the regulation needed on that date, giving a clearly explainable probability of regulation needed intervals for each hour of the day. This technique provides a general view of how much reactive power will be needed in terms of percentiles. Therefore, the resources can be set to a level depending on how much control operation is needed. This gives a long-term visualization of $Q_{loads}(t)$ for a longer horizon, suitable for rough planning purposes. A more accurate forecast curve can be obtained for a shorter forecast horizon using the other methods mentioned in this section, given that the operator uses more recent measurements to serve as inputs.

Figure 34 shows the process for creating the different scenarios and the associated probability distributions, and using this to forecast $Q_{loads}(t)$ for the input dates.

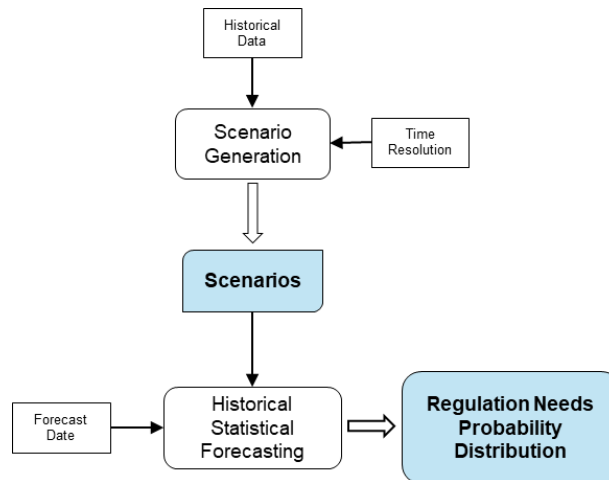


FIGURE 34 - STATISTICAL CLUSTERING FORECAST METHOD

COMPARISON OF THE INPUTS FOR THE DIFFERENT METHODS

The inputs for performing reactive power forecast are dependent on the method used. However, for all three techniques, the process of forecasting is similar in which a model is created using past data. The learning process for each algorithm is different and therefore requires a different input format. Each method required some manipulation of the dataset to create an appropriate input. For the training data, k_{train} measurements, the amount of hours in the training dataset from 2016 - 2018 are given as the input rows. The forecasts always get inputs from 2019, amounting for k_{test} values.

All m features associated to a timestep (an hourly measurement) were lagged N times to create the inputs for the Gradient Boosting method. N is the amount of timesteps selected as “look-back” values, or the number of previous timesteps used to forecast. For example, a week of look-back values would set $N = 24 * 7 = 168$. Figure 35 shows the input format for the training of a Gradient Boosting Model, and the required input format for this model to produce a forecast for reactive power. The training input is a matrix of $k_{train} \times ((m \times N) + 1)$ dimensions, while the inputs for the dataset are a matrix of $k_{test} \times (m \times N)$ dimensions.

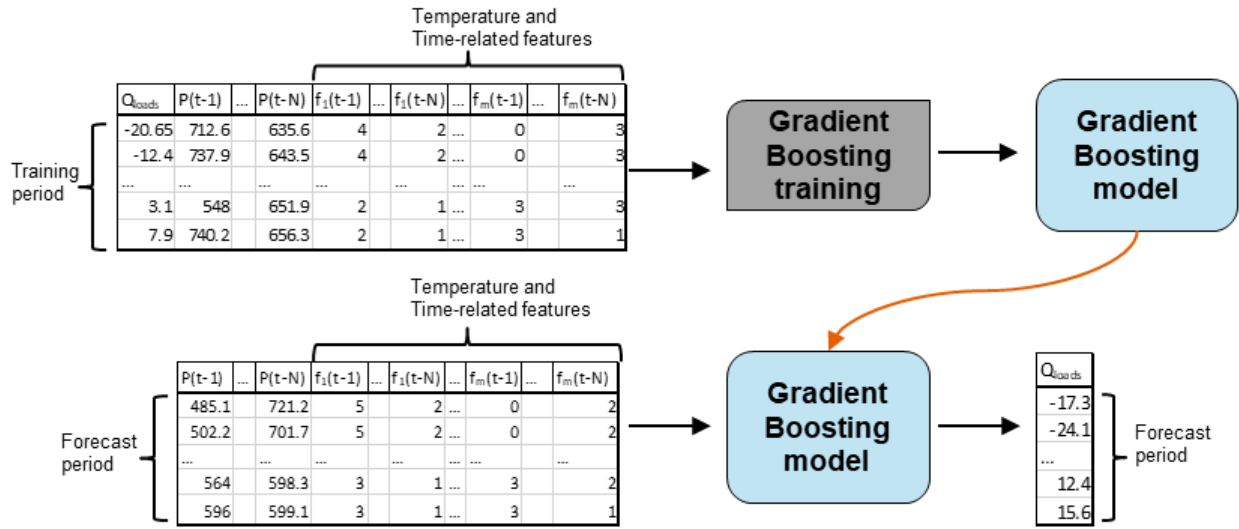


FIGURE 35 - GRADIENT BOOSTING INPUT AND OUTPUT FORMATS

Alternatively, the N lagged features are also needed for the LSTM model training. However, the input format for this algorithm is not a two-dimensional matrix, rather a three-dimensional matrix with the different features as a third axis. Therefore, the training input is in the format $k_{train} \times (N + 1) \times m$, while the input for the forecast is $k_{test} \times N \times m$. Figure 36 shows the relationship between the input and outputs of the LSTM.

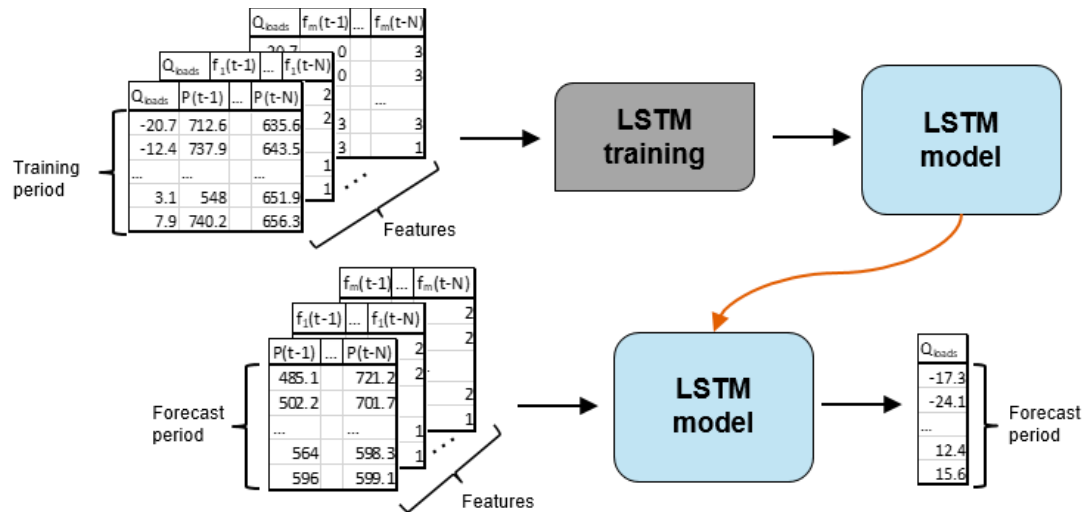


FIGURE 36 - LSTM INPUT AND OUTPUT FORMATS

The statistical clustering method does not require any time-shift or information about previous values of the features to train the model. Instead, it classifies each one of the k_{train} timesteps given in the training dataset into one of the 672 scenarios empirically selected. The inputs for the forecast are then classified into these scenarios based on the time-related features of the k_{test} timestamps given. This process is described in Figure 37.

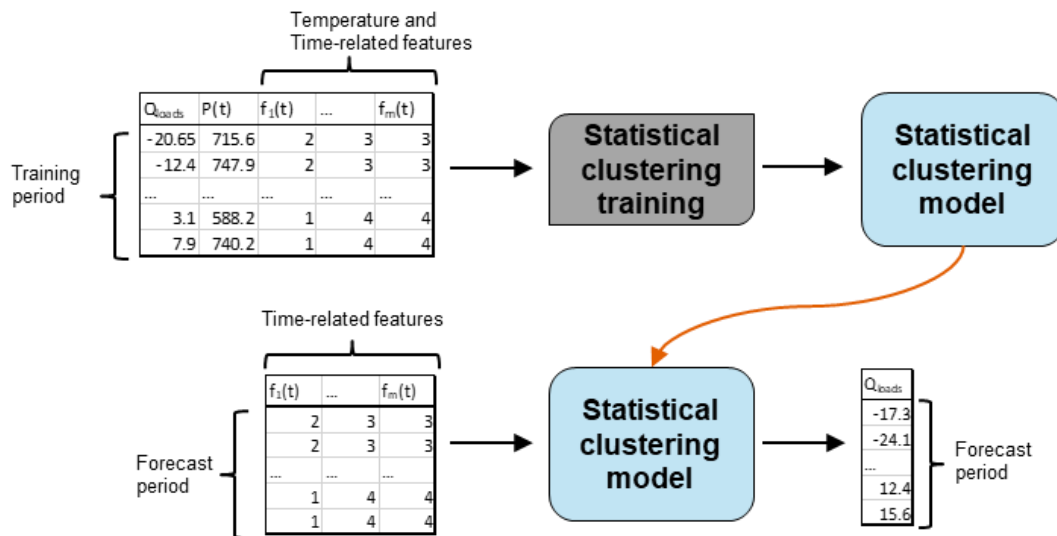


FIGURE 37 - STATISTICAL CLUSTERING INPUT AND OUTPUT FORMATS

The forecast with statistical clustering is performed for the whole test dataset. Therefore, the forecast horizon $F = k_{test}$, and these are equal to the number of hours in the test dataset in 2019. The input data for the model is comprised of only time-related features, which are set for the whole test period, which implies that implementing a rolling window, as was done with Gradient Boosting and LSTM, would serve no purpose in the statistical clustering method.

5.2.2.3 REALIZATION OF THE FORECAST SYSTEM

The realization and integration of the forecast into Helen DSO's systems will be done manually for the purpose of the demonstration period due to the hypothetical nature of the reactive power market. The forecast presented in this deliverable was done by VTT and therefore VTT acts as the forecast provider during the demonstration period. In the demonstration, Helen DSO asks for the forecast for the next week from VTT and VTT provides the forecast as a csv-file. The forecast provided by VTT will tell how much reactive power compensation is needed to comply with the requirements of PQ-window set by the TSO. The forecast is used at Helen DSO to decide how much reactive power compensation and in which times will be asked from the assets participating in the reactive power market demonstration. During the demonstration period, the forecast is updated weekly. The reactive power market demonstration period (technical proof of concept) will be done during 2020.

5.2.3 FORECASTING RESULTS

In all the forecasting techniques implemented in this work, data from 2016-2018 is used as a training set, while for the testing and evaluation data from 2019 is used. This in itself brings a difficulty, that the data gathered was up to the end of May 2019, meaning that the forecast has not been tested against all seasonal conditions that are passed to the models. However, having 5 months as a test set, which comprehends the winter and spring seasons, is already quite representative. The performance of the forecasts with different methods are shown in Table 2 or the full test dataset of January-May 2019.

The results presented in this section are organized according to the forecast horizon, with day-ahead, week-ahead and month-ahead forecasts. All methods are used for all forecast horizons, and their accuracy is compared. To effectively compare the accuracies of the methods, the moment of forecast was arbitrarily set as midnight of 15/3/2019. Therefore, the day-ahead forecast would be for the 15/3/2019; week ahead would comprise of the dates between 15/3/2019-21/3/2019; and the month-ahead forecast is between 15/3/2019-14/4/2019. Selecting arbitrarily one date to execute the forecasts allows for a better visualization of the forecast performance and the forecasted $Q_{loads}(t)$ curves. However, testing the accuracy of the methods in one specific date or range of dates does not provide an indication of the overall accuracy of the methods over the full test dataset (January-May 2019). Thus, the methods are also tested over the full test dataset and the accuracies are compared. The accuracy for forecasting the whole test period of January-May 2019 is also shown, calculated with daily forecasts and a rolling window for Gradient Boosting and LSTM. The required input range k_{test} and forecast range F are also given. The accuracy metrics used are the root mean squared error (RMSE) and the normalized root mean squared error (NRMSE), calculated as:

$$RMSE = \sqrt{\frac{\sum_{t=0}^{t=T} (\hat{y}_t - y_t)^2}{T}} \quad (12)$$

$$NRMSE = \frac{RMSE}{\max(y) - \min(y)} \quad (13)$$

where T is the number of hours in the test dataset, \hat{y}_t are the forecasted values for $Q_{loads}(t)$ and y_t are the reactive power data y for $Q_{loads}(t)$ measured for 2019 in a timestamp t . The NRMSE normalizes the RMSE in relation to the range of values found in the forecast horizon. Therefore, this measure is better suited for comparing forecast accuracy between different methods for the same horizon. RMSE is then used to compare the performance between different forecast horizons.

TABLE 2 - ACCURACY METRICS AND INPUT-OUTPUT FORMATS FOR FORECASTING METHODS FOR FULL TEST DATA FOR 2019

| | Forecast horizon | RMSE (Mvar) | NRMSE | k_{test} | F |
|------------------------|------------------|-------------|--------|------------|------|
| Gradient Boosting | Day-ahead | 6.90 | 0.0613 | 24 | 24 |
| | Week-ahead | 7.11 | 0.0630 | 168 | 168 |
| | Month-ahead | 7.60 | 0.0758 | 672 | 672 |
| LSTM | Day-ahead | 6.68 | 0.0592 | 24 | 24 |
| | Week-ahead | 9.32 | 0.0826 | 168 | 168 |
| | Month-ahead | 12.87 | 0.1223 | 672 | 672 |
| Statistical Clustering | Full dataset | 11.79 | 0.1044 | 2879 | 2879 |

5.2.3.1 DAY-AHEAD FORECAST

Day ahead forecast was performed with all three techniques. The Gradient Boosting method used as input the measurements for active power and time-related information for the past 24 measurements. That is, data for the 14/03/2019 was used as input for the Gradient Boosting method. The LSTM method also used the data for the same day as inputs. Alternatively, the statistical clustering forecast used as input only the time-related information for the forecast horizon F . That is, the method classified each one of the hours of this Spring Friday that was the 15/03/2019 into one of the 672 scenarios and gave as the output the average value of $Q_{loads}(t)$ for similar Spring Fridays.

Figure 38 shows the traced curves for the three forecasting methods implemented. Using data for 14/03 to forecast 15/03, Gradient Boosting yielded an RMSE of 4.5 Mvar, a performance significantly better than the values found for LSTM (10.06 Mvar) and statistical clustering (9.03 Mvar). Table 3 shows the accuracy metrics and the inputs and outputs formats for the day-ahead forecasts. The RMSE values are naturally dependent on the day selected to forecast, and the performance found in forecasting values in 15/03/2019 is not exactly the same as it would be for forecasting a different day. Therefore, a forecast for the whole test dataset, with data from January to May 2019, was performed using the same day-ahead methodology. The accuracy results for the full test dataset is shown in Table 3.

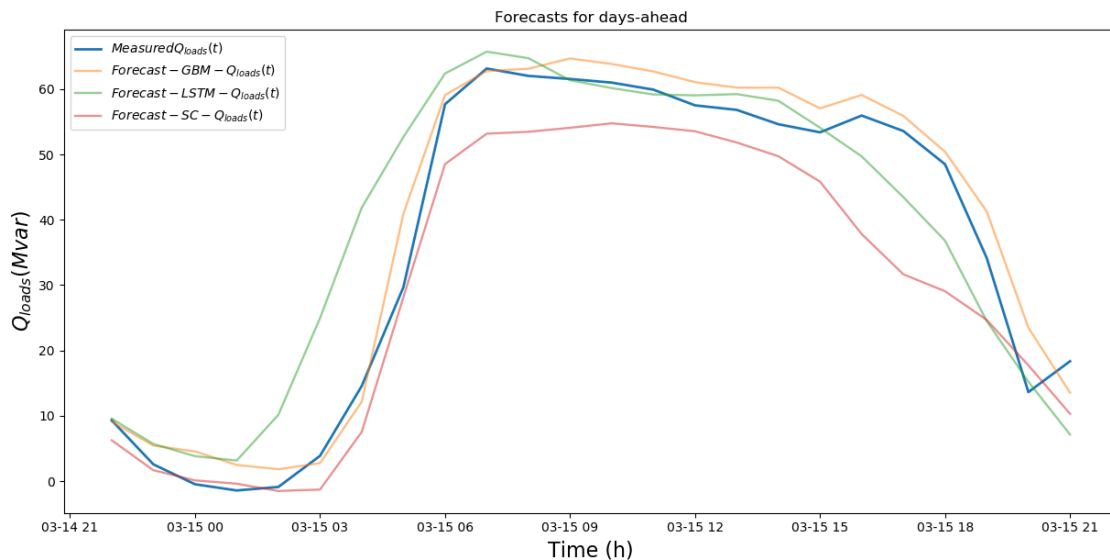


FIGURE 38 - DAY-AHEAD FORECAST CURVES FOR ALL THREE APPROACHES

TABLE 3 - ACCURACY VALUES AND INPUT-OUTPUTS FOR DAY-AHEAD FORECAST

| Forecast horizon | Method | RMSE (Mvar) | NRMSE | k_{test} | k_{test} dates | F | F dates |
|-------------------------|------------------------|-------------|--------|------------|------------------------------|------|----------------|
| 15/03/2019 Day-ahead | Gradient boosting | 4.50 | 0.0692 | 24 | 14/03 | 24 | 15.03 |
| | LSTM | 10.06 | 0.1558 | 24 | 14/03 | 24 | 15.03 |
| | Statistical clustering | 9.03 | 0.1398 | 24 | 15/03 | 24 | 15.03 |
| 2019 Day-ahead | Gradient boosting | 6.90 | 0.0613 | 24 | Day-before rolling window | 24 | Full 2019 data |
| | LSTM | 6.68 | 0.0592 | 24 | | 24 | |
| | Statistical clustering | 11.79 | 0.1044 | 2879 | Full 2019 data | 2879 | |

5.2.3.2 WEEK-AHEAD FORECAST

The week-ahead forecast was performed using inputs from the last 168 timestamps for the Gradient Boosting and LSTM methods. Therefore, $k_{test} = 168$ corresponded to the previous week of 8/3/2019 to 14/3/2019, while the forecast horizon $F = 168$ corresponded to the timestamps between 15/3/2019 - 21/3/2019. Alternatively, the statistical clustering method used the same $k_{test} = 168$, with the inputs being the time-related information for the timestamps of the forecast horizon F .

The Gradient Boosting method was again the one that presented the lowest errors. An RMSE of 6.8 Mvar was roughly 33 % lower than the 10.21 Mvar RMSE achieved with the LSTM method, and 23 % lower than the 8.82 Mvar found with the statistical clustering method. Figure 39 shows the curves for the forecast of $Q_{loads}(t)$ for the week of 15/03/2019 to 21/03/2019. Table 4 shows these results and the format of the inputs and outputs.

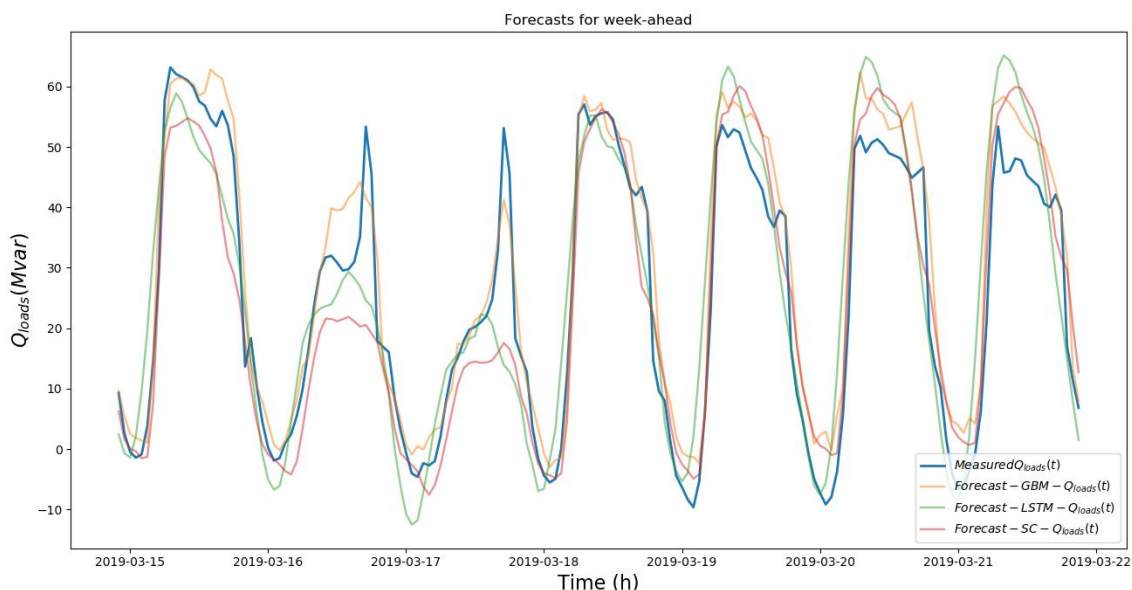


FIGURE 39 - WEEK-AHEAD FORECAST FOR THE THREE FORECASTING METHODS

TABLE 4 - ACCURACY FOR EACH FORECASTING METHOD USING THE WEEK-AHEAD FORECASTING HORIZON

| Forecast horizon | Method | RMSE (Mvar) | NRMSE | k_{test} | k_{test} dates | F | F dates |
|--------------------------|------------------------|-------------|--------|------------|------------------|------|----------------|
| 15/03/2019 Week-ahead | Gradient Boosting | 6.80 | 0.0932 | 168 | 08/03-14/03 | 168 | 15/03-21/03 |
| | LSTM | 10.22 | 0.1403 | 168 | 08/03-14/03 | 168 | 15/03-21/03 |
| | Statistical Clustering | 8.82 | 0.1212 | 168 | 15/03-21/03 | 168 | 15/03-21/03 |
| 2019 week-ahead | Gradient Boosting | 7.11 | 0.0630 | 168 | week-before | 168 | full 2019 data |
| | LSTM | 9.32 | 0.0826 | 168 | rolling window | 168 | |
| | Statistical Clustering | 11.79 | 0.1044 | 2879 | full 2019 data | 2879 | |

Again to account for the possible accuracy variability that comes from selecting different weeks to forecast, the week-ahead forecast method was implemented in a rolling window for the full test dataset of January to May 2019. The LSTM method achieves an accuracy of 9.32 Mvar for the full test duration. Alternatively, Gradient Boosting presented a performance of 7.11 Mvar. As the forecast with the statistical clustering method is not sensitive to a rolling window, it serves as benchmark to compare the Gradient Boosting and LSTM methods against.

5.2.3.3 MONTH-AHEAD FORECAST

The month ahead forecast was performed with $k_{test} = 672$ timestamps as inputs for both the Gradient Boosting and the LSTM methods. Both methods used data from 14/2/2019 to 14/3/2019 to forecast the values of $Q_{loads}(t)$ in the forecast horizon $F = 672$ from 15/03/2019 to 14/04/2019. The statistical clustering method had as inputs the time-related information for the timestamps in the forecast horizon.

The performance of the Gradient Boosting method for the month-ahead forecast produced an RMSE of 7.4 Mvar. This accuracy was very close to the one achieved with the statistical clustering method, which yielded an RMSE of 7.43 Mvar. LSTM method had an RMSE of 17.19 Mvar for the month-ahead forecast. Figure 40 shows the curves for $Q_{loads}(t)$ and the three forecasts for a period of one month.

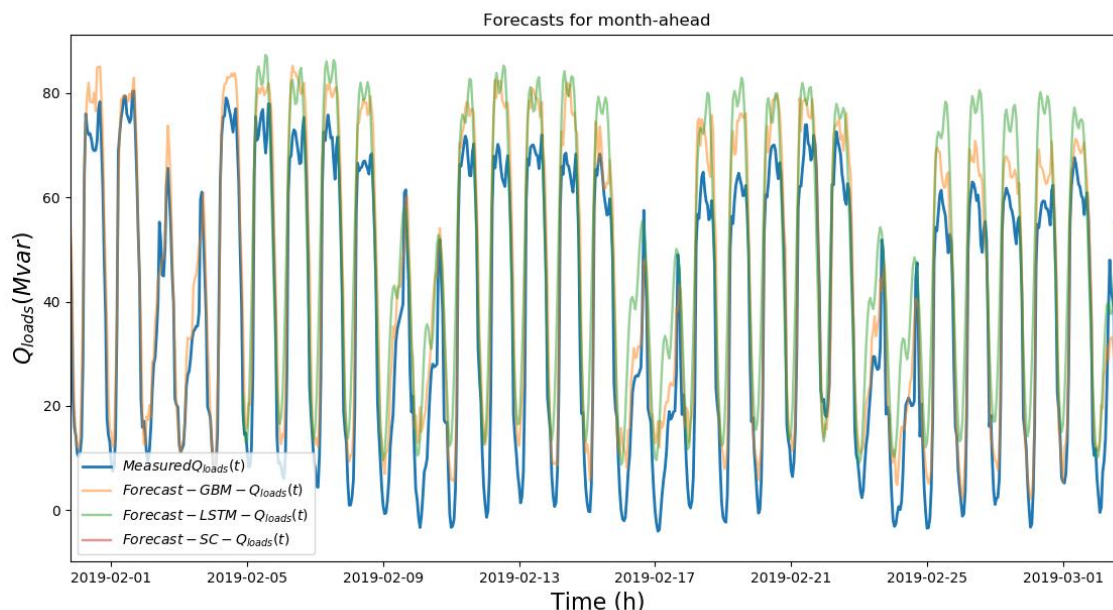


FIGURE 40 - MONTH-AHEAD FORECAST FOR $Q_{loads}(t)$ WITH THE THREE FORECASTING METHODS

Finally, the accuracy of the method over the full test dataset of 2019 was calculated. The month-ahead forecast was implemented in a rolling window. Therefore, only four forecasts are performed in the test dataset with both Gradient Boosting and LSTM methods. Since there are only four months in the full test dataset, the forecast for each month is calculated and concatenated. The performances for the full dataset yielded an RMSE of 7.6 Mvar for Gradient Boosting and 12.87 Mvar for LSTM. Once more, as the statistical clustering method does not benefit from the implementation of a rolling window, its RMSE for the full test dataset remained as 11.79 Mvar. Table 5 shows the results and formats for the inputs and outputs for the forecast with the three different methods.

TABLE 5 - ACCURACY FOR THE MONTH -AHEAD FORECAST WITH DIFFERENT METHODS

| Forecast horizon | Method | RMSE | NRMSE | k_{test} | k_{test} dates | F | F dates |
|---------------------------|------------------------|-------|--------|------------|------------------|------|----------------|
| 15/03/2019 Month-ahead | Gradient Boosting | 7.40 | 0.0928 | 672 | 14/02-14/03 | 672 | 15/03-14/04 |
| | LSTM | 17.19 | 0.2164 | 672 | 14/02-14/03 | 672 | 15/03-14/04 |
| | Statistical Clustering | 7.43 | 0.0936 | 672 | 15/03-14/04 | 672 | 15/03-14/04 |
| 2019 month-ahead | Gradient Boosting | 7.60 | 0.0758 | 672 | day-before | 672 | full 2019 data |
| | LSTM | 12.87 | 0.1223 | 672 | rolling window | 672 | |
| | Statistical Clustering | 11.79 | 0.1044 | 2879 | full 2019 data | 2879 | |

5.2.4 PERFORMANCE OF THE FORECAST SYSTEM

The training of the models requires a varying computing time depending on the model. For Gradient Boosting models, the training ranged from less than one minute to over fifteen minutes for a month-ahead forecast model. For LSTM models, the training times were considerably higher, reaching over one hour for training the month-ahead forecasting model. The statistical clustering forecast method required very little computational resources and was trained in less than one minute. This however needs to be run only on demand and when a significantly large enough amount of recent data is available. There are therefore no specific speed requirements. The forecasts themselves have a lead time of at least 12 hours and, if the model exists and has previously been trained, the computation is of the order of minutes. As regards to time, there is no additional limitation due to the forecasting process.

Regarding the actual performance of the forecasting in terms of accuracy, the implementation and testing with new data will occur during the demonstration period and will be reported in the demonstrator's specific deliverable: D6.9: "Finnish demonstrator - Market based integration of distributed resources in the transmission system operation". The initial accuracy calculations indicated that the LSTM method produces the most reliable forecasts for a forecast horizon of one day (day-ahead). For an horizon of a week-ahead, the Gradient Boosting method produced the lowest errors, with 6.68 Mvar RMSE. For a month-ahead forecast, again the Gradient Boosting method yielded the best results.

5.2.5 APPLICATIONS

The forecasting of the reactive power exchanges for the DSO network can be used by the DSO to determine the strategy to take in order to limit the costs for deviations from the PQ-window determined by the TSO. The shorter term forecasts (days or weeks) can be used to determine the needs for reactive power compensation and to eventually contract a part of it from commercial actors, either using bilateral contracts or by setting up a local reactive power market.

5.3 AMR-CONTROLLED ELECTRIC HEATING HOUSES FORECASTING

5.3.1 INTRODUCTION

In this case, the objective is to forecast the behaviour of habitations in the Helsinki area, which are heated with electricity and equipped with a heat storage system (i.e. a large hot water tank). They are also equipped with relays that can be activated by the DSO. Historically, these were used in order to set the heating systems to run at a fixed time during the night (typically starting at 10 pm). In previous work Koponen and Seppälä (2011), Koponen and Takki (2014), Koponen et al. (2019), a heuristic method for dynamic load control has been developed and tentatively used in order to adjust the consumption and take advantage of the lowest prices on the day-ahead market. Additionally, to support and enable the dynamic load control, a hybrid forecasting model using physical aspects and machine learning methods was developed and simulated. In this work, the model has been improved in order to forecast the state of charge more explicitly. This enables the forecasting and optimization of the resources to provide services such as Frequency Containment Reserves (FCR) and Frequency Restoration Reserves (FRR). When applying electricity heating load resource for these services the heating load would be controlled to support up-regulation by decreasing the load and/or down-regulation by increasing the load. It should be noted however that although the existing smart metering and communication system allows to send dynamic control signals to the houses, the latency in transmitting the control signals to the meters is not suitable to provide a response fast enough for the services considered. This problem can be solved by the roll-out of the next generation of smart meters with a new communication system. The roll out of next generation smart meters is however only in the specification phase and cannot be expected to happen until several years from now. Upgrading the existing communication system would be another option, but it would be too expensive compared to the expected benefits. The results from this forecasting will therefore not be applied in the field test, but some sample scenarios are run and detailed in D6.9: *"Finnish demonstrator - Market based integration of distributed resources in the transmission system operation"*.

In the following, a physically based model is presented first. It forecasts the heating needs, the expected load curves without any dynamic signals being sent and the load variations in response to dynamic control signals. Following it is a description of how the forecasting accuracy is improved by adding a machine-learning model to forecast the residual of the physically based model. The use of a hybrid model combines the strengths of the different approaches and ends up more accurate than its component models applied separately. In Koponen et al. (2019), an explanation of the modelling concepts and analyses with two real short-term load forecasting cases that include active demand is given. In EU-SysFlex, the machine learning model used (a Hierarchical Deep Neural Network, HDNN) is different from the ones used previously (Multi Layer Perceptron MLP and Support Vector Regression (SVR)). The machine-learning model is an application of a rather generic model for short-term forecasting electrical and heating load of buildings that was previously developed and applied in an internal project of VTT.

5.3.2 DESCRIPTION OF THE FORECASTING PROCESS

The houses can be separately controlled. In this study, they are aggregated in two groups and the objective is to forecast the aggregated load for each group. The grouping is due to the fact that the houses have used different values in order to dimension their heat storage. The houses in group 1 and 2 thus have different physical characteristics regarding their heating needs. The models describe the average behaviour of individual houses and can then be multiplied by the number of measured houses to give the aggregated forecast for a group.

5.3.2.1 INITIAL AND INPUT DATA

The data used to forecast the heating consumption of the houses is the following:

- Weather information downloaded from the Finnish Meteorological Institutes open data platform:
 - Hourly outdoor temperature for the Helsinki area
 - Outdoor temperature forecast up to one day ahead.
- Data provided by the DSO:
 - Measured hourly powers of the customers averaged over the modelled group
 - Planned control signals

from 2012 to May 2018.

5.3.2.2 ALGORITHM AND MODELLING

THE PHYSICALLY BASED MODEL

The main component of the physically based model is a simple first order model of the heat storage tank. Its purpose is to forecast the heating load as accurately as possible regarding the load control responses and load saturation. Machine learning methods typically fail with them but are in most other respects better than the physically based models. Figure 41 is a diagram representation of the partly physical model with the measured and forecasted temperatures, hourly power consumptions averaged over the group and the control signals as inputs. The figure shows the inputs in green, some of the internal model components in blue and the outputs in red.

The model also uses values that are calculated from the outdoor temperature using static nonlinear dependencies and the time lag that gives the best correlation. These dependencies are slowly identified on-line from the measured input history and they are:

- Daily energy need (Forecast energy consumption over the 24-hour long periods)
- Forecast of the maximum and minimum powers for the short-term forecast to be made.

In this partly physical model only the heat dynamics of the heat storage are considered. In full storage houses the heat flows from the storage to the house are controlled by the temperature settings of the house so there is no need to model heat dynamics for the houses except for the above mentioned time lag. The internal state of the model represents the state of charge (or assuming perfect mixing the internal temperature) of the heat storage tank. The heating power is always non-negative and smaller than the difference between the maximum and

minimum powers. The storage capacity is estimated based on the dimensioning requirements. It must be large enough to meet the house energy demand over the whole daytime length of the time of day (ToD) grid tariff.

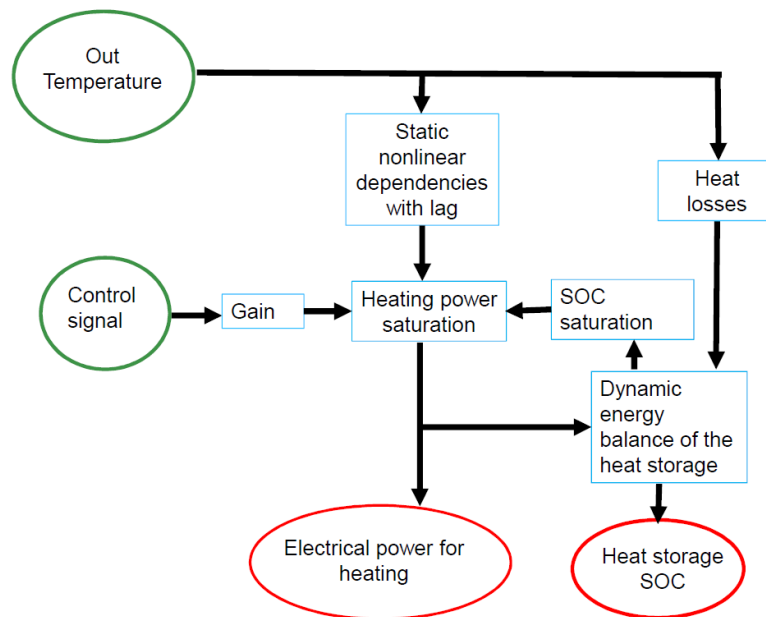


FIGURE 41 - REPRESENTATION OF THE PARTLY PHYSICALLY BASED MODEL FOR ELECTRICALLY HEATED HOUSES WITH AMR-CONTROL CAPABILITIES

A HYBRID MODEL INTEGRATING MACHINE LEARNING METHODS

Models based on machine learning methods often provide better accuracy than a physically based predictive model. Their performance is however subject to large errors in cases such as exceptional weather situations (i.e. input values out of the range of the ones experienced in the historical data) or in forecasting the response to dynamic control signals. Figure 42 shows how the physical and machine learning components of the model are interacting and used to complement each other. In this case, the machine learning method (Hierarchical Deep Neural Network, HDNN) used is different and more modern than the one applied in the previous work (Multi Layer Perceptron, MLP, and Support Vector Regression, SVR). The model implemented is a hierarchical deep neural network utilizing techniques like parameter sharing and sparse interactions. The latter property means that the network is not fully connected. The model forecasts the forecasting error of the physically based model using earlier forecasting errors with day of the week, controls, and outside temperatures as inputs. The model was developed at VTT within other projects (nationally funded ENETE and SGEM projects as well as internal development projects) and applied to the new data in this work.

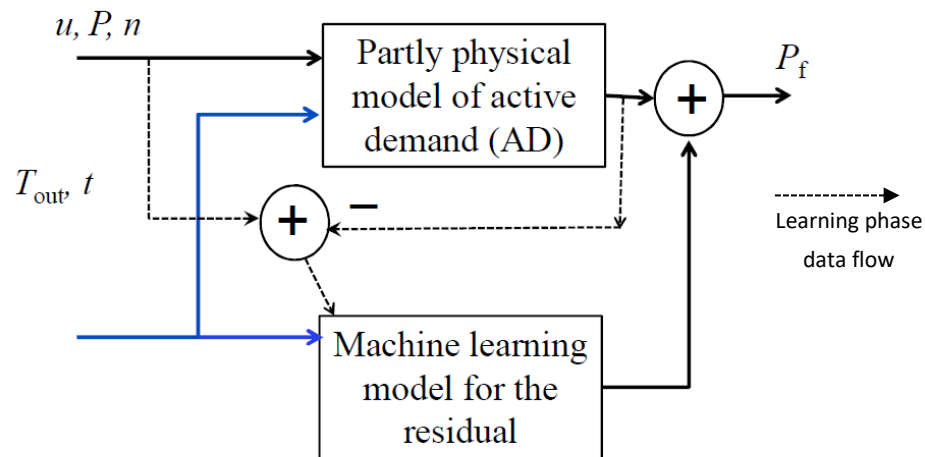


FIGURE 42 - DIAGRAM FOR THE HYBRID FORECASTING MODEL

5.3.3 FORECASTING RESULTS

5.3.3.1 FORECASTING QUALITY BASED ON HISTORICAL DATA

RESULTS FOR THE PHYSICALLY BASED MODEL

Figure 43 shows the aggregated physically based forecasts of Group 1 compared to the corresponding aggregated AMR measurements. The figures show also the forecasted state of charge (SOC) of the heat storage (normalised to 100 kWh/house + bias for readability) and the control signal, because they indicate how much the load can be changed by new control actions such as provision for frequency restoration reserve (FRR). The performance of the physically based model forecast is included in Table 6, along with the results of the hybrid models.

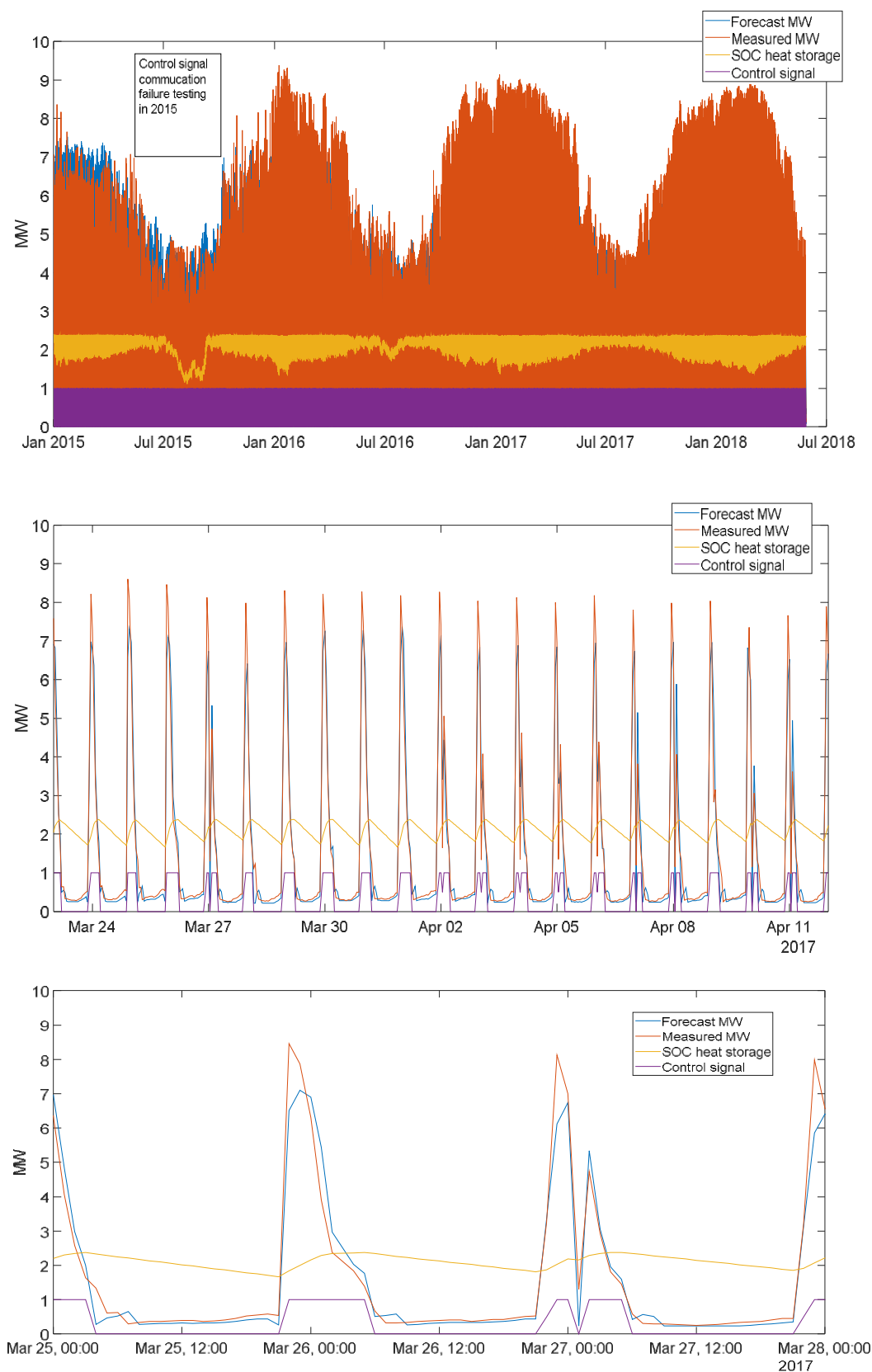


FIGURE 43 - PHYSICALLY BASED LOAD FORECAST: OVERVIEW, OVER A 20-DAY AND OVER A 3-DAY LONG PERIOD.

The dimensioning of the heat storage in the aggregated model is based on the measured responses and the local building requirements. They require that the capacity must be sufficient to meet the full daily heating energy demand by heating only during nights in a sustained -27°C outdoor temperature and taking into account variations in the hot water demand. The aggregated model represents the average behaviour so it is necessary to apply a rather large margin in taking care that all the houses have heat in the storage in all temperature situations. The state of charge (SOC), the state of the control signal and the maximum heating power together define how much control can be applied and in which direction. In practice, the SOC is rarely the active limiting parameter. It is possible to plan the control so that the SOC stays away from its limits. This is however more likely with longer periods of control. For example, preventing the SOC from reaching its required value during the night time could lead to some periods of daytime heating of the storage.

REACTION TO CHANGES IN THE CONTROL SCHEDULE

There is a need to know how much the load can change by following new control actions in order to know the potential that can be offered to frequency services markets and commercial balancing. The following figures show how much potential the model forecasts for individual one hour long load increases and decreases. The actual potential is somewhat smaller because it is necessary to reserve some margin for the forecasting errors. The load increase potential exists only when the heating load is turned off in the initial situation and the load decrease potential only when the load is initially in the on state. The load can be increased only to the extent that the state of charge of the heat storage does not exceed its maximum allowed value. At that point, the temperature in the water tank has reached its maximum and the local control system turns off the heating regardless of the control signal state. With the current installed systems and in the following figures, the loads are controlled so that every night the heat storage reaches its maximum temperature. Thus, the load increase potential is mainly in the afternoons and evenings. If it is expected that load increases will be required in the morning, it is possible to reduce the heating during the night in order not to have a full storage when a load increase would be required. Because the temperatures of the heat storages are not monitored it is necessary to regularly, once or twice a week, allow the heat storage of every house to reach its maximum temperature in order to ensure that the charging state in any house is not reduced too much. The figure shows the potential for load reductions during one hour, but actually nearly always much longer load reductions of the same size can be applied without causing any customer's loss of comfort, because the outdoor temperature is much higher than the heat storage dimensioning temperature. At extremely cold temperatures (below -27°C) the possibilities to control the heating are small because the operational margins become smaller with respect to providing adequate heating for every participating customer.

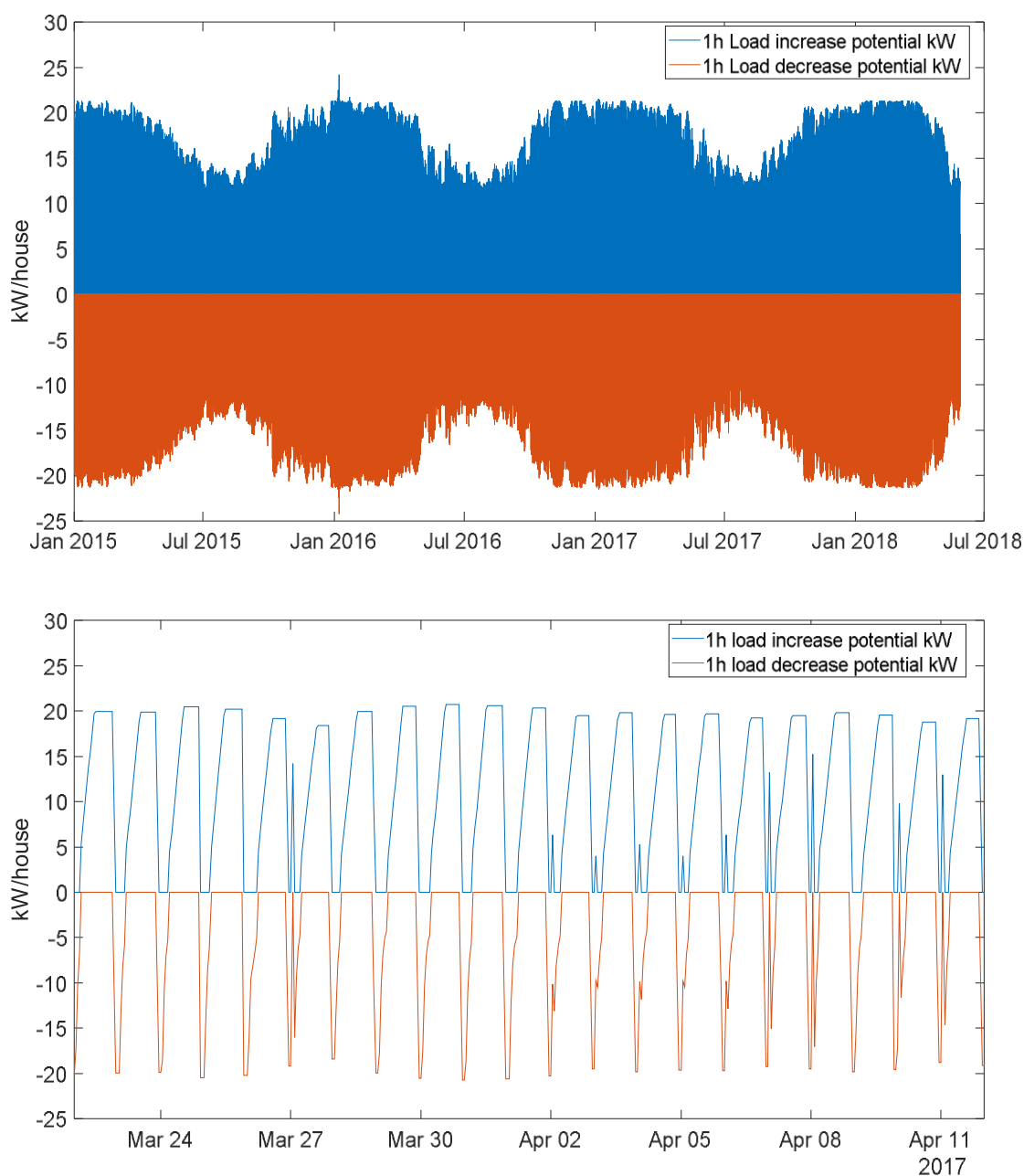


FIGURE 44 - POTENTIAL FOR AN HOUR-LONG LOAD INCREASE OR DECREASE: OVERVIEW AND OVER A 3-WEEK PERIOD

RESULTS FOR THE HYBRID MODEL

The following Table 6 shows the normalised root mean square of the forecasting error NRMSE (%) in the whole verification period (Jan 2015 — May 2018) and in the end part of the verification (April 2016 — May 2018) for the physically based model alone and for the hybrid model (physically based response model + hierarchical deep neural network forecasting the residual). All the models were identified using the time period 1 June 2012 – 1 June 2013. In Table 6, the difference between hybrids 1 and 2 is that hybrid 2 was identified from the residual of the total summed power of both groups while the hybrid 1 identified separate models for each of the two groups. The results for April 2016 – May 2018 are more valid due to the reasons explained next. In 2015 and in early 2016 there were many tests to deliver control signals at short notice causing many houses failing to get the control signals in time. (The meters ignore outdated control signals). These communication failures affect the forecasting

accuracy in the beginning of the period as can be seen in Figure 46. These initial communication performance tests in 2015 only roughly revealed that the smart metering communication system was not capable of controlling the loads for the provision of fast ancillary services, but did not estimate the latencies and reliability of control signal communication of the AMR system with any useful accuracy.

TABLE 6 - COMPARISON OF THE FORECASTING ACCURACY OF THE MODELS

| NRMSE (%) | Jan 2015 — May 2018 | | | April 2016 — May 2018 | | |
|------------------------------------|---------------------|---------|-------|-----------------------|---------|-------------|
| | Group 1 | Group 2 | G1+G2 | Group1 | Group 2 | G1 + G2 |
| Physically based | 48.6 | 54.2 | 45.1 | 39.0 | 49.9 | 37.9 |
| Hybrid 1 (Physically based + SVR) | 47.4 | 40.1 | 37.8 | 38.9 | 35.2 | 30.7 |
| Hybrid 2 (Physically based + HDNN) | 38.2 | 41.7 | 34.3 | 30.3 | 36.9 | 27.9 |

The NRMSE % values are in this case high compared to other forecasting cases, because they are normalised to the mean load that is small compared to the load peaks. Thus, relatively small errors in the forecasting of the daily peak loads result to relatively high NRMSE values. In this case, normalising the RMSE also to the daily peak load, could be used when comparing with the performance in other load forecasting cases. The mean power for group 1 = 1.268 MW and for group 2 = 1.165 MW and the peak powers are 9.136 MW and 8.636 MW respectively.

Figure 45 illustrates the results of the forecasting for the aggregated power of the combined 727 houses of groups 1 and 2.

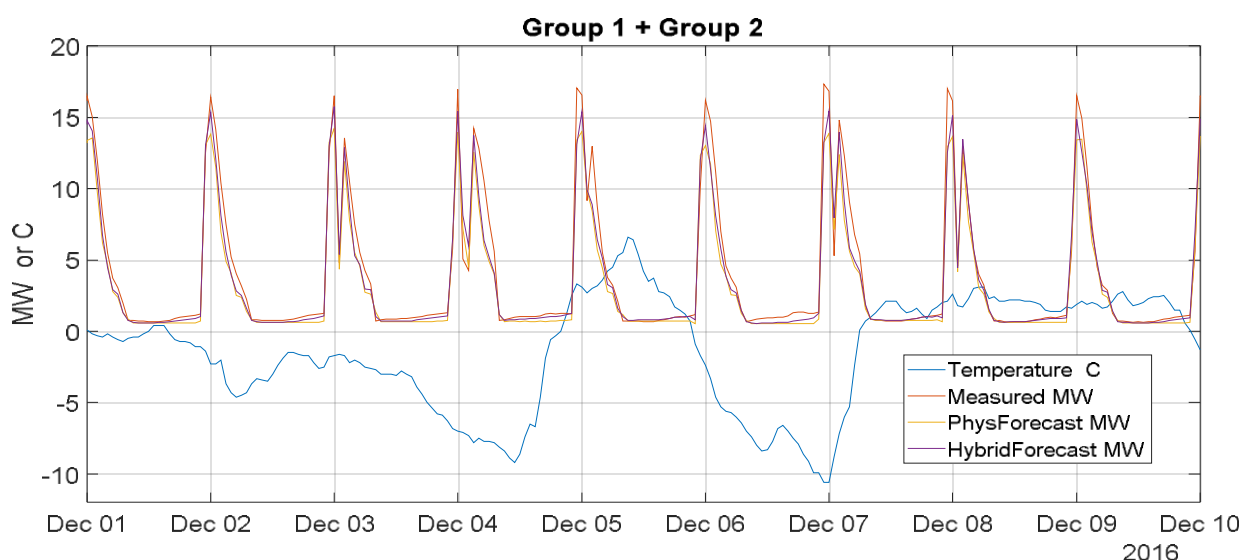


FIGURE 45 - FORECAST RESULTS FOR THE AGGREGATED POWER OF THE 727 HOUSES

Figure 46 shows the respective forecasting errors over the whole verification period.

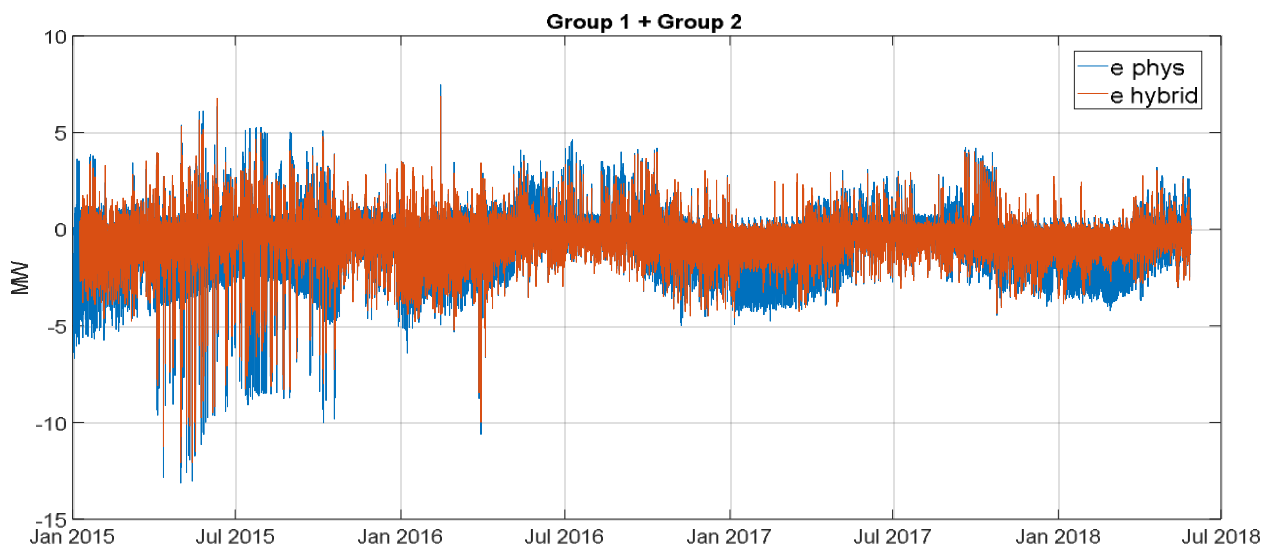


FIGURE 46 - FORECASTING ERROR OVER THE VERIFICATION PERIOD

The following observations can be made regarding the forecasting errors: In the first year there are many large errors caused by failures in control signal communication and related testing. One high peak occurs at the shift from normal time to summer time. Every autumn there are clusters of high errors that the forecasting models cannot explain. Adding the modelling of special days, such as national holidays, is not included and it is expected to improve the forecasting accuracy for those days. More detailed views reveal repeating error patterns. Thus, the forecasting errors give hints that there are still possibilities to improve the forecasting performance by developing and tuning the models or by using a longer identification period for the machine learning than the one-year -period that as was used in this model.

5.3.4 PERFORMANCE OF THE FORECAST SYSTEM

The identification for the physical model and the training for the neural network models require programming and computing times of several hours. The programming time is required due to the fact that new data is not arriving according to communication standards and needs to be fitted into the algorithms. This however needs to be run only on demand and when significant changes happen in the consumers groups. There are therefore no specific speed requirements. The forecasts themselves have a lead time of at least 12 hours and, if the model exists and has previously been trained, the computation is under a minute.

As regards to time, there is no additional limitation due to the forecasting process.

Regarding the actual performance of the forecasting in terms of accuracy, this tool will not be implemented in the field. It will be used within simulations and the results will be reported in deliverable: D6.9: *“Finnish demonstrator - Market based integration of distributed resources in the transmission system operation”*.

5.3.5 APPLICATIONS

The created forecast of the flexibility potential for up and down regulation of electric heating (with heat storage water tank) controlled via AMR meters cannot be utilized in a real environment demonstration during EU-SysFlex due to slowness in the current communication systems that occurs with a large number of AMR meters. The communication channel of current metering system is too slow to meet the requirements of activation times in the TSO ancillary markets. The forecast of AMR electric heating loads developed in T6.3 is being utilized in the AMR simulation cases of T6.4. The objective of the simulations is to analyse the demand response profitability with a few case scenarios. The results of the simulation cases will be presented in D6.9 Market based integration of distributed resources in the transmission system operation.

5.4 EV CHARGING STATION FORECASTING

5.4.1 INTRODUCTION

The objective of the EV charging station forecasting tool is to provide an estimate of the aggregated flexibility that the stations can make available for specific network services. In this case, only public charging stations are taken into account and not private ones. In order to provide services, the mathematical models for the available flexibility of an EV are developed based on the descriptions of different products for the reserve electricity markets. Then, the aggregated probability density function (PDF) of EVs flexibility is obtained and used to estimate the available flexibility for the following day for a group of charging stations. Finally, by performing a stochastic analysis, the maximum expected profit of EVs from participation in the reserve electricity market is calculated (this step is reported in the EU-SysFlex D6.5 - *Optimization tools and first applications in simulated environments*). The proposed methodology is tested using the empirical charging data of EV public charging stations owned by Helen in Helsinki area from 2015 to 2018.

5.4.2 DESCRIPTION OF THE FORECASTING PROCESS

In the Finnish demonstrator, the analysis for the flexibility potential of the EV charging stations is focusing on the provision of Frequency Containment Reserve for Normal operation (FCR-N) and Frequency Containment Reserves for Disturbance situations (FCR-D). The aim of FCR-N is to regulate the power system frequency within a range of 49.9 – 50.1 Hz, during normal dynamic variations, while the FCR-D providers will be activated whenever the frequency is below 49.9 Hz, in case of larger disturbances. According to the market regulations of FCR-N and FCR-D, the flexibility resources must provide their service as long as the frequency is out of the nominal range and they can come back to their nominal consumption/production when the grid frequency is in the nominal range for at least three minutes. However, the regulation allows reserve units with limited capacity, e.g. storage systems, to stop their service after 30 minutes even if the frequency does not come back to the nominal range. It means that the maximum activation time in this case can be considered to be half an hour.

In frequency reserve markets, the reserve providers are compensated for providing capacity and energy. The provided energy is remunerated according to the up- or down-regulating market prices, which are determined in real-time. Since the energy pricing is designed to encourage the providers to alleviate frequency deviations, the energy provided for FCR makes some profit for the flexibility providers. However, the amount of this energy, the price, and the profit are not clear when flexibility providers make the offer a day ahead. On the other hand, the capacity fee is paid based on provided capacity even if it is not used. The capacity fee is paid based on two different agreements: yearly and hourly market agreement. For yearly agreement in 2018, the capacity of FCR-N and FCR-D were paid respectively 14 €/MWh and 2.8 €/MWh. On the hourly market, the capacity fee determines by competition for each hour in a day ahead market.

The FCR-N has a higher reimbursement level in comparison to FCR-D, but it needs to provide continuously the reserve symmetrically in both directions (up- or down-regulation). However, the FCR-D needs to be activated

when the frequency is less than 49.9 Hz; it means it will be only up-regulation reserves. In these circumstances, the demand, e.g. EVs, can provide higher FCR-D than FCR-N, due to the fact that, typically, demand can be decreased or even turned off but it can more rarely be increased over its operating point or at the very least above its nominative power. In the next subsections, this difference and its impact on the flexibility that EV charging stations can provide will be explained in more details.

5.4.2.1 INITIAL AND INPUT DATA

The data used to forecast the flexibility of public EV stations is the following:

- Data about the charging events in the set of stations, provided by Virta and downloaded by Helen:
 - Customer ID
 - Station ID and name
 - Start time
 - End time
 - Energy charged

5.4.2.2 ALGORITHM AND MODELING

EV FLEXIBILITY POTENTIAL

Usually, when an EV is plugged into an electricity source, it is charged with maximum possible power in the beginning of the period, until the battery is fully charged. Figure 47 shows this simple charging profile for an EV

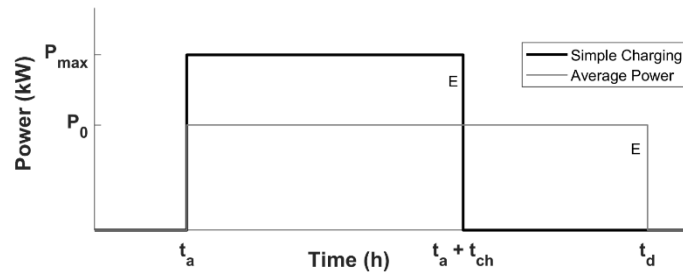


FIGURE 47 - THE SIMPLE CHARGING PROFILE AND AVERAGE POWER CHARGING OF AN EV

arriving at t_a and departing at t_d , with a need for E kWh electrical energy, where a positive value of P represents charging power. This diagram neglects the fix voltage charging stage at the end of the charging cycle. In these circumstances, the required time (t_{ch}) for charging the energy E (kWh) to the EV can be calculated by:

$$t_{ch} = \frac{E}{P_{max}\eta}, \quad (14)$$

where P_{max} is the maximum power of EV chargers and η is the efficiency of the charger.

The flexibility of EVs when they are charging stems from the fact that, often, the plugged-in time ($t_p = t_d - t_a$) is longer than the required charging time (t_{ch}). In this case, the EV may adapt itself to the power system dynamics

without making any change in the final charged energy at the end of the plugged-in period. According to the market regulation, this flexibility can be quantified in down-regulation and up-regulation direction considering power and energy constraints of the EV.

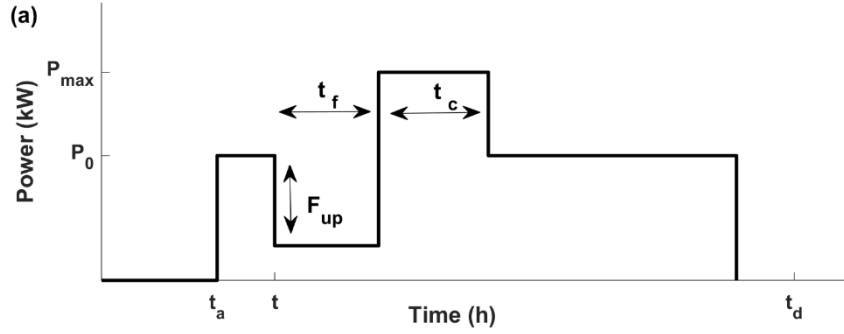


FIGURE 48 - THE CHARGING PROFILES PROVIDING UP-REGULATION RESERVES

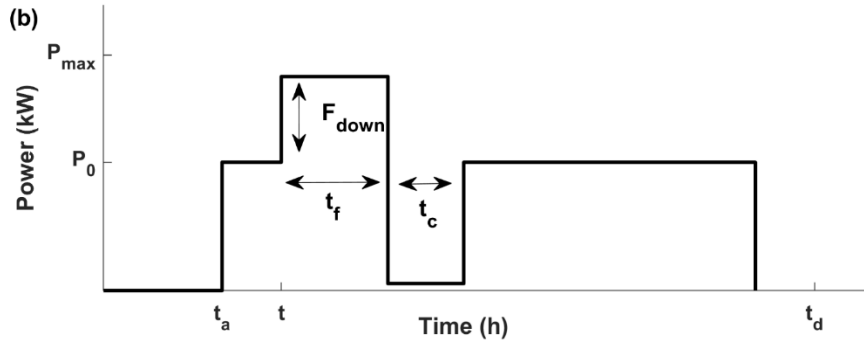


FIGURE 49 - THE CHARGING PROFILES PROVIDING DOWN-REGULATION RESERVES

UP-REGULATION RESERVE

Up-regulation reserve is defined as an increase in generation or a decrease in demand. Therefore here an up-regulation means reducing the charging power. Figure 48 shows a charging profile for an EV providing up-regulation

reserve ($F_{up}(t)$ kW) at time t for t_f hour, while needing t_c hour to compensate for the decrease in the charging profile. This up-regulation power is limited by P_0 , the consumption power of the EV in the moment of providing flexibility.

In addition to this limit, the energy requirement of the EV adds another constraint for up-regulation reserves. Since the flexibility providers must have the ability to continue full activation at least for half an hour ($t_f \geq 0.5$), and providing flexibility should not change the amount of the charging energy in the EV, the following must be satisfied:

$$P_{\max} \eta (t_d - t - 0.5) \geq E - E(t) - 0.5 \eta (P_0 - F_{up}(t)), \quad (15)$$

where $E(t)$ is the charged energy to the EV from t_a until time t . The left term states the maximum possible charging energy into the EV after providing up-regulation reserve and the right term formulates the required energy to the EV after providing the flexibility. Assuming a flat charging profile for the EV before time t , $E(t)$ can be replaced by $P_0 * \eta * (t - t_a)$. In these circumstances, the up-regulation reserve in time t ($F_{up}(t)$) can be calculated as:

$$F_{up}(t) = \min \left(P_0, \frac{P_{\max} \eta (t_d - t - 0.5) + P_0 \eta (t + 0.5 - t_a) - E}{0.5 \eta} \right). \quad (16)$$

In these circumstances, the EV should start to charge with power equal to or greater than the average power (P_{av}) to make sure to reach the required energy level at the end of the charging period.

$$P_{av} = \frac{E}{\eta (t_d - t_a)}. \quad (17)$$

If the EV starts to charge with a power larger than the average charging power it can provide a larger amount of up-regulation reserve at the beginning of the charging period. However, it cannot provide any up-regulation reserve in the later time since the charging power becomes zero due to the required energy or battery capacity.

DOWN-REGULATION RESERVE

Down-regulation reserve is defined as a decrease in generation or an increase in demand. Therefore here down-regulation means the increase of charging power. Figure 49 shows a charging profile for an EV providing down-regulation reserve at time t ($F_{down}(t)$ kW) for t_f hour, while needing t_c hour to compensate the extra charging in the profile. This down-regulation power is limited by $P_{\max} - P_0$.

In addition to this limit, the energy requirement of EV, or the maximum capacity of EV's battery, makes also another constraint in down-regulation reserve. Since the charging energy should be stopped, if the EV charged to the desired amount of energy, and the flexibility should be available at least for half an hour; the following constraint must be satisfied:

$$E(t) + 0.5 \eta (F_{down}(t) + P_0) \leq E. \quad (18)$$

The right term in (18) states the charging energy into the EV after providing down-regulation reserve and the left term formulates the required energy to the EV. Assuming the flat charging profile for the EV before time t , similar to up-regulation, the down-regulation reserve in time t ($F_{down}(t)$) can be calculated as:

$$F_{down}(t) = \min \left(P_{\max} - P_0, \frac{E - P_0 \eta (t + 0.5 - t_a)}{0.5 \eta} \right). \quad (19)$$

In order to provide down-regulation, the EV should start to charge with power less than the maximum power, but definitely more than the average power ($P_{av} \leq P_0 \leq P_{\max}$) to make sure that the EV can reach to the desired energy level if there was no need of down-regulation.

It is worth mentioning that in most of the cases, providing up-regulation by the EV is easier than down-regulation. The reason is the fact that although the plugged-in duration ($t_d - t_a$) is normally more than the required charging time (t_{ch}), it is not very much longer than that in most of the cases, as has been verified from the empirical data.

Therefore, the average power is closer to the maximum power in comparison to zero and $P_{max} - P_o$, the down-regulation limit is less than P_o , up-regulation limit.

MODELS FOR THE FLEXIBILITY POTENTIAL OF EV CHARGING EVENTS

The flexibility providers are compensated for providing capacity and energy, while the energy remuneration cannot be determined a day ahead. Therefore, the following EV flexibility models are based on maximising the flexibility capacity over the plugged-in time.

FCR-N model

The FCR-N providers should offer symmetrical reserves for up- and down-regulation at any time. Therefore, the initial charging power of the EV (P_o) should be selected so that the minimum capacity of up- and down-regulation reserve is maximized over the plugged-in time. It means that the amount of FCR-N flexibility ($F_{FCR-N}(t)$) at time t , can be calculated as follows:

$$F_{FCR-N}(t) = \max_{P_o} \left(\int_{t=t_a}^{t_d} \min(F_{up}(t), F_{down}(t)) dt \right), \quad (20)$$

s.t.

$$P_{av} \leq P_o \leq P_{max}$$

It is a single variable optimization with an upper and lower bound for the variable. This optimization can be solved with different methods. In this case, the MATLAB *fminbnd* function was used.

FCR-D model

Because the FCR-D flexibility is only in the up-regulation direction, the capacity of up-regulation reserve should be maximised over the EV plug-in time, as follows

$$F_{FCR-D}(t) = \max_{P_o} \left(\int_{t=t_a}^{t_d} F_{up}(t) dt \right), \quad (21)$$

s.t.

$$P_{av} \leq P_o \leq P_{max}$$

The flexibility that can be provided decreases when the time t becomes close to the departure time. Therefore, providing the whole flexibility as much as possible in the beginning part of plugged-in time can increase the capacity over time. In these circumstances, $P_o = P_{max}$ maximises (21). Therefore, FCR-D flexibility ($F_{FCR-D}(t)$) can be calculated as follows:

$$F_{FCR-D}(t) = \begin{cases} \min \left(P_{max}, \frac{P_{max} \eta (t_d - t_a)}{0.5 \eta} \right) & t \leq t_a + t_{ch} \\ 0 & t > t_a + t_{ch} \end{cases} \quad (22)$$

PROBABILITY DENSITY FUNCTION OF EV CHARGING EVENTS FLEXIBILITY

The model just described to estimate the flexibility potential of EV charging events includes some variables, such as arriving time, departure time, desired energy level, which are not known in advance. Therefore, the EV flexibility needs to be forecasted. Analysis of the available data revealed that only the time of day had an impact on the occurrence of charging events. For this reason, a general stochastic model over a single day was selected. For this purpose, first, the aggregated PDF of a group of EVs is calculated using historical data to predict the available flexibility in a day ahead market. Then, the expected profit of providing flexibility is maximised using a stochastic optimization.

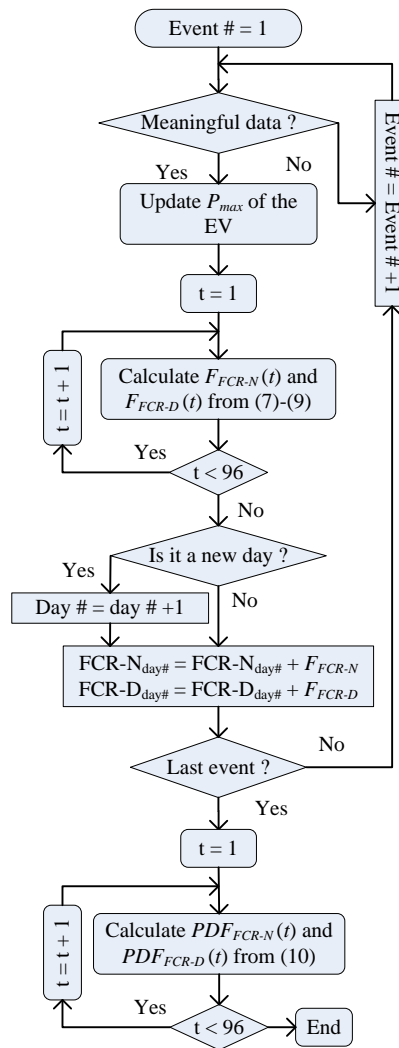


FIGURE 50 - PROCESS USED TO CALCULATE THE AGGREGATED PDF FOR A GROUP OF EVS

In order to obtain the PDF of the aggregated flexibility, the historical data of EV charging events in all available charging stations should be analyzed. Figure 50 shows a flowchart detailing how the PDF of the aggregated flexibility for a group of EVs is calculated. In this flowchart, Event# and day# are used to point respectively the event counter and day counter.

The method calculates the PDF of the aggregated flexibility by analyzing data of all charging events, while the charging stations normally do not have access to EV information, such as EV type and the battery size. However, the available records from the charging stations includes the following charging events data:

- The customer ID encrypted for data protection,
- The station ID, and the maximum station power,
- The type of charging, AC or DC charging,
- The arrival and departure time (t_a and t_d),
- The charged energy (E in kWh).

The flexibility models developed in (20) and (22) need the maximum charging power for each EV ($P_{max,EV,i}$), which is not known by the charging stations. Therefore, the method should estimate this value using the available data. However, before this estimation, since the measured data may include some meaningless records, the data needs to be cleaned up. An EV charging event was simply removed if it showed one of the following issues:

- Missing items,
- Duration plugged-in less than five minutes,
- Energy charged less than 0.1 kWh or more than 100 kWh,
- Charging power more than the charging station rate.

After cleaning-up the data, the maximum charging power for each EV is updated as follows:

$$P_{max,EV,i} = \begin{cases} \max(P_{max,EV,i}, P_{av,EV,i}) & \text{AC charging} \\ P_{max,EV,i} & \text{DC charging} \end{cases}, \quad (23)$$

where $P_{av,EV,i}$ the average charging power of i -th EV, can be calculated using the available data from (17). It is important to notice that when an EV uses direct current (DC) charging, the onboard charger of the EV is bypassed, and therefore the result should not be used for updating the maximum charging power of that specific EV.

After finding the maximum power for each EV, the daily flexibility profile resulting from one charging event can be obtained by solving (20) and (22) respectively for FCR-N and FCR-D in each time interval. Here, each day divided into 96 time-interval to calculate the flexibility profiles with 15-minute resolution. Then, the aggregated daily flexibility profiles is formed by aggregating the results of all the charging events expected to occur in one day.

These daily flexibility profiles are used to calculate the probability of having f kW of FCR-N or FCR-D flexibility at time t , shown by $PDF(f,t)$ in general form. These PDF can be calculated by partitioning the flexibility power to several bins in each time interval and counting members of each bin over to the total numbers, as follows:

$$PDF(f,t) = \frac{N_f(t)}{\sum N_f(t)} \quad (24)$$

where N_f is the number of days that flexibility power calculated from (20) or (22) in time t is equal to f . The function of *histcounts* in MATLAB can perform this partitioning process.

FLEXIBILITY PROFILE ESTIMATION

Based on the PDF, the expected available flexibility profile for the following day can be calculated as follows:

$$F_{ex}(t) = \int PDF(f, t) f(t) df, \quad (25)$$

where $F_{ex}(t)$ is the expected available flexibility in time-interval t , and can be either FCR-N or FCR-D. However, since the flexibility market has a penalty for providing less flexibility than what scheduled, it is not optimum to participate in the market with the expected maximum flexibility. The providers must participate in the market with the optimum profile, which maximises the expected profit.

The profit of the flexibility provider (PR) can be calculated as follows:

$$PR(F, t) = \begin{cases} F \pi_f & f \geq F \\ f \pi_f - (F - f) \pi_{-f} & f < F \end{cases}, \quad (26)$$

where F is the amount that flexibility provider promised for the time; f is the actual amount of flexibility that will happen in real-time and can be estimated using PDF in (24); π_f is the remuneration amount based on €/MW,h; and π_{-f} is the penalty of not providing the promised flexibility. Therefore, the expected profit (PR_{ex}) of the flexibility provider from participating in the reserve market will be:

$$PR_{ex}(F, t) = PDF(f \geq F, t) F \pi_f + \int_0^F (f \pi_f - (F - f) \pi_{-f}) PDF(f, t) df, \quad (27)$$

while

$$PDF(f \geq F, t) = 1 - \int_0^F PDF(f, t) df, \quad (28)$$

where CDF is the cumulative density function. In order to maximize the expected income, F must be selected so that $\partial PR_{ex} / \partial F = 0$. Therefore, the optimum flexibility value (F_{op}) can be calculated from (27) and (28) using Leibniz's rule as follows:

$$\begin{aligned} \frac{\partial PR_{ex}(F_{op}, t)}{\partial F_{op}} &= \\ &= \pi_f - \pi_f CDF(F_{op}, t) - \pi_{-f} CDF(F_{op}, t) = 0, \end{aligned} \quad (29)$$

$$CDF(F_{op}, t) = \frac{\pi_f}{\pi_f + \pi_{-f}}. \quad (30)$$

In other words, the flexibility provider should participate in the reserve flexibility market by amount F_{op} , which satisfies (30). In the current Finnish reserve market regulations, $\pi_f = \pi_{-f}$; therefore, the median of flexibility distribution is the value which maximizes the expected income from participating in the reserve market. In this stage, the flexibility providers could decide which market, e.g. FCR-N, FCR-D, or a combination, has more profit by calculating (30) for all available market, e.g. (20) and (22).

5.4.2.3 REALIZATION OF THE FORECASTING SYSTEM

The realization of the forecasting system is expected to be performed in a fairly manual manner. Currently the forecasting algorithm is run locally on a computer at VTT. The aim is to transfer the forecasting program to the aggregator Helen, so that it can be run locally at Helen. The program is modified by VTT in such a way that it is possible to include new data sets and update the forecast whenever needed. The new data includes new, more recent information about the amount of charging events in the public charging network of Helen. This way, Helen can keep track of the development of the EV flexibility potential. At this stage, no online interfaces are built through which the forecast could be run and updated in a cyclic and regular manner. The reason for this is the uncertainty surrounding the actual usage of EV charging stations for the purpose of TSO ancillary services. Such interfaces can be implemented at a later stage. Moreover, due to the statistical method that is used for the forecasting, the changes in the forecasting result with new, more recent data will not be significant. Only major changes in the amount of charging events will have an effect. This is also one reason why there is no need, at least currently, to update the forecast frequently.

5.4.3 FORECASTING RESULTS

5.4.3.1 FORECASTING QUALITY BASED ON HISTORICAL DATA

CHARGING EVENTS EMPIRICAL MODEL

The first results of the forecasting work for the EV charging station is an empirical model for the behaviour of the EVs connected to them. The data used to obtain it includes the charging records of public EV charging stations in the Helsinki area from Oct. 2014 to Oct. 2018, which contains about 41 000 charging events of about 2 500 customer IDs, after cleaning process.

Figure 51 shows the probability density of the EV arrival time to charging stations during a day. This probability density can be used to allocate the number of charging events per day for each 15-minute time interval. For instance, the probability related to the time interval (8:45-9:00) is 0.03 which means in a day with 33 charging events, it is expected that one event would start during the time interval.

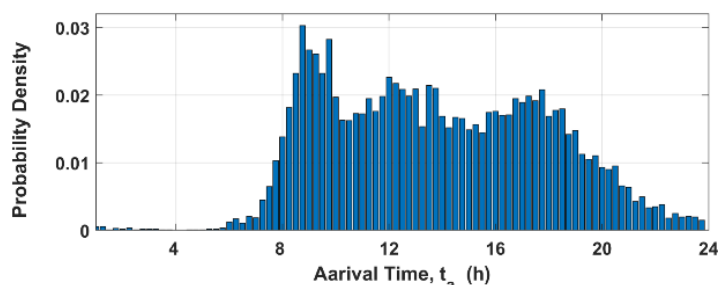


FIGURE 51 - THE PROBABILITY DENSITY OF EVs ARRIVAL TIME, t_a , TO CHARGING STATIONS DURING 2018.

Figure 52 shows the probability density of EV charging duration. The average EV charging time in the public chargers of the Helsinki area is 2 hours and 48 minutes. However, the longest one is more than 14 days (a definite outlier, but showing the variety of the inputs). A probability density function following a Weibull distribution with

optimized shape and scale parameters equal to 2.620 and 0.898, respectively has been calculated to represent distribution of the EV charging duration.

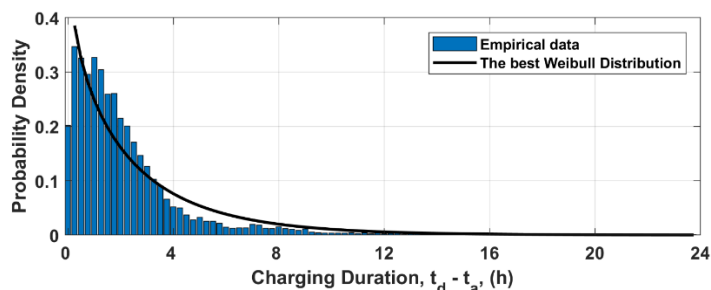


FIGURE 52 - THE PROBABILITY DENSITY OF EVs CHARGING DURATION, $t_d - t_a$, AND THE BEST WEIBULL DISTRIBUTION FIT TO THIS PROBABILITY DENSITY

Figure 53 shows the probability density of EV charging energy (kWh). The average charged energy of an EV in a charging event is about 10 kWh. The best probability density function following a Log-logistic distribution with shape and scale parameters equal to 1.827 and 0.566, respectively has been calculated to represent the EV charging energy distribution.

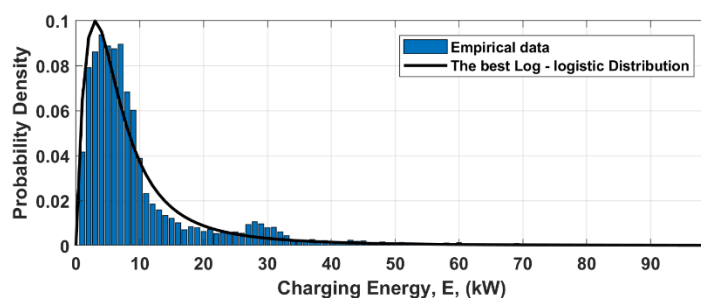


FIGURE 53 - THE PROBABILITY DENSITY OF EVs CHARGING ENERGY, E, (KWH) AND THE BEST LOG-LOGISTIC DISTRIBUTION FIT TO THIS PROBABILITY DENSITY

EV FLEXIBILITY

The aggregated daily profile of FCR-N and FCR-D flexibility and the corresponding PDFs can be obtained by the methodology explained in the description of the forecasting. Figure 54 shows the CDF for FCR-N (a) and FCR-D (b) which can be provided by EV public charging stations of the Helsinki area, based on last year records. Because most EV can provide more up- than down-regulation reserves, as explained in previous chapters, they still have potential to provide FCR-D after providing FCR-N, which is called here FCR-Dn (c).

Using these CDFs, the expected flexibility and the optimum flexibility profile can be estimated using (25) and (30), respectively. Figure 55 shows the expected flexibility profiles, while Figure 56 shows the optimum flexibility profile for different flexibility products. Comparing the two figures shows that the optimum profiles of flexibility, which make the maximum expected profit are quite similar to the expected value. This similarity is due to the fact that the current market regulations have the penalty equal to the remuneration price ($\pi_f = \pi_{-f}$).

It can be noticed that the expected consumption, and thus flexibility, is close to zero during night time. This is due to the fact that the only charging stations considered are public ones and that private charging and the EV owners homes are not included.

Another observation is that the maximum expected FCR-N flexibility of this group of EVs is much lower than the expected FCR-D flexibility (about 12 kW against about 143 kW at 2:00 p.m.). However, the expected profile of FCR-Dn shows that EVs can still provide a considerable amount of FCR-D after providing FCR-N.

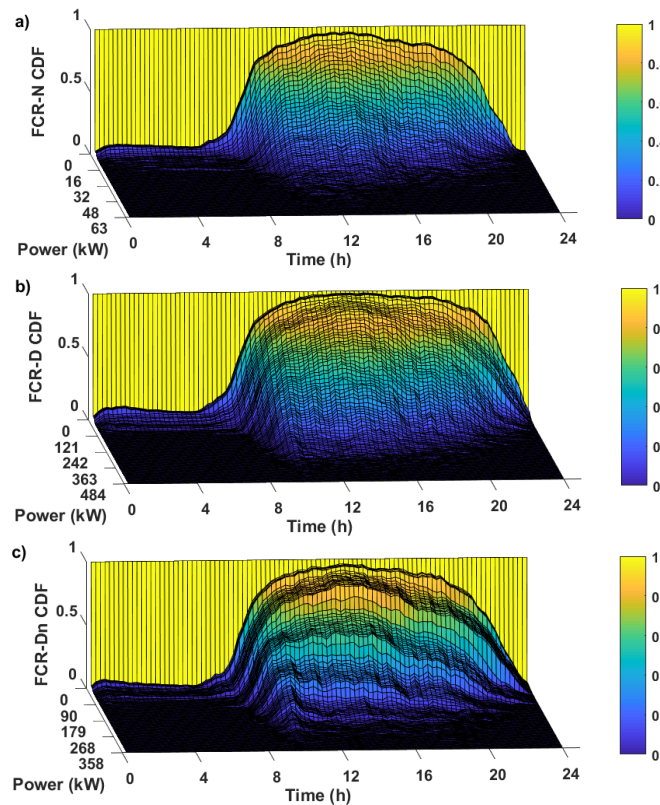


FIGURE 54 - THE CUMULATIVE DENSITY FUNCTION (CDF) OF a) FCR-N, b) FCR-D, AND c) FCR-Dn FLEXIBILITY EACH TIME OF A DAY PROVIDED BY EVs.

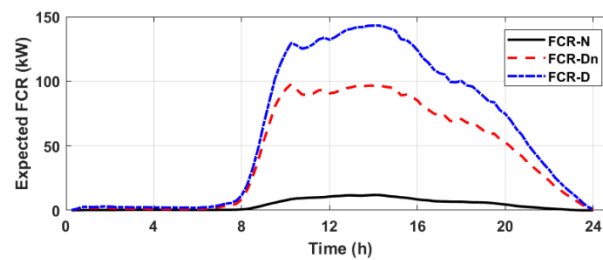


FIGURE 55 - THE EXPECTED FLEXIBILITY PROFILES OF EVs CHARGED IN HELSINKI AREA.

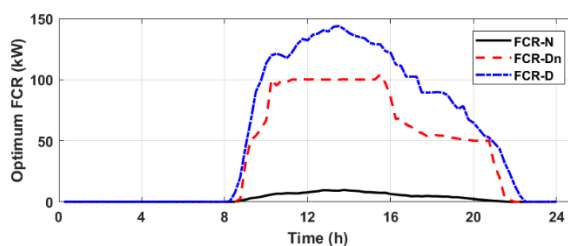


FIGURE 56 - THE OPTIMUM FLEXIBILITY PROFILES OF EVs CHARGED IN HELSINKI.

TABLE 7 - AVERAGE DAILY PROFIT (IN €) CALCULATED FOR PROVIDING FLEXIBILITY PRODUCTS DURING OCT. 2018

| | | FCR-N | FCR-D | FCR-N + FCR-Dn |
|------------------------|------------|-------|-------|----------------|
| Proposed Method | Absolute | 3.846 | 9.452 | 10.99 |
| | Per events | 0.057 | 0.148 | 0.170 |
| | Per kWh | 0.006 | 0.017 | 0.019 |
| Ideal Estimate | Absolute | 5.608 | 16.48 | 17.09 |
| | Per events | 0.080 | 0.238 | 0.247 |
| | Per kWh | 0.009 | 0.027 | 0.028 |

Table 7 lists the average daily profit that could have been obtained from EV flexibility on Oct. 2018 by using the method proposed here and historical data until Sep. 2018. The profit is calculated in for three products provision schemes: providing all the flexibility for FCR-N, FCR-D, or as a combination of FCR-N and FCR-Dn. Although FCR-N has a larger remuneration per capacity, the profit of providing FCR-N is less than FCR-D because EV cannot provide large down-regulation in comparison to up-regulation reserve. Table 7 shows that providing a combination of FCR-N and FCR-Dn is the most profitable choice. The “Ideal Estimate” removes the errors due to forecasting by applying the method directly on the Oct. 2018 historical data. Although such results cannot reasonably be expected, it shows how much the results could be expected to be improved if the forecast could also be improved by, for example, having more historical data available or if the number of EVs and of charging stations were to increase significantly.

Although the FCR-N and FCR-Dn combination is the most profitable, it is difficult to argue that the difference with providing only FCR-D is significant enough to take the risk of reducing the users’ quality of service by not charging the vehicles with the maximum available power and of them unplugging it with an unexpected partial charge. This situation could occur at any time the service is running with FCR-N, but only when it is activated with FCR-D.

The results from this forecasting work are used to determine the curves and prices to be bid on the FCR day-ahead markets. The process to achieve that is detailed in deliverable D6.5.

5.4.4 PERFORMANCE OF THE FORECAST SYSTEM

The training of the models requires a computing time of about an hour. This however needs to be run only on demand and when a significantly large enough amount of recent data is available. There are therefore no specific speed requirements. The forecasts themselves have a lead time of at least 12 hours and, if the model exists and has previously been trained, the computation is of the order of minutes. As regards to time, there is no additional limitation due to the forecasting process. Regarding the actual performance of the forecasting in terms of accuracy, the implementation and testing with new data will occur during the demonstration period and will be reported in the demonstrator's specific deliverable: D6.9: *"Finnish demonstrator - Market based integration of distributed resources in the transmission system operation"*.

5.4.5 APPLICATIONS

The forecast of EV charging stations flexibility potential was done to figure out how much demand response potential currently exists in the public EV charging network of Helen. Currently the flexibility potential is low and limited by the low number of charging events. However, the number of charging events is expected to grow in Helsinki in the future and therefore the available demand response potential is also growing. If the charging stations are aggregated and operated in TSO ancillary services markets, a forecasting tool is essential for an aggregator to determine the correct bid sizes and times.

The EV charging stations flexibility demonstration will be done with a few charging stations located at the office building of Helen DSO (demonstrator with a maximum of four AC charging stations) and one DC charger (50 kW) located in Helsinki. The created forecast of public EV charging stations flexibility is not utilized in the demonstration of T6.4, since the demonstration is done only with a few charging stations. In the case of the office building, the available hours for the flexibility demonstration can be seen from the historical data of the EV stations (e.g. the arrival time of an EV in the morning is usually the same).

5.5 FORECAST FOR CUSTOMER-OWNED BATTERIES

5.5.1 INTRODUCTION

As part of its energy solutions, Helen sells packages including PV panels and a battery. The objective for the customers is to be able to store up their excess PV production during the sunny hours of the day and to consume it during the rest of the time. In EU-SysFlex, Helen evaluates and demonstrates the possibility to use the batteries during the times the consumers do not need them in order to provide system services, such as frequency containment reserves. The priority is to follow the consumer's wishes, which means that, when the PV production exceeds the consumption, the battery has enough storage capacity to absorb it. The forecasting tool created by VTT aims at estimating the production and consumption for a day and determining how much empty storage there should be available in the battery at the time the sun rises.

5.5.2 DESCRIPTION OF THE FORECASTING PROCESS

5.5.2.1 INITIAL DATA: MEASUREMENTS, WEATHER FORECASTS AND META DATA

The data used for the forecasting is the following:

- Measured consumer data, for each minute, provided by Helen:
 - Date and time
 - Consumption
 - PV production
 - Battery charging or discharging power
 - State of Charge of the battery
- Weather information downloaded from the Finnish Meteorological Institutes open data platform:
 - Average daily temperature
 - Hourly solar radiation
- Metadata about the batteries:
 - Rated power
 - Maximum energy storage capacity

The time window included in the historical data was from September 14th, 2018 to October 20th, 2019.

5.5.2.2 ALGORITHMS AND MODELLING

The main objective is that the battery starts to charge, at the time the PV production becomes larger than the consumption, with a State of Charge (SoC) that allows to absorb as much of the excess production as available. In other words the capacity remaining in the battery should be larger than the energy comprised between the production and consumption curves. Figure 57 shows those curves where the production exceeds the consumption first around 7 am. The areas shaded in blue represent the energy that should be stored (if the battery is full, the excess is fed into the distribution network instead) in the battery and the areas in red the energy discharged from the battery (if the battery becomes empty, that required extra energy has to be taken

from the distribution network). The areas before 7 am and after 5 pm are not shaded because the relevant information is how much energy needs to be stored until the time when the consumption takes over (in this case around 5 pm). In other words, starting at 7 am, the blue energy is stored. The two first consumption peaks, in red, require more energy and the quantity to be stored is reset to 0. After that, the energy to be stored does not reach 0 again until 5 pm. The point of interest is the maximum value that this energy to be stored reaches during the day. Putting this in equations, the maximum energy to be stored is the following:

$$E_{st,max} = \max_{h=0 \rightarrow 24} \left(\int_{h_0}^h (P_{prod,h} - P_{cons,h}) \cdot dh \right) \quad (31)$$

where

- $E_{st,max}$ is the maximum energy to be stored in the battery during a specific day, in kWh.
- h_0 is the last time of the day when the integral considered was equal to zero.
- h is the time of day, in hours.
- $P_{prod,h}$ and $P_{cons,h}$ are respectively the power produced and consumed by the household at time h , in kW.

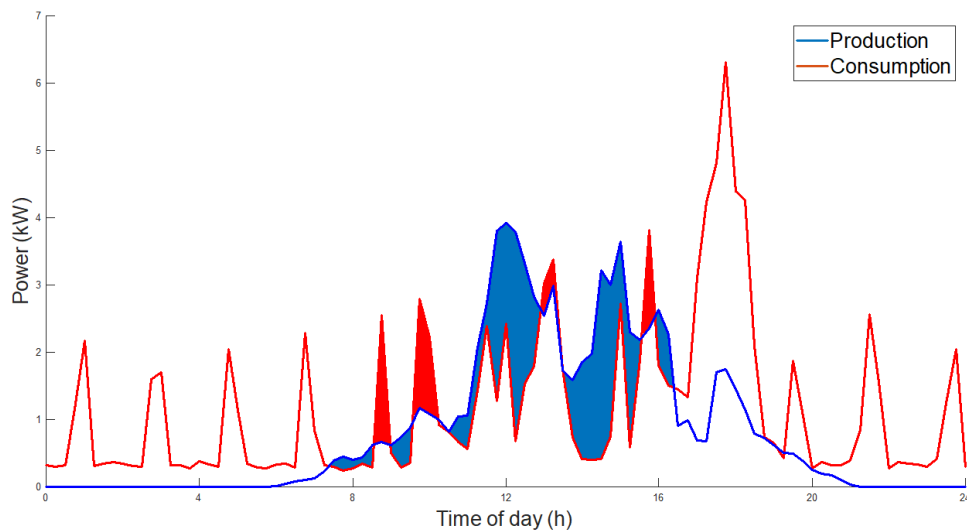


FIGURE 57 - PRODUCTION AND CONSUMPTION CURVES FOR "CONSUMER 1" DURING AUGUST 16TH, 2019.

In order to forecast the behaviour of a household, the first step is to forecast the PV power production. In this case, the forecast is not interested in the most probable values. Its goal is to provide a ceiling for how much PV production can be expected based on the forecasted solar radiations. An accurate forecast is anyway very difficult when dealing with a single installation with limited data about the installation itself and with radiation measurements from a station kilometres away from the installation. Figure 58 shows in blue the points measured between 8 am and 6 pm period and in red a line passing by the origin and chosen so that 80 % of the data fits below it. There can be a number of reasons why the production would be lower than the rated value (clouds, panel orientation not being optimal at that specific time, technical malfunction, measurement system failure, etc.). The points with high produced power during low radiation periods however can be explained only by a difference of radiation between the location of the PV panel and that of the meteorological station.

The red line is chosen as a forecast so that, with specific solar radiation forecasts the odds of the production being higher than the line, including the many errors due to the solar radiation measurement location, is of 20 % for the points with a solar radiation of minimum 200 W/m².

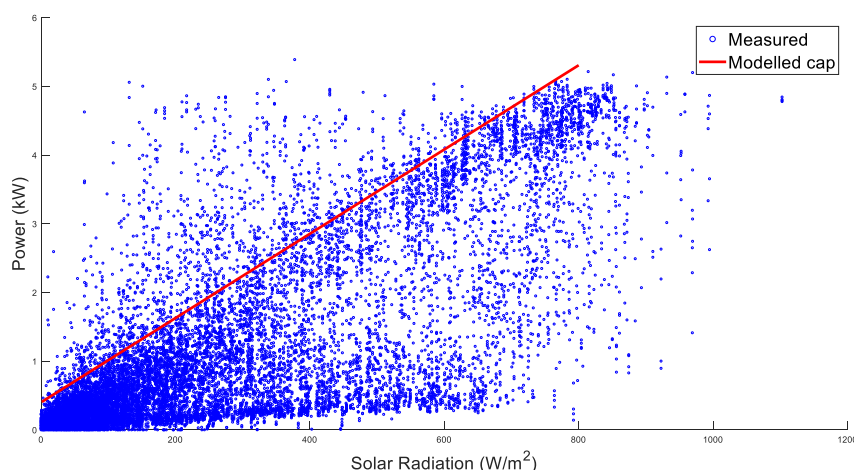


FIGURE 58 - PV PRODUCTION MEASURED AND A MODELLED FORECASTED CAP

The second step is to forecast the consumption. An observation that can be made from the consumption curve in Figure 57 is that the consumption is not smooth. It contains peaks at intervals more or less regular, but with varying period and timing, making them impossible to accurately forecast. Such a behaviour is typical for electric heating systems set to keep the indoor temperature within a certain band and using the thermal inertia of the building to maintain the temperature between the heating periods. As a consequence, for this type of housing, forecasting the power consumption cannot lead to good results. It is more efficient to forecast the energy consumed throughout the day. Another problem encountered here with a direct consumption forecast is that the data is attached to a specific household. Accuracy is possible in forecasting only if the unpredictable variables (such as in this case the consumers behaviour) can be combined between a large number of individuals so that the errors on each of them can cancel each other. That is not possible here and another approach needs to be chosen.

The approach selected is to study the energy consumed by the same individual household on days deemed similar. Weekdays, Saturdays and Sundays show different behaviours. In addition, Figure 59 shows a correlation between the energy consumed until the end of the evening and the outdoor temperature. The linear correlation displayed here in red is only to illustrate the trend, it is not used in the following calculations. There is a high variance in the heating measured for days with the same temperature. Low consumption days can be days when the occupants are not home and the heating system is set on its minimum setting while high consumption days can be the results of things such as the occupants having a sauna evening or forgetting a window opened.

Similar days are thus taken as similar types of weekdays with an average outdoor temperature within 3 degrees of the forecasted temperature for the day studied. Thus, on August 16th, 2019, a Friday, the average daily temperature was of 16.8 degrees and Figure 60 shows the progression through the day of the energy consumed

by this consumer for the 68 weekdays in the data with a recorded average daily temperature between 13.8 and 19.8 degrees.

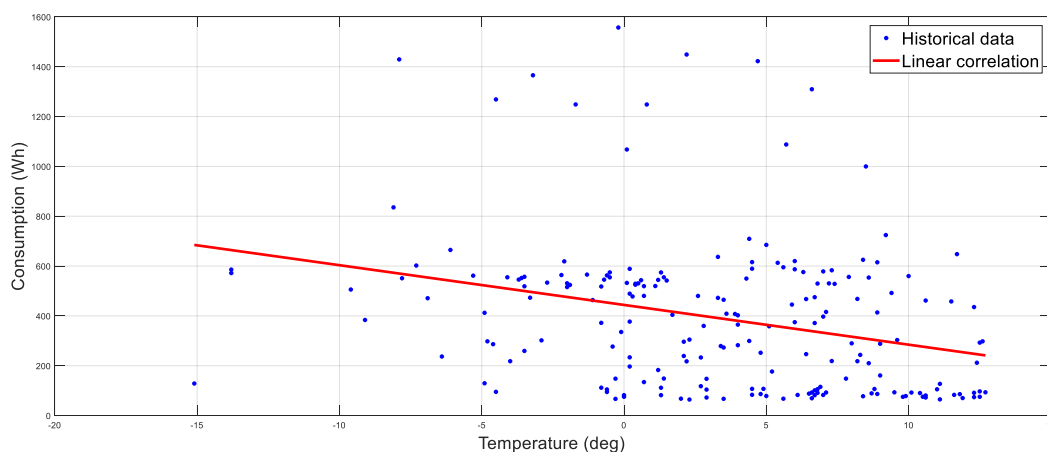


FIGURE 59 -RELATIONSHIP BETWEEN THE ENERGY USED DURING THE DAY AND THE OUTDOOR TEMPERATURE FOR A SINGLE HOUSEHOLD

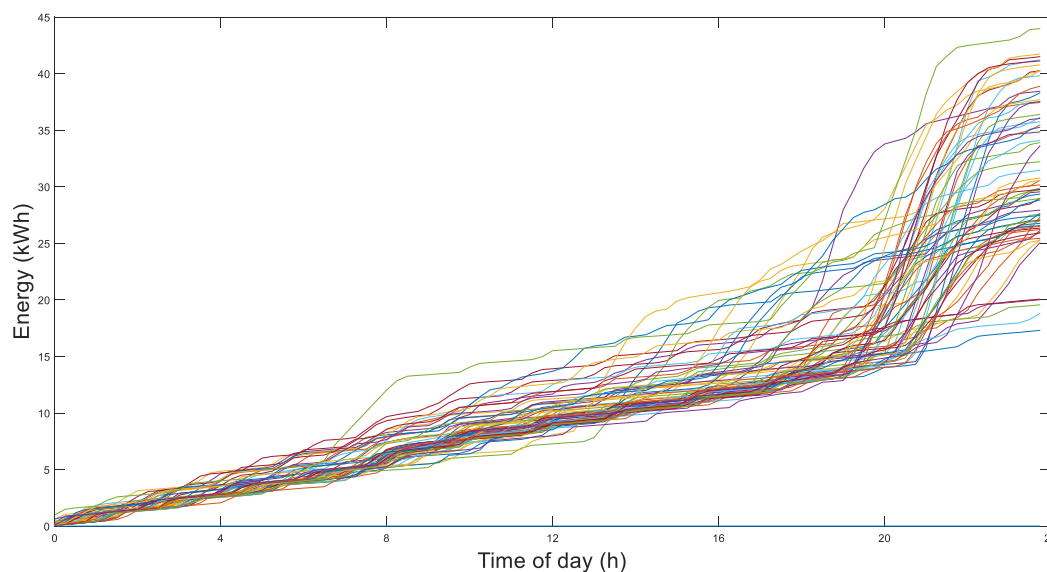


FIGURE 60 - ENERGY CONSUMPTION FOR A SINGLE HOUSEHOLD DURING THE DAY FOR THE DAYS SIMILAR TO AUGUST 16TH, 2019.

The objective of the forecasting, once again, is to prevent situations where the production would be higher than the consumption and the battery would be full. The most conservative approach would be to take the minimum of these recorded curves as the consumption forecast. The choice can however made to take a risk of overestimating the consumption and ignore a certain number of curves. In this case, 10 % of the curves are neglected for the forecast. In that case, the resulting energy curve can be represented again in terms of power consumed.

5.5.2.3 REALIZATION OF THE FORECAST SYSTEM

When fully implemented, the forecast will be run by Helen including:

- the weather forecast data received from a weather forecast provider, and already present in their database for previous purposes.
- Consumer data stored in Helen's database and, if needed, updated with data from the data cloud service provider (Sonnen).

5.5.3 FORECASTING RESULTS

Coming back to the example of August 16th, 2019, the lower bound on the consumption is compared to the actual one in Figure 61. The upper bound of the production as well as the actual one is shown in Figure 62.

The difference between the two curves and their impact on the state of charge (as defined in Equation 30) are shown as forecasted and actual in Figure 63. The main takeaway is that the maximum SoC reached during the day was 87 % while the forecasted one is of 91 %.

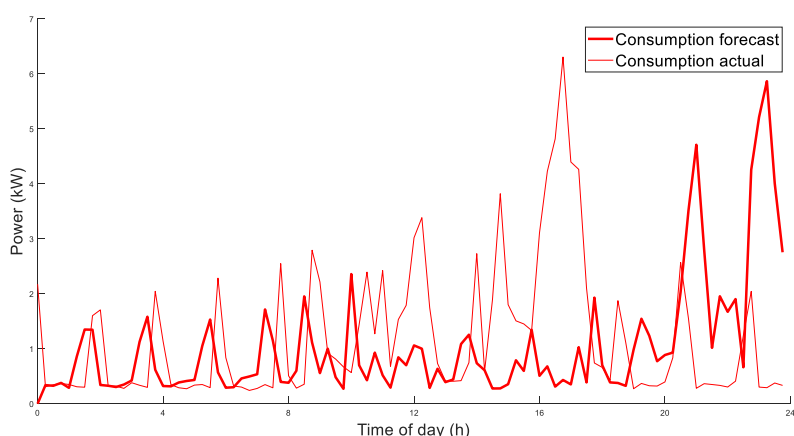


FIGURE 61 - FORECASTED, ENERGYWISE LOWER BOUND AND ACTUAL CONSUMPTION FOR AUGUST 16TH, 2019.

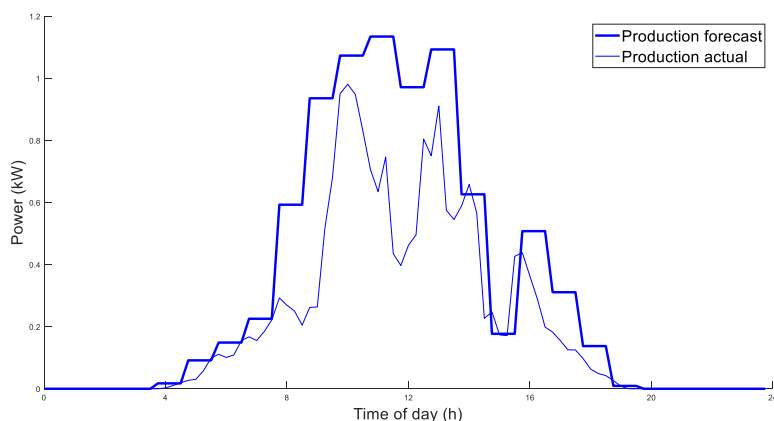


FIGURE 62 - FORECASTED UPPER BOUND ON THE PRODUCTION AND ACTUAL PRODUCTION FOR AUGUST 16TH, 2019.

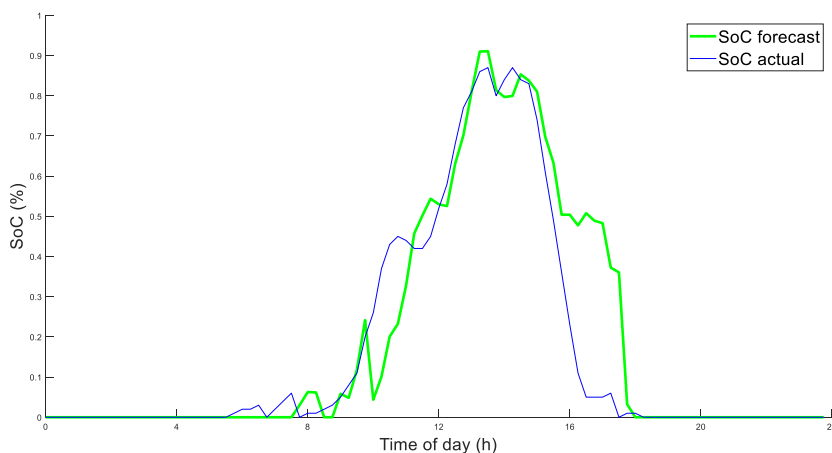


FIGURE 63 - STATE OF CHARGE, FORECASTED "WORST" CASE AND ACTUAL FOR AUGUST 16TH 2019.

5.5.3.1 FORECASTING QUALITY BASED ON HISTORICAL DATA

The forecast as described here has been run over the last 1 year of data (from Oct. 21st, 2018 to Oct 20th, 2019). The results for an individual customer are summarized in Table 8.

TABLE 8 - SUMMARY OF THE RESULTS OF THE FORECASTING TOOL BASED ON ONE YEAR OF HISTORICAL DATA

| | |
|--|---------|
| Number of full battery days identified | 134/141 |
| Number of days when SOC < 5 % identified | 146/170 |
| Number of days when forecast < measured | 11 |

After analysis, it shows that the days when the daily maximum measured SOC was 100 % and the forecast failed to recognize it are due to times when the battery charges itself for maintenance as showed for days 50 to 100 (Dec 9th, 2018 to Jan 28th, 2019). The days when the forecast was less than the measured values are listed in Table 9. The error for most of those is very small. On April 1st, there is an error in the data for the values of the solar radiation. The days in May, the reason for the errors is that the SOC in the measured cases does not reset to 0 in the beginning of the day, as is assumed in the forecast and as would be the case if the installation was used to provide services during the night.

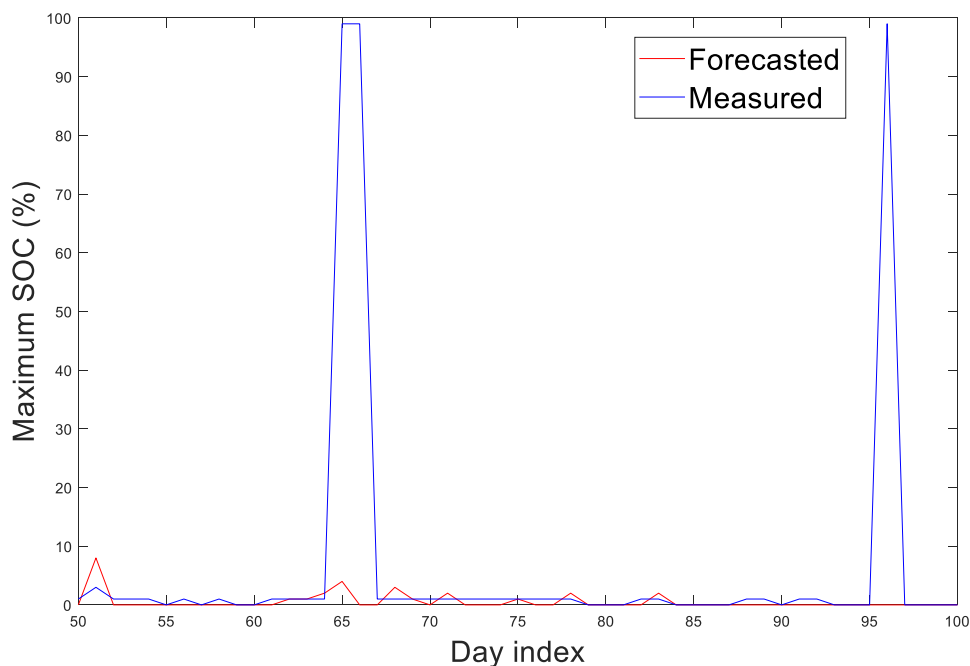


FIGURE 64 - DAILY MAXIMUM SOC MEASURED AND FORECASTED FOR A SINGLE HOUSEHOLD BETWEEN DEC. 9TH, 2018 AND JAN 28TH, 2019.

TABLE 9 - FAILED DAYS, WHEN THE FORECASTED MAXIMUM DAILY SOC IS BELOW THE MEASURED ONE

| Date | Nov 25 | Nov 30 | Apr 01 | Apr 05 | May 14 | May 15 | May 16 | Jun 01 | Jun 07 | Jun 16 | Oct 14 |
|----------------------------------|--------|--------|--------|--------|--------|--------|--------|--------|--------|--------|--------|
| Measured maximum daily SOC (%) | 33 | 5 | 64 | 5 | 53 | 53 | 56 | 32 | 23 | 44 | 9 |
| Forecasted maximum daily SOC (%) | 19 | 2 | 1 | 4 | 2 | 31 | 25 | 31 | 18 | 42 | 7 |

5.5.4 PERFORMANCE OF THE DEMONSTRATION SYSTEM

The most time consuming parts of this tool are to convert the minute-based new data to samples every 15 minutes. Once that is done however, the forecasting itself takes in the order of tens of seconds for each customer. With 11 customers, it remains manageable, but in the future, with more customers, grouping the days for each of them into existing bins would greatly reduce the computing time. The tool would need to be run before the market gate closure for the market window and the following day if the flexibility is to be bid to the TSO ancillary services. There is no real time pressure put on the tool in that regard.

5.5.5 APPLICATIONS

With the information available from the forecast, the aggregator (Helen in this case) can determine at what state of charge the batteries should be when the sun rises. Working backward from it, they can estimate at what time they should stop providing frequency services long enough before so that the battery can be discharged down to the required level. In the example of “Consumer 1”, the rated power of the battery is of 3 kW and the maximum energy contents is of 6 kWh, thus, reserving 2 hours before the production takes over is, in all cases, enough to charge/discharge the battery to the desired level. Another application could be to change the strategy of the consumers and optimize the cost of their consumption using market prices instead of optimizing the energy stored from their PV panels.

5.6 PRELIMINARY CONCLUSIONS FOR THE FINNISH DEMONSTRATOR

This chapter was presenting four forecasting tools developed in the context of the Finnish demonstrator. The first one is for the purposes of the DSO, forecasting the net exchanges of active and reactive power between the DSO's and the TSO's networks. It includes a statistical analyses for operational planning as well and machine learning and neural network methods to forecast the day-to-day operation. By using this type of information, a DSO could better plan its needs for reactive power compensation resources and also have an estimation of the needs for the next few days, allowing it to operate its own resources better as well as to contract the required flexibilities from other actors, such as by setting up a local reactive power market. This forecast will be tested during the implementation of the demonstrator, but only in an off-line advisory mode during the technical proof of concept for the reactive power market.

The other three forecasts are designed to help the aggregator in assessing and bidding its flexibility potential. 727 households with storage heating (i.e. water tank) are forecasted with the intent of controlling their heat storage via the AMR-meters and through this, provide frequency services. The forecast is a hybrid model, including a physically based model for as an initial forecast, and then corrected with neural network algorithms in order to minimize the errors. The output of the tool gives the aggregator a clear view of the aggregated consumption from two groups of households with different dynamics, in cases where their consumption is optimized purely based on day-ahead tariff, but also the details of how the groups would react to different control signals. It allows the aggregator to forecast how the loads will react when they are operated for different services, such as, in the case considered here, for the mFRR market. During the demonstrator, this forecast will be used in order to run simulations of case scenarios.

A statistical analysis is used to forecast the flexibility potential that a set of public EV charging stations in the Helsinki area could provide for frequency containment reserves services. The analysis provides a cumulative density function for the available energy that can be used for upwards regulation (a decrease in consumption) or for symmetrical up- and down-regulation. The outcome is a bidding price and quantity for the frequency markets. The accuracy of the forecast is bounded by the limited number of stations and charging events, but the penetration of EVs in the transport sector in Finland is increasing rapidly and, in a few years, the forecast is expected to become more accurate and the potential flexibility that can be extracted to become more significant.

Finally, a forecasting tool estimates the PV production and the consumption of individual households with a battery energy storage system in order to give an estimate of the allowed state of charge for the battery installation at the time when the sun starts to shine and the PV production overtakes the consumption. This will be used in the implementation phase by the aggregator to determine when the battery can be utilized to provide other services than the maximization of consumption of the local production. The output of this forecast is boundaries on the SOC of the battery which would allow the storage of as much excess PV production during the day as possible. Due to the fact that the forecasting is made individually for different households, the best possible outcome is a conservative boundary with only a limited risk of exceeding it. In the future, with more households equipped with the same system, households could be aggregated for another forecast on the aggregator's side in order to be able to build up service of a size significant enough to form offers on the different markets. The results from the implementation phase for each of the four forecasting tools will be reported in D6.9: "Finnish demonstrator - Market based integration of distributed resources in the transmission system operation".

6 SIMILARITIES, DIFFERENCES AND TRANSFERABILITY OF FORECAST APPROACHES

6.1 OVERVIEW OF THE DIFFERENT APPROACHES AND TECHNIQUES

As it was seen in the previous chapters, three different Demonstrators are set up, acting in LV, MV, and HV voltage levels. All Demonstrators utilize forecast techniques for their own individual purposes. The approaches are partly very different, but share in some cases the same basic assumptions or techniques. In addition, the focus and output is in some cases very similar, even though different approaches are chosen. Table 10 gives an overview of the characteristics of forecast approaches within the three Demonstrators in WP6.

TABLE 10: OVERVIEW OF THE FORECAT APPROACHES AND TECHNIQUES IN THE THREE DEMONSTRATORS WITHIN THE EU-SYSFLEX PROJECT.

| | Finnish Forecast | | | | German Forecast | Italian Forecast |
|--------------------|---|--|---|---|---|---|
| | Forecast of reactive power needs to comply with the PQ window requirements | AMR-Controlled Electr. Heating | Public EV-Charging Stations | | Customer-owned batteries | |
| Description | Forecasting active and reactive power flow at the DSO-TSO connection point | Forecasting the electrical consumption of electrically heated houses | Forecasting the expected flexibility of a set of public charging stations | Forecasting the available flexibility from households combining a battery and PV panels | Forecasting Wind, PV and residual loads at busbars of MV/HV grid points | Forecasting tool for PV and DG in general to monitor and estimate DG on the distribution network |
| Scope | Forecast for the aggregated exchanges at primary substations | Forecast for two aggregated groups of habitations located in a single distribution network | Forecast the flexibility that can be provided for FCR services | Forecast of individual households to extract capacity for reserves services | Forecast at MV and HV-level to support grid optimization at HV-level | Forecast of generation at MV and LV level, aggregated for substation (point of connection for MV producers, MV/LV transformer for LV producers) |
| Innovation | Forecasting reactive power of vertical power flow under consideration of compensation requirements on different time horizons | Hybrid model for load forecasting and dynamic response to control signals | Linking the flexibility potential to the specific FCR market | Study based on production and consumption of individual households. | Intra-Day forecast of disaggregated producers based on aggregated power measurement | Providing nowcast of active power and reactive power values of PV generators, loads and other sources. |

| | | | | | | |
|------------------------|---|--|---|--|--|--|
| Forecast-Target | Active power, P Reactive power, Q | P for two aggregated sets of habitations | P up- and down-regulation potential for FCR markets | Limitations on the SOC of the battery when the PV production starts. | P for Wind, PV, residual load and Q for vertical power flow | P produced by PV plants (working in case of “clear sky”) with an adjustment considering the weather conditions. |
| Input-Data | P and Q historical time series (2016-2019) | Outdoor temperature and its forecast. Averaged measured P of the customers. Control signals. | Charging events history | Production, consumption and SOC for individual consumers. Temperature and solar radiation data. | NWP-Model (CD2, ICON), Measurements at MV/HV transformers with status information (P,Q). Daytime information. Installed capacity of Wind and PV in MV and LV. | Weather forecasts; Electrical grid connection status; Installed power of single power plants directly connected to MV feeders; Aggregation of generators for each MV/LV distribution transformer in case of DG located on LV network; Historical recordings (when available) |
| Type of Model | Statistical analysis, Gradient Boosting, LSTM | Physical based model complemented with DNN for the residuals | Statistical analysis | Statistical analysis | Physical Approach, LSTM | PV model (inspired to the PVUSA rating methodology) that provide the forecast of the average active power generated in a time interval as a function of the average values of the meteorological variables in the same interval |
| Lead Times | 12 – 36 h, 1 – 7 days | 12 – 36 h | Not applicable | 12 – 36 h | 0-72 h | 0 – 72 h |
| Update Cycle | By request of Helen DSO | Not applicable (used for simulation cases) | Not applicable | 24 h | 15 min. | 24 h |

| | | | | | | |
|------------------------|--|--|--|---|--|---|
| Time Resolution | 1 hour | 1 hour | 1 hour | 15 min | 15 min | Time step of 60 minutes. |
| Applicability | Determine reactive power compensation needs for the DSO | Habitations with electrical heating and local heat storage | Determine the price and volumes to be bet on the FCR markets | Determine a potential that could be used on reserves markets. | Grid optimization, Congestion management | Apply the observability of system for TSO and improve the grid management for DSO. |
| Limitations | Accuracy limited by other input: forecasts (GB); underground cabling network status information (LSTM) | Model specific to the considered loads. | Based on a limited data set. A better model could most likely be defined with more available data. | Accuracy limited by data from individual consumers with small installations. No aggregation is made for now | Intraday Forecast limited in performance due to input measurements only available at transformer stations. | The forecast algorithm does not take into account the actual availability of all the Distributed Generators |

The prediction systems were adapted for each demonstrator in such a way that they provide the demonstrator with the optimal amount of data it needs for its operation. Despite this very strong focus on the demonstrators, similar concepts are found in the three national systems. The Italian and German forecasting systems are used to predict the active power of individual generators and their aggregation to grid stations. These forecasts are based on weather forecasts and measured values and are calculated for points in time up to 72 hours into the future. Both systems use physical models to calculate wind and PV power, but the approaches to transform weather variables such as radiation and wind into active power differ slightly. And although the online data sources differ in resolution and quality (the Italian system receives SCADA data directly from the generators, while the German system depends on the measurements at the substations' transformers), the measurements entering the system online are from the same type, e.g. active power of the producer. Compared to the forecast system in the Italian demonstrator, the forecast in the German demonstrator will be executed as an intra-day prediction. This means that the forecast is updated every 15 minutes.

In order to get an exact forecast, the integration of online measurements is necessary. In contrast to the Italian system, however, no Scada measurements are online available at the renewable energy sources, but only measurements at the transition points to the High Voltage Level. Therefore it is necessary to develop new methods how these measurements are used in order to integrate them into the forecast, which is located in the transition from low voltage to medium voltage level. The challenge here is the boundary condition that the measurement is a sum measurement over all generators and consumers, from which the renewable sources must first be separated or other substitutions like the selection of best fitting weather ensembles must be made. Therefore, the forecasting system must be adapted to the special conditions found in this distribution system and must be designed exactly for this.

From an algorithmic point of view, several prediction systems use machine learning approaches, including the Finnish systems for predicting active and reactive power flow in the PQ-window and electric heating loads of houses and the German system for predicting the P/Q behaviour of loads. Particularly noteworthy here is the Long-Short-Term Memory (LSTM), which are used in both the Finnish demonstrator and the German demonstrator. While the Finnish prediction uses them beneath other models to predict the active and reactive power flow in the PQ-window for one week in the future, the German prediction forecasts the active and reactive power of the loads for a few hours up to days in the future. Interesting here is that although the context of the target variable is different, parts of the input data are very similar. This includes the measured active and reactive power and temperature as well as the day of the week.

6.2 COMPARISON BETWEEN THE APPROACHES FROM THE THREE DEMONSTRATIONS

6.2.1 SCOPE AND INNOVATIONS

As already mentioned above and seen in Table 6, the German Demonstrator and Italian one use forecast approaches which obtain similar information. Both approaches forecast the generation of decentralized generation units which are located in mid-voltage grids and also at the low voltage level. In the German approach, these determined and forecasted generations are aggregated onto HV-MV substations, in order to use them in HV state estimation and grid optimization. The approach is quite different for the Finnish demonstrator, which is dedicated to specific assets: electric heating loads in consumer households, public charging stations for electric vehicles and houses with battery energy storage system and PV panel installations. In a fourth tool, the Finnish forecast is estimating the energy exchanges at the TSO-DSO interconnection (between HV and EHV, 110 kV and 400 kV in this case) in order to determine the compensation needs to stay within the PQ-window set by the TSO. This latter approach is similar to the approach in the German Demonstrator, where, after determining the energy generated in MV grids, the residual energy exchange between MV and HV grids is determined and forecasted. These forecast data include consumers from MV and indirectly also LV as well as generation which are not Wind or PV related. Eventually, the PQ-window at interconnection points between TSO and DSO are computed and provided to the grid operators.

All of these approaches serve the purpose to complete the information needed to fulfil the different Demonstrator objectives. Their innovation stems from the fact that such information was partly not available or used before EU-SysFlex.

In the German case, a mix between bottom-up and top-down approaches are used. LV and MV generating units are forecasted and aggregated onto MV-HV substations. This generation value is then subtracted from the aggregated measurements at these substations. This way, a distinction between generation and consumption at HV level is achieved.

In the Italian Demonstrator, up-to-date information about production and consumption in MV grids is required in order to provide input for optimization purposes. This is achieved via an innovative approach using standard load profiles, physical PV generation models and current weather data, as well as weather forecast. Within this approach, besides forecast for the next 72 hours, current generation and consumption values for all assets in the MV grid can be obtained. This nowcast is then used to estimate the current grid state and perform optimization of P-Q flexibilities at MV-HV substation level.

Similar to these innovative approaches, the Finnish Demonstrator forecasts the reactive power flows going through the TSO and DSO interface. Besides this tool, the Finnish Demonstrator also developed three other forecasting tools that are aimed the purposes of an aggregator. The first one is a hybrid model for the forecasting of electric heating loads that can dynamically respond to control signals from an aggregator. The second one uses information about the charging behaviour of electric vehicles to assess the flexibility potential to participate to the frequency containment process. The third one estimates the production and consumption of individual households in order to determine how much of their installed battery storage system can be used to provide flexibility services.

6.2.2 INPUT DATA AND MODELLING

As general basic input, it was shown, that time series (measured and generic ones) and weather data serve in all three demonstrations. These are measurements at substations and in some cases also at device level as well as generic load profiles. The usage of physical models which taking weather data as inputs is also present in most of the cases. For all three demonstrators, the determination of P and /or Q values at interconnection points, follows similar ways and uses similar data.

In order to correlate weather information with historical measurements and then make prediction of future values, LSTM models are used in the German case for residual load forecasts and in the Finnish case for vertical power flow forecasts. For the prediction of generation, physical models are used in the German and Italian cases. In both cases, the current and predicted weather conditions are used in the models, and energy generation can be determined.

Regarding forecast horizons and timely resolutions, various differences between the approaches can be seen from Table 6. The lead time, which describes the forecast horizon, is similar in the German and Italian cases. In the Finnish cases, there are some differences depending on the application. The forecasts for the AMR-controlled houses, for the compliance to the PQ requirements and for the customer-scale batteries have a lead time of 12 to 36 hours. The compliance tool to the PQ window requirements has also developed 1 – 7 day estimations.

Considering the frequency of forecast update (update cycle), strong differences between the approaches arise. In the Italian and German cases, a fixed update cycle of 24 h and 15 minutes, respectively are used. In the Finnish cases, updates of forecast data are only done by request. This depends on the data deliveries from field measurements and weather forecasts. The time resolution of forecast data has the same order of magnitude for all cases, but depends on the applications of the forecasts.

6.2.3 APPLICATIONS AND LIMITATIONS

The main application for all approaches in German and Italian demonstrations is to enhance the information exchange between DSO and TSO. In order to achieve this, forecasts are used to update grid states in the German and Italian cases, enabling state estimation and optimization of P-Q flexibility. In the Finnish case, the approaches are targeted to help the DSO to stay within PQ-window set by the TSO and on the other hand and to help the aggregator in the determination of bidding times and bid volume to the TSO ancillary services. The PQ-window compliance forecasting tool is utilized in the reactive power market demonstration (proof of concept). Forecasts for electric heating loads controlled via AMR meters serve to optimize local heat storage and bidding volumes on the TSO ancillary markets in the simulation scenarios. The flexibility forecasts of public EV charging stations and customer-scale batteries are also targeted to determine the correct bidding volumes and times for the aggregator.

However, these applications are limited in applicability, performance and accuracy. For example, in the German case, intraday forecast is limited in performance due to input measurements only available at transformer

stations. Also the amount of information limits the usage within the demonstrator functionalities. A 15 minute resolution is already the lower limit of which can be processed within the demonstrator.

In the Italian case, the limitations related to the forecast algorithm must be identified in the regulatory aspects that underlie relationship between the DSO and the owners of the distributed power plants. More in detail, the day-by-day forecast of generation from distributed generators does not take into account the actual availability of all the plants (e.g. ordinary or not ordinary maintenance for generators). It is important to specify that the Italian regulation frame does not foresee an integration between planning and operational processes of DSOs and activities at distributed generation plants.

In the Finnish case, the accuracies of the forecasts are limited due to reasons specific for the forecasting problem. In the forecast of reactive power compensation needs to comply within the PQ-window, the accuracy is limited by some input data that the model uses, i.e. underground cable network status information and weather forecasts. The forecast of expected flexibility of a set of public EV charging stations of Helen is limited due to the rather low number of charging stations and charging events. It is expected that with the higher number of charging stations better forecasts can be created. The forecast of electrical consumption of electrically heated houses is specific to the type of housing included in the data sets. The customer-scale battery forecast is limited by the fact that the targets are individuals, making it possible to only limit the risks of exceeding the limits allowed.

7 CONCLUSION

This deliverable presents the different forecast approaches used in the three Demonstrators in Workpackage 6 of the H2020 project “EU-SysFlex”. It gives also insides to the individual techniques and methods, which range from standard load profiles and physical asset models over statistical analysis and application of artificial neural networks. These conducted forecast methods are applied on real test data as well as generic and simulated and these first and preliminary results are also given in this deliverable.

The objectives of the forecasting approaches within each individual demonstrations are quite different and vary in voltage level and type of assets. For the Finnish demonstration, which considers assets and prosumers in low-voltage grids, like households, storage and also electric vehicles the objective and purpose of the forecast is on the one hand, to sell flexibilities through a retailer at the TSO flexibility markets and on the other hand, to determine a reactive and active power window at DSO-TSO interface.

In the Italian and German demonstrations, which act at the interfaces between DSO and TSO, the aims of forecasts are similar but not equal. In the German case, forecast is mainly needed as basic data input for generation of future (0-72 h) grid states on which determination of PQ-flexibility bands at asset level but also at TSO-DSO interface level takes place. In the Italian case, also the current grid state (nowcast) is determined via forecasting in combination with load profiles as well as a 72 h forecast. In both cases the grid state will be determined and Q-flexibility at a HV/MV substation are computed.

In the German demonstrator an optimization of the electrical grid regarding active and reactive power as well as congestions is carried out by the DSO in the high voltage distribution grid. As input for the optimization intra-day and day-ahead forecasts are needed. These forecasts are divided into wind, PV and residual load forecasts at grid connections in HV and aggregated at HV/MV substations. The forecast system consists of two approaches, the physical modelling for the wind and PV forecasts and the machine learning approach by using a LSTM in a deep neural network architecture for the residual load forecast. Analysis of the system and the final deployment steps are still in progress so that a final evaluation is yet to be done in Deliverable 6.7. First results are shown for the vertical power flow forecasts as a pre step of the residual load forecasts. The results are shown in more detail for one transformer and additionally an overview of the results for all transformer is given. Forecasts with a shorter forecast horizon of up to 4 hours perform well, especially for the forecast horizon up to one hour. However, the results for the higher forecast horizons also show that there is still a need for further investigation. The result of these evaluations and the addition of wind and PV forecasts are finally shown in Deliverable D6.7.

The forecast tool used in the Italian Demonstrator represents an important instrument not only within EU-SysFlex objectives but also for normal distribution network operations.

The Italian Demonstrator makes use of the forecast system, which consists of the estimation and real-time monitoring of distributed generation connected to LV and MV level, to which the nowcast functionality is added.

The forecast tool currently exploits weather forecast data and works within E-distribuzione systems for state estimation scopes, finalized mainly to support voltage regulation function (mainly by means OLTCs) and other

function to reach an evolved operation of distribution network, like optimal scheme, supporting for network planning and so on.

For this reason, this functionality is necessary to satisfy also EU-SysFlex objectives, in which flexibilities owned and managed by the DSO (including the OLTC itself) are involved in addition to RES. In this context, nowcast functionality is aimed at improving the accuracy of forecast providing an “almost” real time information about renewable production. This information are obtained by processing weather data coming from a weather station that is going to be installed close to the demonstration site. However, it should be noted that the actual availability and level of efficiency of distributed power plants can also constitute a limitation to the correct functioning of the forecast tool because, according to the Italian regulatory framework, owners of DG are not required to provide updates about it. On the other hand, with this kind of application, it might possible to better evaluate and improve the quality of forecast, by considering some new input parameters depending on the position of the weather station and the closest renewable plants.

For the residual load forecast, a clusterization of customers is performed within a specific categorization based on the season and the day of the week. These clusters take into account of historical curves and real time measurements. This kind of elaboration is then performed also for Distributed Generation, even if the output data are used for state estimation and optimization in case forecast tool output should not be available.

In the Finnish case, there are four different forecasting tools. For two of them the available data is sufficient to run machine learning and neural network methods. The first one, the forecast of the active and reactive power exchanges between the DSO and TSO, requires first to identify the contribution from various variables (connection of underground cables, activation of existing reactive power control assets) which need to be subtracted from the historical time series for the algorithms to provide accurate results. For the second one, the forecast of the consumption profiles of houses equipped with controllable heating systems and a heat storage, the neural network is used to mitigate the errors from a physically based model. The takeaway is that in both cases the machine learning methods could not be left unchecked and that some underlying method has to be implemented in order to prevent very high inaccuracy in situations occurring too rarely. In the two other cases, the data is so sparse that accurate results from an actual forecasting model are not possible. In those cases, the estimations are based on statistical analyses. The potential for the participation to frequency containment reserves of the TSO is identified for public EV charging stations of Helen in the Helsinki region. For this identification it was required to model how individual charging events could provide symmetrical up- and down- or only up-regulation (a decrease in charging power) and to apply it to the probability of the occurrence and size of charging events. In the last forecasting tool, the photovoltaic production and the electricity consumption of households is estimated individually for each of the households. The objective is to minimize the risk that the utilization of their battery system by the aggregator for TSO ancillary services would prevent the household from storing its excess PV production. The result for this one is a range of allowed states of charge for the battery in the beginning of the day. The outcome of the forecasting tool for the TSO - DSO interactions can be used by the DSO in order to dimension its needs for reactive power and in potentially setting up a reactive power market. The outcome of the three others is used in the Finnish Demonstrator to help the aggregator provide services to the TSO by creating bids on the reserve markets.

In a comparison between the approaches from the three teams (chapter 6) it was shown, that the requirements on forecast approaches, stemming from the various business and hence related system use cases, can differ significantly. Hence also the forecast approaches differ from each other. But there are also similarities between the approaches and realizations.

Concerning the scope of the approaches in the three demonstrators, the German and Italian demonstrators have partly similar purposes. Hence the final usage of the forecast approaches is very similar. Both demonstrations predict node values for MV (Italy) and HV (Germany) on which future grid states are computed and evaluated. In addition to this, the Italian demonstration also use the forecast in order to obtain a “Now Cast”. Also, in both cases, different optimizations are applied and the results are used for operational planning purposes. One approach (the 4th) in the Finnish case is also related to this scope, but mainly to estimate the needed amount of reactive power which need to be compensated in order to stay in a defined PQ-window. For their other approaches, the scope is quite different, since they aim at forecasting of specific kinds of assets in consumer households are public charging structure.

As input data and used models, it was seen, that all approaches rely on historical time series as basic input in order to create their forecast models and adjust them. The kind of time series differs vastly and are of course dependent on the scope of each forecast. But for example, the forecasting of P or Q at interconnection points, the input time series are almost identical in type.

The correlation models used in the approaches differs again. LSTM for example is used in the Finnish and German case in order to estimate vertical and residual load flows respectively. Physical models on the other hand are use in the Italian and German approaches for estimating energy injections from renewable weather dependent assets like Wind and PV plants.

Also, a wide spread was found in lead times, they range from 12 hours to up to 7 days. Related to this are also the update cycles, which also have a wide range between 15 minutes and 24 hours.

In general and in conclusion, one can say, that forecast approaches within WP6 of EU-SysFlex are very individual and specific to their related scope and task. Like the whole demonstrations are highly specialized to fulfil their purposes, the forecasts utilized in the project are carefully chosen and elaborated in a way each application can get the best results out of it.

Even though there are some differences and some similarities within the approaches, one can see that there are already solutions starting from household level, via low- and mid-voltage grid levels up to high voltage grids which all serve the main purposes of making operational grid planning more feasible and secure. This besides further aspects, serves the WP6 objectives which are

- Improve TSO-DSO coordination;
- Provide ancillary services to TSOs from distribution system flexibilities;
- Investigate how these flexibilities could meet the needs of both TSOs and DSOs,

and are hence well aligned with the purpose of this workpackage.

8 REFERENCES

- Baldi et al. (2012) Baldi, Di Lembo, Nebiacolombo, Corti “MONITORING AND CONTROL OF ACTIVE DISTRIBUTION GRID”, May 2012, Lisbon, Cired Workshop
- Bianchini et al. (2013) Bianchini, Paoletti, Vicino, Corti, Nebiacolombo “Model estimation of photovoltaic power generation using partial information”, 2013 IEE PES Innovative Smart Grid Technologies Conference EUROPE (ISGT Europe 2013), Copenhagen, Denmark
- Dows and Gough (1995) R.N. Dows and E.J. Gough. PVUSA procurement, acceptance, and rating practices for photovoltaic power plants. Technical report, Pacific Gas and Electric Company, San Ramon, CA, 1995.
- Fritz et al. (2017) Fritz, Rafael; Good, Garrett; Braun, Axel; Dobschinski, Jan; Hagedorn, Renate; Siefert, Malte (2017): Abschlussbericht EWELINE : Erstellung innovativer Wetter- und Leistungsprognosemodelle für die Netzintegration wetterabhängiger Energieträger. With assistance of TIB-Technische Informationsbibliothek Universitätsbibliothek Hannover, Technische Informationsbibliothek (TIB).
- Gazzetta Ufficiale della Repubblica Italiana Gazzetta Ufficiale della Repubblica Italiana, “gazzettaufficiale.it”
- Giannitrapani et al. (2015) Antonio Giannitrapani, Simone Paoletti, Antonio Vicino, Donato Zarrilli “Bidding Wind Energy Exploiting Wind Speed Forecasts”, September 2015, Published in IEEE Transactions on Power Systems (Volume: 31, Issue: 4 , July 2016)
- Greff et al. (2017) Greff, Klaus; Srivastava, Rupesh Kumar; Koutník, Jan; Steunebrink, Bas R.; Schmidhuber, Jürgen (2017): LSTM: A Search Space Odyssey. In IEEE Trans. Neural Netw. Learning Syst. 28 (10), pp. 2222–2232.
- Hochreiter and Schmidhuber (1997) Hochreiter, S.; Schmidhuber, J. (1997): Long short-term memory. In Neural computation 9 (8), pp. 1735–1780.

| | |
|----------------------------|--|
| Soler et al. (2019) | Robert Soler (EDF); Ye Wang (EDF); Danny Pudjianto (Imperial College); Pirjo Heine (Helen Electricity Network); Suvi Takala (Helen); Antti Hyttinen (Helen); Miguel Jorje Marques (EDP); Nuno Lopes Filipe (EDP); José Villar (Inesctec); Bernardo Silva (Inesctec); Sahra Vennemann (Innogy); Maik Staudt (Mitnetz); Jens Schwedler (Mitnetz); Kalle Kukk (Elering); Simone Tegas (EDIS); Carla Marino (EDIS); Daniele Clerici (RSE); Diana Moneta (RSE). Report on the selection of KPIs for the demonstrations. D10.1. dated 8.2.2019. accessed 21.2.2019 http://eu-sysflex.com/wp-content/uploads/2019/02/EU-SysFlex-D10.1-Report-on-the-selection-of-KPIs-for-the-demonstrations.pdf |
| Misesti (2011) | Misesti, D’Orazio, Valtorta, Corgiolu, De Bianchi, Di Marino “FUNCTIONAL SPECIFICATION OF THE DSO SCADA SYSTEM TO MONITOR AND CONTROL ACTIVE DISTRIBUTION GRIDS”, June 2011, Frankfurt, CIRED |
| Koponen et al. (2019) | Koponen, Pekka; Niska, Harri; Mutanen, Antti: ” Mitigating the Weaknesses of Machine Learning in Short–Term Forecasting of Aggregated Power System Active Loads”, <i>IEEE INDIN19</i> , 22-25 July 2019, Helsinki-Espoo, Finland 8 p. |
| Koponen and Seppälä (2011) | Koponen, Pekka; Seppälä, Joel: ”Market price based control of electrical heating loads”. Proceedings of the 21st International Conference on Electricity Distribution, <i>CIRED 2011</i> , Frankfurt, 6-9 June 2011. Paper 0796, 4 p. |
| Koponen and Takki (2014) | Koponen, Pekka; Takki, Pekka: “Forecasting the responses of market based control of residential electrical heating loads”, <i>CIRED 2014 Workshop</i> , 11-12 June 2014, Rome Italy, Paper 0178. 5 p. |
| McLean (2008) | McLean, J. R. (2008): TradeWind WP2.6 - Equivalent Wind Power Curves. Garrad Hassan and Partners Ltd. |
| Pan and Yang (2010) | Pan, Sinno Jialin; Yang, Qiang (2010): A Survey on Transfer Learning. In <i>IEEE Trans. Knowl. Data Eng.</i> 22 (10), pp. 1345–1359. |
| Pihkala et al. (2019) | Pihkala, Atte; Takala, Suvi; Heine, Pirjo: Analysis of Changing Consumer Reactive Power Patterns in Distribution Grids. The 11th International Conference on Power Quality and System Reliability, Kärđla, Hiiumaa Island, Estonia, June 12-15 2019, 6 p. |
| Rumelhart et al. (1986) | Rumelhart, David E.; Hinton, Geoffrey E.; Williams, Ronald J. (1986): Learning representations by back-propagating errors. In <i>Nature</i> 323 (6088), pp. 533–536. |

- Saint-Drenan et al. (2015) Saint-Drenan, Y. M.; Bofinger, S.; Fritz, R.; Vogt, S.; Good, G. H.; Dobschinski, J. (2015): An empirical approach to parameterizing photovoltaic plants for power forecasting and simulation. In Solar Energy 120, pp. 479–493.
- Salz (2020) Salz, Martin (2020): Hyperparameter Tuning mit AutoML für Zeitreihenprognosen im Energiesektor. Masterthesis.
- Takala et al. (2019) Takala, Suvi; Pihkala, Atte; Heine, Pirjo: Control of Reactive Power in Electricity Distribution Companies. CIRED 2019, 25th International Conference on Electricity Distribution, Paper 1448, June, 3-6, 2019, Madrid, Spain, 5 p. <https://cired-repository.org/handle/20.500.12455/412>, ISBN 978-2-9602415-0-1, ISSN 2032-9644

9 COPYRIGHT

Copyright © EU-SysFlex, all rights reserved. This document may not be copied, reproduced, or modified in whole or in part for any purpose. In addition, an acknowledgement of the authors of the document and all applicable portions of the copyright notice must be clearly referenced.

Changes in this document will be notified and approved by the PMB. This document will be approved by the PMB.

The EC / Innovation and Networks Executive Agency is not responsible for any use that may be made of the information it contains.

This project has received funding from the European Union's Horizon 2020 research and innovation programme under EC-GA No 773505.